

The role of *Slc1a1* in OCD-relevant behavior and associated neural activity

by

Jared Michael Kopelman

B.A. Pomona College, 2011

Submitted to the Graduate Faculty of the
School of Medicine in partial fulfillment
of the requirements for the degree of
Doctor of Philosophy

University of Pittsburgh

2020

UNIVERSITY OF PITTSBURGH

SCHOOL OF MEDICINE

This dissertation was presented

by

Jared Michael Kopelman

It was defended on

August 3, 2020

and approved by

Anthony Grace, Professor, Department of Neuroscience

Mary Torregrossa, Associate Professor, Department of Psychiatry

Nathan Urban, Professor, Department of Neurobiology

Christopher Pittenger, Associate Professor, Department of Psychiatry, Yale University

Committee Chair: Rebecca Seal, Associate Professor, Department of Neurobiology

Dissertation Director: Susanne Ahmari, Associate Professor, Department of Psychiatry

Copyright © by Jared Michael Kopelman

2020

The role of *Slc1a1* in OCD-relevant behavior and associated neural activity

Jared Michael Kopelman, PhD

University of Pittsburgh, 2020

Obsessive compulsive disorder (OCD) is a severe neuropsychiatric illness with a lifetime prevalence of 2-3%. While the causes of OCD are unknown, there is a significant genetic component in the etiology of the disorder. Multiple studies have identified association of polymorphism in *SLC1A1* with OCD, with the most common polymorphism resulting in increased expression of the encoded protein, excitatory amino acid transporter-3 (EAAT3), the neuronal glutamate transporter. Subsequent studies in rodents have identified a potential role for *Slc1a1*/EAAT3 in OCD-relevant behavior. In this dissertation, I followed up on these studies first by investigating the effect of overexpressing *Slc1a1* on OCD-relevant behaviors in mice. I found a significant effect of *Slc1a1* overexpression on amphetamine-induced behaviors, but no effect on baseline grooming behavior or anxiety-like behavior. *Slc1a1*-overexpressing (OE) mice consistently showed potentiated hyperlocomotion in response to a low dose of amphetamine and potentiated stereotypy behavior in response to a high dose of amphetamine. This potentiated response to the high dose of amphetamine was associated with increased cFos expression in the ventromedial striatum. I then used an unbiased machine learning algorithm to cluster behaviors in *Slc1a1*-OE mice and controls following administration of low dose amphetamine, high dose amphetamine, or vehicle. I found that this approach was able to successfully identify amphetamine-induced behaviors that differed between *Slc1a1*-OE mice and controls and showed that the behavioral response to amphetamine is potentiated in *Slc1a1*-OE mice relative to controls. Using this automated scoring, I found that stereotypy behavior was positively correlated with the

number of cFos positive D1-neurons in the ventral striatum and negatively correlated with the number of cFos positive D2-neurons in the dorsal striatum. In contrast, locomotor behavior was positively correlated with the number of cFos positive D2-neurons in the dorsal striatum, indicating that there may be distinct populations of cells that drive distinct amphetamine-induced behavioral response. Lastly, I tested the effect of genetic ablation of *Slc1a1* or pharmacological inhibition of EAAT3 on OCD-relevant behaviors in *Sapap3*-KO mice. I found no significant effects of manipulating *Slc1a1*/EAAT3 on any of the behaviors tested. Together, these data point toward a role for *Slc1a1*/EAAT3 in abnormal repetitive behavior.

Table of Contents

Preface.....	xiv
1.0 Introduction.....	1
1.1 Obsessive Compulsive Disorder	1
1.1.1 Burden of OCD.....	2
1.1.2 OCD Treatment.....	2
1.1.3 Neurobiology of OCD	3
1.1.3.1 Structural studies.....	4
1.1.3.2 Functional Studies	4
1.1.3.3 Neural Networks in OCD	5
1.1.4 Genetics of OCD.....	6
1.1.4.1 Twin and Family Studies.....	6
1.1.4.2 Association studies.....	7
1.1.4.3 Glutamate Genetics in OCD	7
1.1.4.3.1 SLC1A1 in OCD	8
1.1.4.3.2 SAPAP/DLGAP in OCD.....	8
1.1.4.4 Genome-wide association studies in OCD	9
1.2 Glutamate system	10
1.2.1 Glutamate receptors	11
1.2.2 Glutamate transporters	13
1.3 EAAT3.....	14
1.3.1 Localization.....	14

1.3.2 Function	15
1.3.3 EAAT3 in Disease.....	17
1.4 Glutamate in OCD.....	19
1.5 Models of repetitive behavior	21
1.5.1 Genetic models of repetitive behavior	22
1.5.2 Circuit models of repetitive behavior	23
1.5.3 Drug induced repetitive behavior	24
1.6 Goals of this dissertation.....	26
2.0 EAAT3 overexpression increases susceptibility to the development of amphetamine-induced repetitive behaviors	27
2.1 Introduction	27
2.2 Methods	30
2.2.1 Mice	30
2.2.2 Behavioral testing.....	31
2.2.2.1 Anxiety tests	31
2.2.2.1.1 Open field test.....	31
2.2.2.1.2 Elevated plus maze test.....	32
2.2.2.1.3 Light dark test	32
2.2.2.1.4 Grooming assessment.....	32
2.2.2.2 Amphetamine-induced hyperlocomotion	32
2.2.2.3 Amphetamine-induced stereotypy	33
2.2.3 DeepLabCut.....	33
2.2.4 Behavioral Segmentation of Open-field in DeepLabCut (B-SOID)	34

2.2.5 Western blot.....	34
2.2.6 Immunohistochemistry	35
2.2.7 RNAScope	36
2.2.8 Statistical analysis	37
2.3 Results.....	38
2.4 Discussion	52
3.0 Examining the therapeutic potential of EAAT3 ablation or inhibition in the <i>Sapap3</i>-knockout mouse model of OCD	56
3.1 Introduction	56
3.2 Methods	59
3.2.1 Mice	59
3.2.1.1 <i>Sapap3</i> mice	59
3.2.1.2 <i>Slc1a1</i> -STOP mice	60
3.2.1.3 <i>Sapap3/Slc1a1</i> mice.....	60
3.2.2 Behavioral testing.....	61
3.2.2.1 Anxiety tests	61
3.2.2.1.1 Open field test	61
3.2.2.1.2 Elevated plus maze test.....	61
3.2.2.1.3 Light dark test	62
3.2.2.1.4 Grooming assessment.....	62
3.2.3 EAAT3i delivery.....	62
3.2.4 Western Blot	63
3.2.5 In situ.....	63

3.2.6 Statistical analysis	64
3.3 Results.....	65
3.4 Discussion	73
4.0 Conclusions.....	77
4.1 Dissertation background.....	77
4.2 Summary of findings	79
4.2.1 Chapter 2: EAAT3 overexpression increases susceptibility to the development of amphetamine-induced repetitive behaviors	79
4.2.2 Chapter 3: Examining the therapeutic potential of EAAT3 in the <i>Sapap3</i> - knockout mouse model of OCD	83
4.3 Grooming/ anxiety-like behaviors in <i>Slc1a1</i> -OE mice	85
4.4 Mechanisms of amphetamine-induced behaviors.....	87
4.5 Possible mechanisms underlying effect of EAAT3 on amphetamine-induced behavior and neural activity.....	88
4.6 Automated scoring of amphetamine-induced behavior	89
4.7 Future directions	90
Appendix A Supplemental Data	92
Bibliography	111

List of Tables

Table A-1 Table of statistics for two-way repeated measures analysis of cFos in striatal subregions.....	96
Table A-2 Correlation between stereotypy behavior and cFos expression in striatal subregions	97

List of Figures

Figure 1-1 The role of EAAT3 signaling at the glutamatergic synapse	17
Figure 2-1 <i>Slc1a1</i> -OE mice show increased EAAT3 protein expression that can be reversed by doxycycline administration	39
Figure 2-2 <i>Slc1a1</i> -OE mice show potentiated behavioral response to both low-dose and high-dose amphetamine.....	41
Figure 2-3 <i>Slc1a1</i> -OE mice show increased stereotypy behavior following amphetamine and increased cFos expression in the ventral striatum.....	43
Figure 2-4 Amphetamine increases cFos across striatal subcompartments.....	45
Figure 2-5 <i>Slc1a1</i> -OE mice show a potentiated response to amphetamine	48
Figure 2-6 <i>Slc1a1</i> -OE mice have show increased cFos in D1-neurons following high dose amphetamine.	50
Figure 2-7 Striatal subregion cFos expression in D1 and D2 neurons is significantly correlated with distinct behavioral responses to amphetamine	51
Figure 3-1 <i>Sapap3</i> -KO mice on a 129s background show a robust anxiety-like behavioral phenotype.....	67
Figure 3-2 Administration of an EAAT3 inhibitor does not normalize compulsive grooming behavior in <i>Sapap3</i> -KO mice	68
Figure 3-3 <i>Slc1a1</i> -STOP mice show ablated <i>Slc1a1</i> mRNA and EAAT3 protein expression	69
Figure 3-4 <i>Slc1a1</i> ablation does not rescue anxiety-like behavior in <i>Sapap3</i> -KO mice.....	72
Figure 3-5 <i>Slc1a1</i> ablation does not normalize grooming in <i>Sapap3</i> -KO mice	73

Figure A-1 <i>Slc1a1</i>-OE mice show no differences in grooming levels compared to controls	92
Figure A-2 Anxiety-like behavior in lifetime and adult-specific <i>Slc1a1</i>-OE mice	93
Figure A-3 <i>Slc1a1</i>-OE mice show no consistent anxiety-like behavioral phenotype	94
Figure A-4 Amphetamine significantly increases cFos in subregions throughout dorsal and ventral striatum	95
Figure A-5 Traces of B-SOID scored behavior, separated by genotype and drug treatment	99
Figure A-6 Pie charts of B-SOID scored behavior, separated by genotype and drug treatment	100
Figure A-7 Amphetamine increases overall cFos expression and D1 neuron cFos expression throughout the striatum and D2 neuron cFos in the NAc	101
Figure A-8 Amphetamine increases cFos in dorsal and ventral striatum	102
Figure A-9 Shank3-KO mice show increased grooming relative to WT mice, and this increased grooming is blunted by the administration of an EAAT3 inhibitor (EAAT3i, 30 mg/kg)	103
Figure A-10 <i>Sapap3</i>-KO mice show increased EAAT3 protein expression but no change in EAAT3 function	104
Figure A-11 <i>Sapap3</i> mice on C57Bl/6 background show an inconsistent anxiety-like phenotype	105
Figure A-12 <i>Sapap3</i>-KO mice on both C57Bl/6 and 129S background show lower levels of locomotion relative to <i>Sapap3</i>-WT mice	106
Figure A-13 Administration of an EAAT3 inhibitor blocks amphetamine-induced inhibition of midbrain dopamine firing rate	107

Figure A-14 *Slc1a1* mRNA expression in the whole mouse brain as measured by *in situ* hybridization histochemistry in *Slc1a1*-WT (A) and *Slc1a1*-STOP mice 110

Preface

This dissertation and the work completed throughout my time in graduate school would not have been possible without the help of countless mentors, collaborators, co-workers, friends, and family. I want to highlight first my advisor, Dr. Susanne Ahmari. Susanne is a phenomenal mentor, who taught me how to think about science in a truly translational way. Her passion and dedication to understanding the neurobiology of OCD and to using that understanding to help patients is genuinely inspiring. I have had many other great mentors throughout my time in graduate school, including my MSTP Career Advisor, Dr. Vishwajit Nimgaonkar, and the MSTP Program Director, Dr. Richard Steinman, both of whom have been tremendously supportive of me throughout this journey. I would like to thank the members of my committee who have guided me and helped shape this work, Dr. Tony Grace, Dr. Becky Seal, Dr. Mary Torregrossa, Dr. Nathan Urban, and my outside examiner, Dr. Chris Pittenger. I hope to continue these relationships throughout my career. I would also like to acknowledge mentors of mine from previous points in my life who encouraged me along this path, including Dr. Carolyn Thomas, Dr. Richard Lewis, Dr. Nicole Weekes, and Dr. Christopher Lowry.

There are too many people who helped with this work in the Ahmari Lab and the larger Pittsburgh neuroscience community for me to thank them all individually. However, without their help, this work would not have happened. I especially would like to thank my fellow graduate students in the lab, Dr. Zoe LaPalombara, Dr. Sean Piantadosi, and Dr. Victoria Corbit, who were with me in lab for most of my PhD and who helped with innumerable parts of this project. I have learned a tremendous amount from current and former Ahmari Lab post docs Dr. Lizzie Manning, Dr. James Hyde, Dr. Jesse Wood, and Dr. Britny Hildebrant. Perhaps no one in the lab has been

more instrumental in the day-to-day completion of this work than the Ahmari Lab manager, Dr. Jamie Pierson. Thank you all for all the help.

There are a variety of people who kept me grounded outside of lab and helped me maintain a work/life balance. These include my MSTP classmates Dr. Elliot Collins and Dr. Colleen Judge, and my former medical school classmates Drs. Lili and Patrick Polsunas, all of whom have enriched my life tremendously. Pittsburgh would not be the same without you. I would also like to thank my girlfriend and partner, Carmen Fernandez Fisac, who has been so much to me throughout the past few years, including my rock, my motivational speaker, and my Spanish/Matlab tutor. You have been so supportive of me through the good and the bad, and I am forever grateful to have you in my life and by my side. Thank you to our dog, Freddie, for being a very good boy. And lastly, I would like to thank my family. My parents, Steve and Laura, and my sisters Samantha and Nicole, have been unconditionally supporting and loving, and I could not have done this without you.

1.0 Introduction

1.1 Obsessive Compulsive Disorder

Obsessive Compulsive Disorder (OCD) is a debilitating neuropsychiatric disorder affecting 2-3% of the population worldwide (Kessler et al. 2005; Robins et al. 1984). It is characterized by obsessions, which are recurrent intrusive thoughts or urges, and compulsions, which are repetitive behaviors that are often stereotyped and excessive. These behaviors are voluntarily undertaken, but nonetheless difficult to control, and they may be performed to relieve the anxiety associated with unwanted obsessions (Pauls et al. 2014). There is tremendous heterogeneity within the diagnosis of OCD, not only in the manifestation of an individual's particular obsessions and compulsions, but also in the severity of the disorder. Common obsession/compulsion pairs include intrusive harm-related thoughts/checking and fear of contamination contamination/washing, although these are by no means the only symptom categories, and many patients show symptoms from more than one category (Robbins et al. 2019). OCD symptoms often present in childhood, and for many patients the disorder results in severe, lifelong disability (Ruscio et al. 2010). In many cases an individual's insight into the excessive or irrational nature of their compulsions is preserved, and the symptoms of OCD are sometimes referred to as ego-dystonic - that is, there is a mismatch between the patient's subjective goals and the intrusive thoughts that constitute the disorder. This can make the disorder incredibly difficult for both patients and clinicians alike, as it can prevent patients from seeking care or lead them to minimize their symptoms due to shame regarding the irrational nature of their obsessions (Fernandez et al. 2018).

1.1.1 Burden of OCD

The burden of OCD is high on both a societal and an individual level. Eaton et al. (2008) report that OCD costs \$10.6 billion per year in treatment, with an estimated \$40 billion in lost productivity in the US alone (DuPont et al. 1995). The worldwide prevalence of OCD is 50 million, reflecting a tremendous global economic burden of the disease (Koran 2000). Furthermore, individuals diagnosed with OCD experience a poorer quality of life, worse academic and job outcomes, and impairments in interpersonal relationships (Koran 2000; Koran et al. 2007). All of this combines to make individuals with OCD approximately 10 times more likely to die of suicide than the general population (Fernández de la Cruz et al. 2017). Improved treatment and access to treatment are clearly needed.

1.1.2 OCD Treatment

Current standard-of-care treatments for OCD include pharmacotherapies and psychotherapy. The first-line drug for OCD treatment is a serotonin-reuptake inhibitor (SRI) such as fluoxetine, often at a higher dose than used for depression or anxiety and with a longer treatment course required to see effects (Pittenger et al. 2005). This can result in significant side effects for a subset of patients (Del Casale et al. 2019). Cognitive behavioral therapy (CBT) with exposure response prevention has also been shown to be effective for some OCD patients (McKay et al. 2015). This involves exposing patients to stimuli that trigger their obsessions in a controlled, therapeutic environment while preventing them from engaging in their compulsions, and is thought to break the connection between obsessions and compulsions and allow patients to inhibit their compulsions in the future (Pence et al. 2010). While these treatments are helpful for many patients

with OCD, they are not effective in up to 50% of patients, they are not curative, they are not accessible for all patients (especially CBT), and many patients continue to suffer from significant impairments despite an improvement in symptoms with treatment (Hirschtritt et al. 2017). These therapies have been the mainstay of OCD treatment for the past 3 decades, and newer treatments are clearly needed. However, a lack of understanding of the etiology and underlying neurobiology of the disorder have hampered the development of novel OCD treatments.

1.1.3 Neurobiology of OCD

A considerable body of neuroimaging work has served to delineate the structural and functional underpinnings of OCD. While there is much debate about, and ongoing work investigating, the exact nature of the brain changes seen in OCD, there is a consensus that alterations in cortico-striatal-thalamo-cortical (CSTC) circuits are at least partly responsible for the symptomatology of the disorder. This model, also known as the frontostriatal or corticostriatal model of OCD, is based on structural and functional alterations in various nodes of classical cortico-basal ganglia loops (Alexander et al. 1986; Alexander et al. 1990). These “loops” refer to segregated sensorimotor, associative, and limbic regions of the basal ganglia that are thought to be involved in motor, cognitive, and emotional aspects of behavior, respectively (Milardi et al. 2019). Early studies in OCD patients found alterations in the orbitofrontal cortex (OFC), anterior cingulate cortex (ACC) and caudate nucleus in OCD patients relative to controls, all crucial nodes of the CSTC circuit.

1.1.3.1 Structural studies

Early computerized tomography (CT) and magnetic resonance imaging (MRI) studies showed a decrease in the volume of the caudate nucleus in OCD patients compared to healthy controls and controls with other psychiatric disorders (Parmar and Sarkar 2016). More recent voxel-based morphometry studies have explored the whole brain for candidate regions and found a reduction in gray matter in a variety of cortical areas including the OFC and ACC (de Wit et al. 2014; Pujol et al. 2004). Subsequent studies and meta-analyses have largely replicated these results as well as implicated structural changes in a variety of other regions in OCD, with differences between study findings likely attributable to medication status, psychiatric comorbidities, sample heterogeneity, small sample sizes, or differences in imaging technique or analysis approach (de Wit et al. 2014; Radua and Mataix-Cols 2009; van den Heuvel et al. 2009).

1.1.3.2 Functional Studies

In addition to these structural imaging studies, functional neuroimaging has provided us with tremendous insight into the neurobiology underlying OCD. Similar to the structural studies, functional studies also have implicated regions of the CSTC circuit, with positron emission tomography (PET) studies showing an increase in glucose metabolism in OFC and caudate nucleus of OCD patients compared to controls (Baxter et al. 1987; Baxter et al. 1988; Nordahl et al. 1989). This increased activity is seen in OCD patients at baseline, has been found to be normalized by effective treatment, and in some cases has been shown to correlate with OCD symptom severity (Baxter et al. 1992). A similar pattern has been shown in both PET and functional magnetic resonance imaging (fMRI) studies of symptom provocation. By-and-large, these studies show increased activity of OFC and caudate nucleus when individuals are shown symptom-triggering images specific to their subtype of OCD— for example, an individual with contamination/washing

OCD being shown images of garbage or dirt. In contrast to the results seen during symptom provocation, fMRI studies during cognitive tasks such as reversal learning or inhibitory control have shown a decrease in OFC activation, indicating that dysfunction of this region may be domain-specific in OCD (Chamberlain et al. 2008). Further evidence for a causal role for abnormal CSTC circuitry in OCD comes from work in animal models of compulsive behavior (see 1.5 Models of repetitive behavior section below).

1.1.3.3 Neural Networks in OCD

More recent work has added nuance to this model of CSTC circuit dysfunction and implicated other regions, both within the basal ganglia and throughout the brain. While early imaging studies have mostly implicated regions of the caudate nucleus (or dorsal striatum), more recent work also has implicated more ventral regions of the striatum in OCD as well. The nucleus accumbens (NAc) and adjacent ventral capsule has been a successful target of deep brain stimulation (DBS) for OCD (Denys et al. 2010). This region receives a large cortical projection from the ACC, which has been implicated in OCD in imaging studies and which has also been a successful surgical target for the treatment of refractory OCD (Dougherty et al. 2002). Recent resting state fMRI approaches have shown reduced functional connectivity between OFC and caudate and increased functional connectivity of the ventral striatum, again reinforcing the involvement of more distributed CSTC circuits in the disorder (Harrison et al. 2009; Vaghi et al. 2017). The role of these more traditionally “emotional” regions of extended CSTC circuitry in OCD is supported by evidence that OCD is at least partially a disease in which the normal process of behavioral selection is corrupted by dysregulated emotional states (Wood and Ahmari 2015). Furthermore, a recent mega-analysis implicated structural changes in a variety of cortical regions, including the ACC, the prefrontal cortex, the temporal lobe, parietal cortex, and cerebellum

(Fouche et al. 2017). At least some of this broad neural involvement might be due to different subtypes of the disorder (Morein-Zamir et al. 2014; van den Heuvel et al. 2009). Indeed, OCD may be a disorder that has CSTC circuit dysfunction at its core, but with abnormalities within other circuits determining which specific symptoms of OCD are expressed.

1.1.4 Genetics of OCD

1.1.4.1 Twin and Family Studies

While the cause of OCD is unknown, a significant body of evidence from twin and family studies has revealed a role for genetic susceptibility in the etiology of OCD. Studies examining the concordance rate of OCD in monozygotic twins and comparing this to the rate in dizygotic twins allows researchers to get a crude sense of the genetic contribution to the risk of OCD. Twin studies place the heritability of adult-onset OCD at 27-47% and pediatric-onset OCD at 45-65% (Grados and Wilcox 2007; Pauls 2008; van Grootheest et al. 2005). Family studies have supported these results and found strong evidence that at least some cases of OCD are familial. Many family studies have found a significantly increased risk of OCD in family members of affected individuals, with a meta-analysis of five OCD family studies estimating $OR = 4.0$ (95% CI =2.2-7.1) (Hettema et al. 2001), indicating that the risk for relatives of an OCD proband was ~8.2%, significantly greater than a risk of ~2.0% for control relatives. More recent population-based studies have similarly reported odds ratios of 4-6 for first-degree relatives of OCD patients with some evidence for increased heritability in early-onset OCD (Mataix-Cols et al. 2013; Steinhausen et al. 2013). Family studies also show that relatives of OCD probands have an increased risk of other OCD-spectrum disorders as well, such as tic disorders, grooming disorders, body dysmorphic disorder, and somatoform disorders (Bienvenu et al. 2000; Grados et al. 2001).

1.1.4.2 Association studies

Given the heritable nature of the disorder, researchers have spent the last several decades searching for individual genes that may contribute to OCD risk. Initial studies focused on serotonin-system genes, as the most effective drugs for OCD are serotonin reuptake inhibitors. Many of these candidate gene studies have shown association of OCD with one or more single nucleotide polymorphisms (SNPs) of serotonin system genes (Taylor 2013), as well as other candidate genes related to the dopaminergic system (Goodman et al. 1990) and neuropeptide systems (McDougle et al. 1999). A meta-analysis found significant association between OCD and alleles of the serotonin transporter (*5-HTTLPR*) and a serotonin receptor gene (*HTR2A*), and an association in males between OCD and alleles of *COMT* and *MAOA*, both genes involved in dopamine metabolism (Taylor 2013). However, none of these candidates has proved to reliably replicable, and none has reached genome-wide significance in GWAS studies (see 1.1.4.4 Genome-wide association studies below).

1.1.4.3 Glutamate Genetics in OCD

The most fruitful source of information regarding the genetic underpinnings of OCD has come from investigation of the glutamate system (Fernandez et al. 2018; Rajendram et al. 2017). The role of glutamate in OCD was first based on imaging and other biological evidence rather than genetic studies per se (See 1.4 Glutamate in OCD section below). Multiple lines of evidence have implicated glutamate-related genes, including the glutamate transporter gene *SLC1A1* and the *SAPAP/DLGAP* family of scaffolding genes.

1.1.4.3.1 SLC1A1 in OCD

Initial linkage studies of OCD identified suggestive linkage to chromosome 9p24 (Hanna, Veenstra-VanderWeele, et al. 2002), a result which was replicated in a subsequent study (Willour et al. 2004). This chromosomal region contains the gene *SLC1A1* (Solute Carrier, Family 1, member 1) which encodes the neuronal glutamate transporter, EAAT3. Multiple association studies since then have identified association of various polymorphisms of *SLC1A1* with OCD and with antipsychotic-induced compulsions (Arnold et al. 2006; Cai et al. 2013; Dickel et al. 2006; Samuels et al. 2011; Shugart et al. 2009; Stewart et al. 2007; Veenstra-VanderWeele et al. 2012; Wendland et al. 2009). Most of these polymorphisms cluster in the 3' region of the gene, with the rs301430 polymorphism being the one most commonly implicated in OCD. This gene has been the primary candidate for association with OCD for many years, due to the number of studies implicating polymorphisms of this gene with OCD, although a meta-analysis failed to find significant association of any individual *SLC1A1* allele with the disorder (Stewart, Mayerfeld, et al. 2013), likely due to the low sample size for each individual polymorphism.

1.1.4.3.2 SAPAP/DLGAP in OCD

The first evidence for the role of *SAPAP/DLGAP* in OCD came from a mouse model of compulsive behavior (Welch et al. 2007). Mice with genetic deletion of *Sapap3* show compulsive grooming behavior and increased anxiety-like behavior (see 1.5 Animal models of repetitive behavior section below). *Sapap3* is a member of the SAPAP (or DLGAP in humans) family of proteins, membrane-associated guanylate kinases that interact with other proteins to form scaffolding complexes within the postsynaptic density of excitatory (glutamatergic) synapses and regulate neurotransmission (Rasmussen et al. 2017). *DLGAP3*, the human homolog of *Sapap3*, has been associated with disorders of compulsivity such as Tourette's syndrome (Crane et al. 2011)

and grooming disorders such as trichotillomania and pathologic nail biting or pathologic skin picking (Bienvenu et al. 2009). Another study found multiple rare *DLGAP3* missense variants that had higher prevalence in trichotillomania and OCD relative to controls. In addition, two SNPs of *DLGAP1*, a different member of this gene family, were identified as having low p-values in the first genome-wide association study of OCD, although they did not reach genome wide significance (Mattheisen et al. 2015).

1.1.4.4 Genome-wide association studies in OCD

Despite the plethora of candidate gene association studies in OCD and other psychiatric disorders, there are significant limitations to this approach. Most psychiatric disorders, including OCD, are polygenic by nature, with few cases having a gene with large effect size. Therefore, the sample sizes of these association studies are likely too small to detect most of these small effect-size genes. Furthermore, the genes chosen for association studies are necessarily chosen *a priori*, based on biological and/or linkage studies. Given the enormous number of SNPs within the human genome and our nascent understanding of the biology of OCD, the probability of choosing a correct gene, and the correct SNP within that gene, is low. Furthermore, candidate gene studies are susceptible to false positives due, among other things, to differences in background ancestry, and therefore SNP frequency, between cases and controls (Fernandez et al. 2018). Due to these weaknesses, as well as improved and cheaper sequencing technologies, researchers have increasingly turned from candidate gene studies to genome wide association studies (GWAS).

To date, two consortiums have undertaken GWAS studies of OCD (Mattheisen et al. 2015; Stewart, Yu, et al. 2013). Neither of these studies has found hits that reached genome-wide significance. However, there is reason to think that these studies are underpowered, as both studies combined have only 2688 patients, which is likely smaller than the number of subjects needed to

detect genes of small effect size, as we learned from GWAS studies of schizophrenia, which needed 36989 cases and 113075 controls in order to find 108 significant risk genes (Schizophrenia Working Group of the Psychiatric Genomics Consortium 2014). Furthermore, a comparison of the SNPs with the lowest p values (i.e. closest to being “hits”) shows significant overlap between the two studies (Stewart, Mayerfeld, et al. 2013), giving hope that increasing sample size will lead to reliable genetic findings in OCD. Some of the strongest signals from these studies include: *DLGAPI* (the homolog of *Sapap3* in mice), mentioned above; a SNP near the gene *BTBD3*, a protein involved in dendritic plasticity, which achieved significance in an analysis that only included trios; a SNP near the gene *FAIM2*, a protein involved in intracellular signaling; and a SNP near *PTPRD*, a protein involved in the differentiation of glutamatergic and GABAergic synapses. More research is needed, particularly in the form of larger GWAS studies, to definitively say whether *SLC1A1* or any other specific gene is associated with increased risk of OCD.

1.2 Glutamate system

Glutamate is the primary excitatory neurotransmitter in the brain, comprising ~40% of all CNS neurotransmission (Zhou and Danbolt 2014). It has broad importance in brain functions including behavior, cognition, learning, and memory, and the glutamate system is highly conserved across evolution (Greer et al. 2017). Perhaps unsurprisingly due to its importance in normal brain function, alterations in the glutamate system have been implicated in a variety of psychiatric and neurological conditions. Glutamate is packaged into synaptic vesicles within axon terminals by proteins known as vesicular glutamate transporters (VGLUTs), a process that is dependent on the proton electrochemical gradient (Shigeri et al. 2004). It is released in a Ca^{2+}

dependent process of vesicle fusion following the arrival of a propagating axon potential at the terminal. Following release from a presynaptic neuron, glutamate acts on the post-synaptic neuron by binding to a variety of receptors (e.g. ionotropic and metabotropic), which results in depolarization of the postsynaptic neuron. Because of its potent excitatory effects, excess glutamate has the potential to cause excitotoxic cell damage and death. Therefore, regulation of Glu at the synapse and termination of its signaling are of vital importance to maintain both the health of the brain and information flow within neural circuits. As there are no extracellular enzymes that degrade glutamate, reuptake mechanisms are responsible for maintaining appropriate concentrations of glutamate at the synapse (Danbolt et al. 2016).

1.2.1 Glutamate receptors

Molecular cloning has identified several different families of glutamate receptors (Hollmann and Heinemann 1994; Nakanishi 1992; Ozawa et al. 1998; Sommer et al. 1992). One of these families was found to be activated by the glutamate analogue N-methyl-D-aspartate (NMDA) and was therefore coined as the NMDA-receptor family (Monyer et al. 1992). These are ionotropic receptors that are composed of a combination of structurally distinct subunits (NR1, NR2A, NR2B, and NR2B), the pattern of which varies by brain region. The second class of receptor is activated by alpha-amino-3-hydroxy-5-methyl-4-isoxazole propionic acid (AMPA) and is known as AMPA-receptors (Borges and Dingledine 1998). These receptors are similarly ionotropic, but have very different activation profiles and dynamics, resulting in differing effects on response in the postsynaptic cell. Both AMPA-receptors and NMDA-receptors are critical for long term potentiation (LTP), a mechanism of synaptic strengthening thought to underly much learning and memory within the CNS. In LTP, activation of NMDA-receptors results in an influx

of Ca^{2+} and activation of CaMKII, which results in increased trafficking of AMPA receptors to the cell surface and increased response to subsequent stimulation of the cell (Herring and Nicoll 2016). Kainate receptors are a third class of ionotropic glutamate receptors identified initially by their response to the drug kainate. Kainate receptors have limited distribution in the brain relative to AMPA- and NMDA-receptors, and their role is less well defined. AMPA and kainate receptors respond to most of the same agonists/antagonists, and are therefore sometimes referred to as non-NMDA receptors, despite cloning studies which indicate that they are distinct receptor families (Ozawa et al. 1998). The ionotropic glutamate receptors are cation channels that allow for the influx of either Na^+ exclusively or Na^+ and Ca^{2+} upon binding by glutamate (or another antagonist). AMPA and Kainate receptors have quick activation profiles, but desensitize quickly, while NMDA receptors require depolarized membrane potential and binding by the co-agonist, glycine, for activation, but then desensitize more slowly (Traynelis et al. 2010)

Metabotropic glutamate receptors (mGluR1-8) are a superfamily of G-protein coupled receptors that mediate the slower effects of glutamate (Nakanishi et al. 1994) These receptors couple to GTP-binding proteins and modulate the production of intracellular messengers. mGluRs can be classified into three distinct subtypes: Group I-III. Group I receptors, which include mGluR1 and mGluR5, couple to $G_{q/11}$ and stimulate polyphosphoinositide hydrolysis. These receptors are located perisynaptically to postsynaptic specializations of glutamatergic synapses. Group II receptors, which include mGluR2 and mGluR3, and Group III receptors, which include mGluR4, mGluR6, mGluR7, and mGluR8, are both coupled to $G_{i/o}$ and inhibit the cyclic adenosine monophosphate. These two groups represent the classical inhibitory autoreceptor mechanism suppressing excess transmitter release from presynaptic glutamatergic terminals (Niswender and Conn 2010).

1.2.2 Glutamate transporters

The reuptake of glutamate following release and receptor activation is largely accomplished by a class of transmembrane transport proteins known as excitatory amino acid transporters (EAATs). There are five known EAATs, which share 35-65% amino acid homology and have some basic properties in common (Amara and Fontana 2002). However, each receptor has unique distinct cellular and development expression profiles, pharmacology, and roles in glutamatergic signaling (Shigeri et al. 2004). The EAATs are secondary active transporters, which translocate $1H^+$, $3NA^+$, and counter-transport $1K^+$ for each substrate molecule. This co-transport provides the energetic driving force to transport glutamate against a thousand-fold concentration gradient (Nicholls and Attwell 1990; Zerangue and Kavanaugh 1996). EAATs are homotrimers with non-covalent connections between the subunits. They have 8-10 transmembrane helices with intracellular N- and C-termini (Bjørn-Yoshimoto and Underhill 2016).

An overview of each of these five receptors will be given here, with additional information given about EAAT3 later, as it is the focus of this dissertation. EAAT1, also known as the glutamate/aspartate transporter (GLAST), is expressed in astrocytes throughout the brain. In the retina it is the primary glutamate transporter (Lehre et al. 1995). EAAT1 knockout mice develop normally, but they exhibit impaired glutamate homeostasis and altered behavior in adulthood. EAAT2, also known as glutamate transporter 1 (GLT-1), is responsible for the bulk (95%) of glutamate uptake within the CNS. Because of this, it is considered to be the only glutamate transporter necessary for viability, and indeed, EAAT2-knockout mice have ~50% mortality by 1 month of age, showing increased susceptibility to seizures and blunted growth prior (Tanaka et al. 1997). EAAT2 is located primarily on astrocytes, although it appears to be expressed at lower levels in neurons as well (Lehre and Danbolt 1998). EAAT4 is localized primarily to the dendrites

of Purkinje cells in the cerebellum, and EAAT4-knockout mice show no overt phenotypes (Dehnes et al. 1998; Fairman et al. 1995; Huang et al. 2004). The role of EAAT5 is less well known, as there does not exist an EAAT5-knockout mouse, but it has been reported that EAAT5 is preferentially expressed in the retina (Arriza et al. 1997; Eliasof et al. 1998).

1.3 EAAT3

1.3.1 Localization

EAAT3 (also known as excitatory amino acid carrier-1, or EAAC1) is expressed throughout the mature brain, with enrichment in the basal ganglia, cortex, hippocampus, and cerebellum (Holmseth et al. 2012). It is also expressed outside the CNS, where it appears to be the primary glutamate and aspartate transporter in many tissue types including intestine, kidneys, liver, heart, and skeletal muscle (Bjørn-Yoshimoto and Underhill 2016; Kanai and Hediger 1992; Velaz-Faircloth et al. 1996). Within the CNS, EAAT3 is located on neurons. Early reports of EAAT3 showed expression in astrocytes and oligodendrocytes as well (Conti et al. 1998; Kugler and Schmitt 1999), reports that seemed to be confirmed with more recent studies of EAAT3 expression in astrocytic cell cultures (DeSilva et al. 2009; Liang et al. 2014). In the case of initial studies, these are likely spurious results due to non-specific antibody binding, which is common as antibodies to EAAT3 are notoriously nonspecific and rigorous controls were not used (Holmseth et al. 2006). The more recent reports of EAAT3 expression in cultured glia are likely a result of the technique used and not likely to reflect *in vivo* expression of EAAT3. Indeed, the most rigorous study of EAAT3 expression that used EAAT3-knockout mice as controls found no detectible

EAAT3 in astrocytes or oligodendrocytes of mature rat brains (Holmseth et al. 2012). Within the plasma membrane, EAAT3 is localized primarily to the peri-synaptic area of postsynaptic neurons, with a substantial portion EAAT3 located intracellularly under basal conditions, and very little if any located presynaptically on axon terminals (Danbolt et al. 2016; Holmseth et al. 2012). Indeed, there appears to be a sequence on the c-terminus of EAAT3 that restricts its expression to the dendritic compartment, at least in hippocampal neurons (Cheng et al. 2002).

1.3.2 Function

Canonically, EAAT3 has three roles at the synapse, shown in Figure 1-1 (Wadiche et al. 1995). EAAT3 1) modulates peri-synaptic glutamate concentration and reduces activation of NMDA and metabotropic glutamate receptors by competing for free glutamate (Diamond and Jahr 1997; Grewer et al. 2000); 2) takes up glutamate for the synthesis of GABA in postsynaptic cells (Mathews and Diamond 2003); and 3) takes up cysteine for the synthesis of the antioxidant glutathione (Aoyama et al. 2006). These are not the only roles that have been suggested for EAAT3, but they are the ones best supported by the body of available evidence.

The localization of EAAT3 postsynaptically, as well as its ~100 fold lower levels of expression compared to EAAT2, indicates that it is not primarily responsible for the recycling of glutamate. Indeed this role is performed primarily by EAAT2 on astrocytes, which convert glutamate to glutamine before shuttling it back into to the presynaptic neuron for re-synthesis into glutamate (Albrecht et al. 2010). Furthermore, there is evidence that EAAT3 has a role in regulating the concentration of glutamate near receptors, rather than bulk clearance of glutamate. Indeed, disruption of EAAT3 appears to affect both AMPA and NMDA receptor currents (Jarzylo and Man 2012; Li et al. 2017; Scimemi et al. 2009; Underhill et al. 2014). NMDARs have been

shown to respond to non-locally released glutamate spillover at peri-synaptic sites, and experiments in rat hippocampal slices indicate that EAAT3 regulates this spillover-dependent activation (Diamond 2001; Scimemi et al. 2004). This regulation may be dependent on EAAT3 trafficking; as mentioned above, a large pool of EAAT3 protein is located intracellularly, available for insertion into the plasma membrane. Depolarization of the plasma membrane due to high frequency stimulation has been shown to inhibit EAAT3 transport to the membrane, which could allow for increased NMDA-receptor activation and promote long term potentiation, a form of neural plasticity (Diamond 2001). EAAT3 activity has also been shown to regulate AMPA-receptors. Blocking EAAT3 activity in the hippocampus was shown to activate peri-synaptic NR2B-containing NMDA-receptors, leading to a reduction in GluR1- and GluR2-containing AMPARs (Scimemi et al. 2004).

EAAT3 has also been shown to be important for the synthesis of GABA. In the hippocampus, blockage of EAAT3 results in a decrease in the amount of GABA available in post-synaptic cells and a subsequent reduction in inhibitory currents (Mathews and Diamond 2003; Sepkuty et al. 2002). In addition to facilitating the uptake of glutamate, EAAT3 is also at least partially responsible for the uptake of cysteine into neurons. Cysteine is a precursor for glutathione, an important antioxidant involved in protecting neurons from free radicals. Neurons from EAAT3-knockout mice are more sensitive to oxidative stress induced by H₂O₂ (Aoyama et al. 2006; Berman et al. 2011; Choi et al. 2014). Older EAAT3-knockout mice were shown to have signs of oxidative stress, including cortical thinning and ventricular enlargement, and have decreased performance on the Morris water maze. These phenotypes can be reversed by administering *N*-acetylcysteine, a precursor to glutathione that bypasses the need for cysteine (Aoyama et al. 2006; Cao et al. 2012).

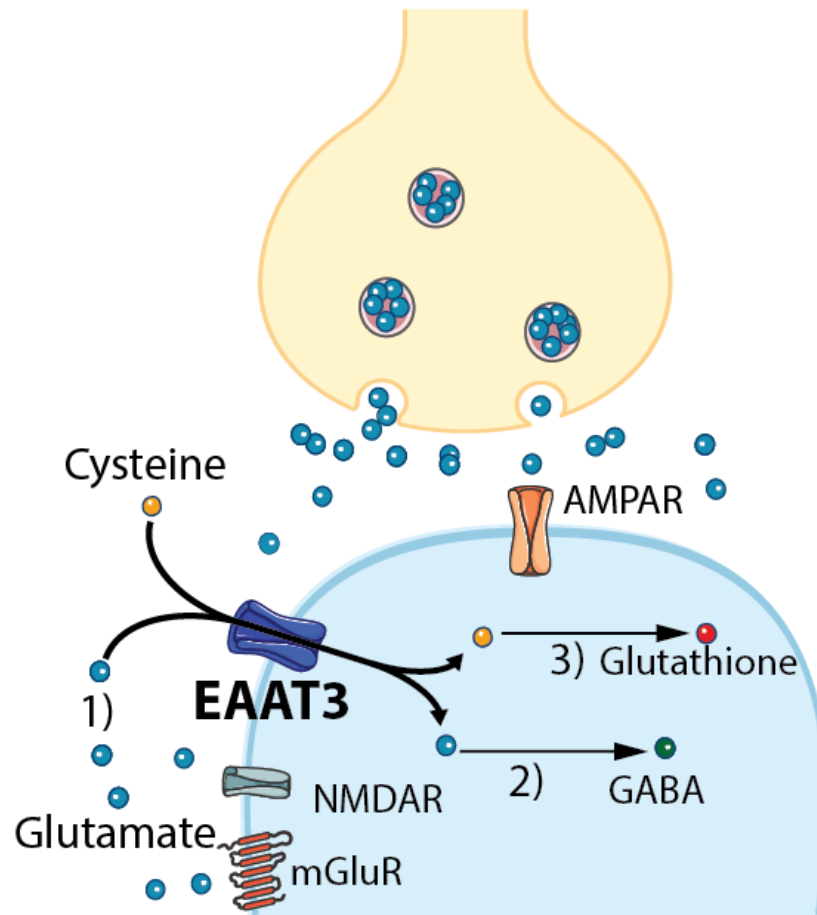


Figure 1-1 The role of EAAT3 signaling at the glutamatergic synapse

At the synapse, EAAT3 has 3 canonical roles: 1) modulates glutamate concentrations around peri-synaptic receptors, 2) provides glutamate as a substrate for GABA synthesis, and 3) provides cysteine as a substrate for glutathione synthesis

1.3.3 EAAT3 in Disease

EAAT3 has been implicated in several human diseases. The most concrete link is between EAAT3 deletion and dicarboxylic aminoaciduria. Three individuals have been described in the

literature with complete loss of EAAT3 function (Bailey et al. 2011), two siblings with a missense SNP variant and one individual with a 3 base pair exonic deletion of the *SLC1A1* gene. These individuals all showed increased glutamate and aspartate in the urine, likely due to the lack of EAAT3 in the kidney, where it is responsible for the reuptake of these amino acids from the glomerular filtrate. Two of these individuals had a history of kidney stones, and one of them had a history of compulsive-like behavior, although a full psychiatric history was not available (Bailey et al. 2011). EAAT3 knockout mice also develop dicarboxylic aminoaciduria, further supporting this connection (Peghini et al. 1997).

Post-mortem studies of schizophrenia have shown some alterations in EAAT3 transcripts (Hu et al. 2015; McCullumsmith and Meador-Woodruff 2002). Furthermore, deletion of the promoter region and first exon of *SLC1A1* was identified in a Paluan family with multiple generations affected by schizophrenia or schizoaffective disorder (Myles-Worsley et al. 2013). An *SLC1A1* SNP was identified in a case-control study of schizophrenia with nested replication (Horiuchi et al. 2012). However, this gene was associated with increased *SLC1A1* expression. Furthermore, this SNP (or any other *SLC1A1* SNP) has not been identified in GWAS studies of schizophrenia (Pardiñas et al. 2018). As such, the role of *SLC1A1*/EAAT3 in schizophrenia remains unclear.

As mentioned above, *SLC1A1* is the most commonly-associated OCD gene. Furthermore, the most commonly-associated polymorphism of this gene is the rs301430 allele (Veenstra-VanderWeele et al. 2012). Importantly, this polymorphism increases expression of the encoded protein, the neuronal glutamate transporter excitatory amino acid transporter-3 (EAAT3). The OCD-linked C allele is associated with increased *SLC1A1* expression in lymphoblastoid cells, human postmortem brain, a luciferase reporter assay, and transfected HEK cells, where there is

also a functional increase in EAAT3 protein as evidenced by increased glutamate uptake (Veenstra-VanderWeele et al., 2012; Wendland et al., 2009). This suggests that OCD susceptibility may result from increased *SLC1A1* expression, and that reducing levels of EAAT3 may be protective against the development of OCD.

1.4 Glutamate in OCD

In addition to the genetic evidence discussed above for a role of glutamate in OCD, there are several other lines of evidence tying abnormalities in the glutamatergic system to OCD (Pittenger et al. 2011). Two studies have shown increased glutamate in the cerebrospinal fluid of unmedicated OCD patients (Chakrabarty et al. 2005). Magnetic resonance spectroscopy (MRS) studies complement these results and provide some regional specificity. MRS studies in OCD to date have used low magnetic field strengths which are unable to distinguish between glutamate and glutamine. Therefore, they present results of a composite measure of both molecules known as Glx. Glx is often interpreted as glutamate, but it is important to note that they are different signals, with some recent evidence that the ratio of glutamate/glutamine may be important in psychiatric disorders (Yüksel and Öngür 2010). Early MRS studies reported increased Glx in caudate in a sample of 11 pediatric patients (Bolton et al. 2001), an increase that was reversed with successful treatment with paroxetine. Studies in adults have shown decreased Glx in OCD patients (Rosenberg et al. 2004). Other studies have failed to find a clear relationship between Glx signal and OCD (Bartha et al. 1998; Starck et al. 2008; Whiteside et al. 2006), and larger sample sizes are likely needed to define clearly the relationship between OCD and glutamate concentration in various brain regions. A recent study of post-mortem human brain samples pointed to widespread

alterations in the glutamatergic system of OCD patients compared to matched controls (Piantadosi et al. 2019). Specifically, this study found a reduction in transcripts encoding proteins related to excitatory synaptic structure and function in OFC of OCD subjects relative to controls. This finding was at least somewhat specific, as they found minimal evidence for differences in transcripts related to inhibitory synaptic structure.

Lastly, several drugs affecting the glutamatergic system have shown promise in treating OCD patients (Marinova et al. 2017; Pittenger 2015). The mechanism of these drugs is disparate, and some appear to target the same pathway in opposite directions. That two drugs with opposing mechanisms have been proposed as treatments for the same disorder supports the fact that we have much to learn about the role of glutamate in OCD. These drugs have been proposed as adjunctive therapies in combination with psychotherapy or as a second-line treatment for individuals who do not respond to SRIs. Riluzole, a drug approved for the treatment of amyotrophic lateral sclerosis, inhibits glutamate release and reuptake by astrocytes. Results from riluzole trials have been mixed, with one study showing no effects on treatment-resistant OCD in children (Grant et al. 2014), another study showing a trend toward statistically significant effects in treatment-resistant adults (Pittenger et al. 2015), and one study showing efficacy in adults (Emamzadehfard et al. 2016). N-acetylcysteine (NAC), an antioxidant and precursor to cysteine, modulates the cystine-glutamate transporter and is used clinically for the treatment of acetaminophen overdose. Results from trials of NAC have been promising, with some showing an improvement in Y-BOCS scores in the NAC group (Afshar et al. 2012; Paydary et al. 2016), and some showing no benefit overall, but improvement in specific symptom domains such as compulsions (Sarris et al. 2015) or anxiety (Costa et al. 2017). Memantine, an uncompetitive NMDA receptor antagonist that is approved for treatment of Alzheimer's disease, has been used in several trials of OCD patients with promising

results from two randomized clinical trials showing symptom reduction in OCD patients (Ghaleiha et al. 2013). Ketamine, a non-competitive NMDA receptor antagonist has recently shown tremendous promise for the treatment of severe depression and has been suggested as a possible treatment for OCD (Bloch et al. 2012; Rodriguez, Levinson, et al. 2016; Rodriguez, Wheaton, et al. 2016), although larger randomized controlled trials are needed. Several other compounds with glutamatergic activity have been suggested as OCD therapeutics, including glycine (an NMDA receptor co-agonist), sarcosine (an inhibitor of the glycine transporter-1), and D-cycloserine (a partial NMDA receptor co-agonist). While early investigation into the potential of these compounds to treat OCD has been promising, many of the studies are small and are designed to utilize these compounds as adjuvants to the treatments patients are currently receiving (most commonly SRIs). As such, it remains to be seen whether they will usher in a new class of first-line OCD treatments.

1.5 Models of repetitive behavior

Pathological repetitive behavior is found in variety of psychiatric and neurological disorders, including OCD, autism, Tourette syndrome, substance abuse, schizophrenia, Parkinson's disease, and dementias (Lewis and Kim 2009). Repetitive behavior refers to a broad class of actions, characterized by their repetition, rigidity or inflexibility, and lack of obvious function. They can vary from lower-order sensory-motor behaviors to higher-order insistence on sameness or resistance to change. Studies of neural circuitry in different psychiatric disorders have found CSTC circuit abnormalities related specifically to repetitive behavior across diagnoses, indicating potentially shared neural mechanisms despite wide differences in the exact nature of

repetitive behavior exhibited (Muehlmann and Lewis 2012). There are many models of repetitive behavior, often found within broader models of a psychiatric or neurological disorder. Here I will discuss several genetic, circuit, and pharmacological manipulations that result in repetitive behavior in mouse models.

1.5.1 Genetic models of repetitive behavior

Repetitive behavioral phenotypes have been observed in a variety of mutant mouse models. As mentioned above, mice with global knockout of *Sapap3* display increased repetitive grooming behavior that leads to severe lesions (Welch et al. 2007). In addition, these mice show increased anxiety-like behaviors and abnormalities in reversal learning (Manning et al. 2019). The overgrooming and anxiety-like phenotypes in these mice can both be reversed with a chronic, but not acute, course of fluoxetine, similar to the course required for the treatment of human OCD. This phenotype was localized to the striatum, as rescue of striatal *Sapap3* expression reversed both the overgrooming and anxiety-like behavior phenotypes. Further work has implicated cortico-striatal, rather than cortico-thalamic synapses in this phenotype (Wan et al. 2014), and shown that strength of specific M2-striatal projections seem to be increased in these mice (Corbit et al. 2019).

Repetitive overgrooming has been observed in several other mutant mouse lines. These include *Slitrk5*-KO mice. SLITRKs are transmembrane proteins located throughout the brain that appear to direct neurite outgrowth, and rare variants of this family have been associated with Tourette syndrome (Abelson et al. 2005). Similar to *Sapap3*-KO mice, *Slitrk5*-KO mice display compulsive grooming resulting in lesions and anxiety-like behavior, both of which can be reversed with chronic SRI administration (Shmelkov et al. 2010). These mice also show abnormalities of

CSTC circuitry, including increased activity (measured by FosB immunoreactivity) in the OFC and altered signaling at striatal synapses.

Genetic models related to autism spectrum disorders display a range of repetitive behaviors (Bey and Jiang 2014). These include syndromic models with defined somatic abnormalities as well as a variety of neurobehavioral phenotypes. Examples include mutations in MeCP2, observed in Rett syndrome patients, that result in repetitive forelimb movements; mutations in FMR1, observed in Fragile X Syndrome, that result in compulsive grooming; and mutations in SNC1A, observed in Dravet Syndrome, that result in repetitive circling (Bhakar et al. 2012; Han et al. 2012; Shahbazian et al. 2002). The most well-studied genes in non-syndromic autism are the *SHANK* gene family. SHANK proteins are master scaffold proteins, and SHANK1-3 have been strongly implicated in autism from human genetic studies (Jiang and Ehlers 2013). SHANK3 is the most well-characterized of these genes, and *Shank3*-KO mice show a robust over-grooming phenotype (Kouser et al. 2013).

1.5.2 Circuit models of repetitive behavior

A recent model of OCD-relevant behavior used optogenetic activation of a cortico-striatal circuit to induce increased grooming in mice (Ahmari et al. 2013). Repeated, but not acute, photoactivation of a circuit from the medial OFC (mOFC) to the ventromedial striatum (VMS) over the course of several days was sufficient to induce progressive overgrooming in wildtype mice. This overgrooming lasted for 2 weeks following cessation of stimulation and was reversible with a chronic course of fluoxetine. Overgrooming was correlated with a potentiation of mOFC to VMS evoked firing rate, which was also normalized with chronic fluoxetine.

In addition, mice with Tropomyosin receptor kinase B (TrkB) receptor deletion specifically in direct-pathway D1-expressing neurons show repetitive rotations and head-tic behaviors (Engeln et al. 2020). This phenotype appears to be dependent upon excessive activation of these direct-pathway neurons, as chemogenetic inhibition of striatal D1 neurons reverses the repetitive behavioral phenotype. This phenotype is only partially penetrant, and examination of D1-neuron gene expression and cell morphology in the mice exhibiting repetitive behaviors revealed broad changes in neuronal projection and synaptic structure genes as well as dendritic spine loss and dendritic atrophy, indicating that alterations in D1 striatal neurons can result in expression of a repetitive behavioral phenotypes.

D1 cholera toxin (D1CT) mice were engineered to express intracellular cholera toxin in D1+ neurons in the piriform cortex layer II, somatosensory cortex layers II-III, and the intercalated nucleus on the amygdala (Campbell et al. 1999). Cholera toxin is a neuropotentiating enzyme that activates stimulatory G-protein signal transduction in these neurons. D1CT mice have a variety of behavioral abnormalities, including repetition of a normal behaviors and expression of novel repetitive leaping behavior and nonaggressive biting of siblings. This model highlights the wider circuits that are potentially involved in the generation of repetitive behavior, as well as the diversity of behaviors in mouse models that can potentially be labeled as repetitive.

1.5.3 Drug induced repetitive behavior

The most thoroughly studied repetitive behaviors are those induced by the administration of drugs. Early experiments showed that administration of dopamine or dopaminergic agonists such as cocaine (a dopamine re-uptake inhibitor), amphetamine (a dopamine releasing agent), or

apomorphine (a dopamine-receptor agonist) resulted in the induction of stereotyped behavior in rodents (Kim and Lewis 2009). Lesion and microinjection experiments highlighted the importance of activation of dopaminergic receptors within the striatum for stereotypy induced by dopaminergic drugs, and showed that the cortical and thalamic inputs into striatum could have potentiating effects on drug-induced stereotypy within the striatum (Muehlmann Lewis 2012). More recent work has shown a critical role for D1 receptors in the striatum in drug induced stereotypies (Chartoff et al. 2001; Lee et al. 2018), as well as a role for activation of the striosomal compartment of the striatum (which is enriched in D1 receptor expression) relative to the matrix compartment of the striatum (Canales and Graybiel 2000).

Studies have also combined genetic manipulations with drug challenge. A recent example of this investigated the effect of high-dose amphetamine on mice with genetic knockout of histadine decarboxylase (*Hdc*), the key enzyme for the synthesis of histamine (Baldan et al 2013). *HDC* mutations have been implicated as a rare genetic cause of Tourette Syndrome, and mice with complete (*Hdc*-KO) or partial (*Hdc*-HET) ablation of *Hdc* show increased stereotypy in response to amphetamine. These mice also show increased activation of cells in the striosome compartment of the striatum (as measured by cFos) and altered dopamine release in striatum. This study shows a clear effect of a genetic risk gene on altering neural activity in basal ganglia circuits and subsequent induction of repetitive behavior in mice.

1.6 Goals of this dissertation

In this dissertation I examine the role of *SLC1A1*, a gene that has been associated with OCD, in behaviors and neural activity in mice. I do this by first overexpressing *Slc1a1* in OCD-relevant brain regions in mice, thus modeling the expected effects of the most commonly-reported OCD-associated polymorphism within this gene. Next, I test the therapeutic potential of ablating expression of this gene or the activity of its protein product in an OCD-relevant mouse model.

2.0 EAAT3 overexpression increases susceptibility to the development of amphetamine-induced repetitive behaviors

2.1 Introduction

Obsessive compulsive disorder (OCD) is a debilitating neuropsychiatric disorder with a lifetime prevalence of 2-3% (Kessler et al. 2005; Ruscio et al. 2010). It is characterized by intrusive thoughts or urges known as obsessions, and repetitive behaviors known as compulsions, which are often performed to relieve anxiety associated with obsessions (Pauls et al. 2014). Current standard of care treatments for OCD include cognitive behavioral therapy and serotonin reuptake inhibitors (SRIs). While these treatments are beneficial for many, up to 50% of OCD patients receiving them remain symptomatic (Dougherty et al. 2004; Koran et al. 2007), and better treatments based upon the underlying neurobiology of the disorder are needed.

Neuroimaging studies of OCD have identified abnormalities in cortico-striato-thalamo-cortical (CSTC) circuitry in OCD patients, with studies consistently showing hyperactivity of cortical and striatal regions (Menziés et al. 2008; Radua et al. 2010). Some studies have also reported increased glutamatergic signal in the caudate, measured by magnetic resonance spectroscopy, and increased glutamate in the CSF of a subset of OCD patients (Pittenger et al. 2011; Rosenberg et al. 2000; Starck et al. 2008). Animal models have further implicated particular glutamatergic inputs from cortex to striatum in OCD-relevant behaviors (Ade et al. 2016; Ahmari et al. 2013; Burguière et al. 2013; Corbit et al. 2019; Shmelkov et al. 2010; Wan et al. 2014; Welch et al. 2007), indicating that dysfunction of these circuits may be relevant for abnormal repetitive behaviors across species.

Early linkage studies of OCD implicated chromosome 9p24 region in the pathogenesis of the disorder (Hanna, Piacentini, et al. 2002; Willour et al. 2004). This region contains the gene *SLC1A1*, which encodes the neuronal glutamate transporter, EAAT3, and subsequent association studies have implicated various polymorphisms of this gene with OCD (Arnold et al. 2006; Cai et al. 2013; Dickel et al. 2006; Samuels et al. 2011; Shugart et al. 2009; Stewart et al. 2007; Veenstra-VanderWeele et al. 2012; Wendland et al. 2009). The most commonly-associated of these polymorphisms is the rs301430C allele. This allele results in increased expression of SLC1A1 in human postmortem brain, lymphoblastoid cells, and a luciferase reporter assay (Veenstra-VanderWeele et al. 2012; Wendland et al. 2009). This indicates that elevated levels of *SLC1A1*/EAAT3 may result in increased risk of OCD in humans and may lead to OCD-relevant behaviors in model systems.

EAAT3 is highly expressed in cortical and striatal regions (Danbold 2012), and animal studies have linked *Slc1a1*/EAAT3 to abnormal repetitive behaviors. We previously found no differences in baseline grooming or anxiety-like behavior in a mouse model of EAAT3 ablation (Zike et al. 2017). However, we found that mice lacking EAAT3 expression are protected against the development of drug-induced repetitive behavior. Specifically, these mice had reduced hyperlocomotion in response to low or moderate dose amphetamine, reduced stereotypy in response to high dose amphetamine, and reduced grooming in response to a dopamine D₁ receptor agonist. In addition, a recent study by Delgado-Acevedo et al. (2019) examined the effect of forebrain overexpression of EAAT3 on behavior and neural activity. They found that overexpressing *Slc1a1* resulted in increased anxiety-like behaviors and repetitive behaviors in mice, including increased grooming that was reversed by the administration of a serotonin reuptake inhibitor (SRI). Furthermore, they found abnormalities in cortico-striatal synapses, including

changes in NMDA receptor subunit expression and altered NMDA-dependent synaptic plasticity. However, they did not examine the impact of EAAT3 OE on drug-induced repetitive behavior.

Amphetamine is a dopamine-releasing agent that is used clinically as a treatment for ADHD. However, it can also be a drug of abuse, and at high doses, it has been shown to induce abnormal repetitive behavior, including hyperlocomotion and stereotypy. These two behaviors occur along a dose-response continuum, with lower doses leading to a predominance of hyperlocomotion and higher doses leading to a predominance of stereotypy (Yates et al. 2007). Amphetamine has been reported to induce or worsen OCD symptoms in a small subset of patients, and dopamine antagonists are sometimes used as an adjuvant with SRIs for treatment of OCD (Denys et al. 2004; Thamby and Jaisoorya 2019). Dopamine has also been heavily implicated in other repetitive behavior disorders such as tic disorders, and correspondingly, previous studies have used amphetamine challenge to induce stereotypy in a genetic mouse model of Tourette syndrome (Baldan et al. 2014).

In this study, we tested whether overexpression of *Slc1a1* exacerbated behavioral response to amphetamine, consistent with human genetic studies implicating this gene in OCD and a preclinical mouse study that was published shortly before we completed this work implicating this gene in OCD-relevant behaviors (Delgado-Acevedo et al 2019). We found that mice overexpressing EAAT3 show an increased behavioral response to both low and high dose amphetamine. Use of an unbiased machine-learning classifier to characterize amphetamine-induced behaviors showed that EAAT3 overexpression potentiated the behavioral response to amphetamine. We show that this increased susceptibility to the effects of amphetamine is associated with D1 neuronal activation in the ventromedial striatum. Lastly, we show that

stereotypy behavior and locomotor behavior following amphetamine were correlated with distinct patterns of cFos expression in dorsal and ventral striatum.

2.2 Methods

2.2.1 Mice

All procedures were carried out in accordance with the guidelines set out by the NIH in the Guide for the Care and Use of Laboratory (Guide for the Care and Use of Laboratory Animals, 1996) and were approved by the University of Pittsburgh Institutional Animal Care and Use Committee (IACUC). All mice were housed in cages of 3-5 mice/cage with *ad libidum* to food and water. Mice were on a 12hr:12hr light/dark cycle, with lights on at 7:00AM and lights off at 7:00PM, and all behavioral testing was conducted during the light cycle.

Slc1a1-OE mice were bred by crossing *Slc1a1*-NeoSTOP-tetO mice (Zike et al. 2017) with ROSA26-flippase mice to excise the NeoSTOP cassette. Forebrain-specific overexpression achieved by crossing these *Slc1a1*-tetO mice on a 129S6/SvEv background with CaMKII-tTA mice on a C57Bl/6 background (Fig. 2-1A), resulting in *Slc1a1*-tetO/*CaMKII*-tTA experimental mice on a mixed 129S6/SvEv;C57Bl/6 background. For the doxycycline dose-response experiment, mice were fed were fed doxycycline at doses of 0, 50, 100, 200, or 400 mg/kg in their chow for 4 weeks prior to sacrifice (Envigo Custom diet in LabDiet 5P76, ProLab IsoPro RMH 3000). For lifetime overexpression, breeding pairs were fed 50 mg/kg doxycycline chow, and mice were continued on this diet following weaning. For adult-specific overexpression, breeding pairs were fed 400 mg/kg doxycycline chow and switched to 50 mg/kg doxycycline chow at 8 weeks of

age (Fig. 2-1D). The dose-response cohort consisted of 3 mice/group. The initial lifetime overexpression behavioral cohort consisted of 25 tTA+ mice and 20 tTA-, while the initial adult-specific overexpression cohort consisted of 21 tTA+ and 17 tTA- mice. The first cFos cohort included 16 tTA+ mice and 16 tTA- mice, while the second cohort consisted of 21 tTA+ and 22 tTA- mice. All mice were 3-6 months at time of testing.

2.2.2 Behavioral testing

All testing was conducted between the hours of 8:00AM and 6:00PM. Mice were habituated in their home cages to the testing room for 20-40 minutes prior to testing. Each behavioral apparatus was washed with 70% EtOH and allowed to dry completely between mice.

2.2.2.1 Anxiety tests

Anxiety testing occurred in unhandled, naïve mice prior to any other testing. The tests were conducted in the following order: open field (OF) test, elevated plus maze (EPM) test, and light dark (LD) test, with one day between tests.

2.2.2.1.1 Open field test

Mice were placed into the center of a 41 cm X 41cm Plexiglas open field chamber under room lights for 30 minutes. Locomotor activity was scored by detecting interruptions of infrared beams by the body of the mouse; data was collected and analyzed using Motor Monitor (Kinder Scientific). The total distance as well as the time and distance in the center (10 cm X 10 cm) of the chamber was recorded.

2.2.2.1.2 Elevated plus maze test

The elevated-plus maze is a cross maze that consists of two open and two closed 30×5 cm arms. Top-view video was recorded using an Any Maze video camera, and automated tracking of the mouse (Any Maze). Time spent in the open arms, distance traveled in the open arms, and total distance traveled was recorded for 5 minutes.

2.2.2.1.3 Light dark test

The light dark chamber consists of two equally sized chambers (24cm x 24cm), one enclosed and dark and one brightly lit (~300lux). Mice are placed in the dark side of the chamber and allowed to freely explore both sides for 10 minutes. Locomotor activity was scored by detecting interruptions of infrared beams by the body of the mouse; data was collected and analyzed using Motor Monitor (Kinder Scientific). The total distance as well as the time and distance in the light and dark sides of the chamber was recorded.

2.2.2.1.4 Grooming assessment

For assessment of grooming behavior, mice were placed in a plexiglass chamber (20 cm x 20cm) and video recorded (Cannon) for 30 minutes. A trained experimenter blind to group then scored the amount of time spent grooming during the three sessions.

2.2.2.2 Amphetamine-induced hyperlocomotion

Mice were weighed prior to being placed into the center of a 41 cm X 41cm Plexiglas open field chamber under for 30 minutes. Mice then received intraperitoneal injections of either saline or 3.0 mg/kg D-amphetamine (Sigma-Aldrich) and were placed back in the locomotor chamber for another 60 minutes. One week later, mice were treated given the other treatment in a crossover

design. Locomotor activity was scored by detecting interruptions of infrared beams by the body of the mouse; data was collected and analyzed using Motor Monitor (Kinder Scientific).

2.2.2.3 Amphetamine-induced stereotypy

Mice were weighed prior to receiving either saline or a high-dose (8.0 mg/kg) of D-amphetamine via intraperitoneal injection. Mice placed into small (20 cm x 20 cm) Plexiglas chambers and were video recorded for 90 minutes following injection. An experimenter blind to genotype, drug treatment, and timepoint scored 3 two-minute time bins (cohort I) or 9 two-minute time bins (Cohort II). Stereotypy was defined as stationary head bobbing, sniffing, shuffling, or licking motion lasting at least one second. Interrater reliability for this behavior exceeded 0.90.

2.2.3 DeepLabCut

For cohort III, mice were weighed before being placed in small (20 cm x 20 cm) Plexiglas chambers for 30 minutes. After 30 minutes they were removed from the chamber and injected with VEH, 3.0 mg/kg amphetamine, or 8.0 mg/kg amphetamine before being placed back into the chamber. For this experiment, behavior was recorded from below at 60fps using hand-held video cameras (Cannon). Videos were then analyzed using DeepLabCut (DLC) (Mathis et al. 2018; Nath et al. 2019). DLC uses convolutional neural networks to estimate 3D-poses. We manually labeled the location of the paws, nose, and tail base in 833 frames taken from a subset of behavioral videos. We then trained the network to predict the location of these 6 body parts in every other frame of the video, using a GPU (RTX 2080Ti in an Alienware R8). We evaluated and refined the labels 2X until the tracking was sufficiently good.

2.2.4 Behavioral Segmentation of Open-field in DeepLabCut (B-SOID)

B-SOID is an unsupervised learning algorithm that serves to discover and classify behaviors in an unbiased fashion (Hsu and Yttri 2019). This algorithm segregates statistically different, sub-second rodent behaviors, using novel expectation maximization fitting of Gaussian mixture models on t-Distributed Stochastic Neighbor Embedding (t-SNE). The original features taken from dimensionally-reduced classes are then used build a multi-class support vector machine classifier that can decode actions. We trained this classifier using three one-minute videos taken from each mouse in the experiment: one minute during habituation, one minute during early drug response, and one minute during late drug response. We did this in order to ensure that all drug responses were represented. We then used this trained classifier to analyze all data from every mouse.

2.2.5 Western blot

Western blot was performed according to Zike et al. (2017). Briefly, brains were extracted from mice after rapid decapitation and immediately frozen on an ice-cold metal platform. Sections were cut on a microtome and the whole striatum was dissected and homogenized. Protein concentrations of all samples were determined by a bicinchoninic acid (BCA) protein assay (Thermo Fisher Scientific). Equal amounts of protein were incubated with a Laemmi sample buffer for 5 minutes at room temperature. Samples were analyzed by SDS/PAGE followed by Western blotting. EAAT3 protein was visualized using a rabbit anti-EAAC1/EAAT3 antibody (1:1,000 dilution; EAAC110A, Alpha Diagnostics).

2.2.6 Immunohistochemistry

Following the 8.0 mg/kg amphetamine challenge, mice in Cohort II were sacrificed and perfused with 4% paraformaldehyde and post-fixed overnight at 4 °C, transferred to 30% sucrose solution until they sank, then frozen on dry ice and sliced on a cryostat into 35 um coronal sections. Sections were stored in 1X PBS/0.1% sodium azide until use. Sections were washed in Tris-buffered saline (TBS), incubated in 0.03% H₂O₂ for 10 minutes, washed again in TBS, and blocked in 3% normal goat serum before being blocked in anti-cFos primary antibody (1:1000 dilution, Millipore Sigma) for 48 hours at 4 °C. Sections were washed in TBS+ (0.3% Triton X-100; Sigma) and incubated in anti-rabbit biotinylated secondary antibody (1:500 dilution) for 2 hours, blocked in tertiary avidin-biotin complex solution (Vector) for 1 hour, and then stained with 3,3'-Diaminobenzidine chromogen (DAB; Sigma) for 5 minutes. In between these steps, sections were washed with TBS+. Sections were mounted on glass slides, dehydrated with ethanol, coverslipped with DPX and imaged with a light microscope. cFos positive cells were quantified using cellSens (Olympus).

For the double-labeling protocol of cFos and striatal patch compartment, sections were first taken through the cFos staining above and then repeated with anti-mu opioid receptor (MOR, specific to striosome compartment of striatum) primary antibody (1:1000 dilution; Millipore Sigma) for 24 hours at 4 °C. Additionally, DAB-Nickel was used in place of DAB. Sections were mounted on glass slides, coverslipped with DPX and imaged with a light microscope. MOR+ patch compartment was identified by an experimenter, and cFos within these regions and within MOR-putative matrix compartment was quantified using cellSens.

2.2.7 RNAScope

For cohort III, mice were sacrificed immediately following the end of the behavior session. We performed RNA ISH for Fos, Drd1, and Drd2 mRNAs as described previously (Caprioli et al 2017). We rapidly extracted and froze brains on dry ice. Brains were stored at -80°C until use. Brains were sliced on a cryostat at 16µm and collected directly onto Superfrost Plus slides (Fisher Scientific). We used an RNAScope Multiplex Fluorescent Reagent Kit (Advanced Cell Diagnostics) and performed the ISH assay according to the user manual for fresh-frozen tissue and as described previously. We fixed brain slices in 4% Phosphate buffered saline for 20 min at 4°C. We rinsed the slices three times in PBS and dehydrated the slices in 50, 70, 100, and 100% ethanol. We dried the slides at room temperature for 10 min, and to limit the spreading of the solutions, we drew a hydrophobic barrier on slides around brain slices. We then treated the slides with protease solution (pretreatment 4) at room temperature for 20 min. We then applied target probes for Fos, Drd1, and Drd2 to the slides and incubated them at 40°C for 2 h in the HybEZ oven. Each RNAScope target probe contains a mixture of 20 ZZ oligonucleotide probes that are bound to the target RNA, as follows: Fos-C3 probe (GenBank accession number NM_022197.2); Drd1-C1 probe (GenBank accession number NM_012546.2); and Drd2-C2 probe (GenBank accession number NM_012547.1). Next, we incubated the slides with preamplifier and amplifier probes (AMP1, 40°C for 30 min; AMP2, 40°C for 15 min; AMP3, 40°C for 30 min). We then incubated the slides with fluorescently labeled probes by selecting a specific combination of colors associated with each channel, as follows: green (Alexa Fluor 488 nm), orange (Alexa Fluor 550 nm), and far red (Alexa Fluor 647 nm). We used AMP4 Alt4 to detect triplex Drd2, Fos, and Drd1, in far red, green, and red channels, respectively. Finally, we incubated sections for 20 s with DAPI.

We washed the slides with one washing buffer two times in between incubations. After air drying the slides, we coverslipped them with Fluroshield mounting medium.

2.2.8 Statistical analysis

Data were analyzed using Prism (GraphPad, La Jolla, CA, USA). Two-tailed, unpaired Student t-test or two-way ANOVA with Sidak's post-tests were used to analyze the primary data, except for locomotor and automated stereotypy curve data, which was analyzed using non-linear curve fit analysis. Specific statistical analyses for each data set are described in results and in the figure legends. All data are reported as the mean \pm standard error of the mean. Geisser-Greenhouse corrections were used for ANOVA where appropriate. Pearson correlations were used for analysis of cFos and behavioral data.

2.3 Results

To examine the effect of *Slc1a1* overexpression on behavior and neural activity in mice, thus modeling the effects of the most common OCD-associated polymorphism, we generated *Slc1a1*-overexpressing (OE) mice. *Slc1a1*-OE mice were bred by first crossing *Slc1a1*-tetO-STOP mice with Flippase mice in order to excise the Neo-STOP construct (Figure 2-1A). The resulting progeny were then crossed with *CaMKII*-tetracycline transactivator (tTA) mice in order to overexpress *Slc1a1* selectively in forebrain neurons in a doxycycline-dependent manner. To validate this system, we measured levels of EAAT3, the protein product of *Slc1a1*, in *Slc1a1*-tetO/*CaMKII*-tTA mice given different doses of doxycycline (0 mg/kg, 50 mg/kg, 100 mg/kg, 200 mg/kg, or 400 mg/kg) in their chow for four weeks. They were then sacrificed, and Western blots were performed to measure EAAT3 levels in striatum (Figure 2-1B, C). As expected, we saw a dose-dependent effect of doxycycline on EAAT3 expression (one-way ANOVA, $F(7, 16) = 53.81$, $p < 0.001$). *Slc1a1*-tetO/*CaMKII*-tTA mice receiving 0 mg/kg doxycycline show ~55 times the level of expression seen in *Slc1a1*-WT and *Slc1a1*-tetO mice. Overexpression was normalized by increasing levels of doxycycline, with mice on the highest dose of doxycycline (400 mg/kg) showing levels of expression comparable to WT mice. EAAT3 expression in the no-doxycycline group was supraphysiological. We therefore chose 50 mg/kg doxycycline to generate a level of overexpression more consistent with that generated by the OCD-associated polymorphism. All cohorts were therefore comprised of *Slc1a1*-tetO/*CaMKII*-tTA mice receiving 50 mg/kg doxycycline (*Slc1a1*-OE mice; tTA+), and *Slc1a1*-tetO mice lacking tTA littermate controls (tTA-). For lifetime overexpression, mice were born and raised on 50 mg/kg doxycycline, whereas for adult-specific overexpression, mice were born and raised on 400 mg/kg doxycycline and switched to 50 mg/kg at 8 weeks of age (Figure 2-1D).

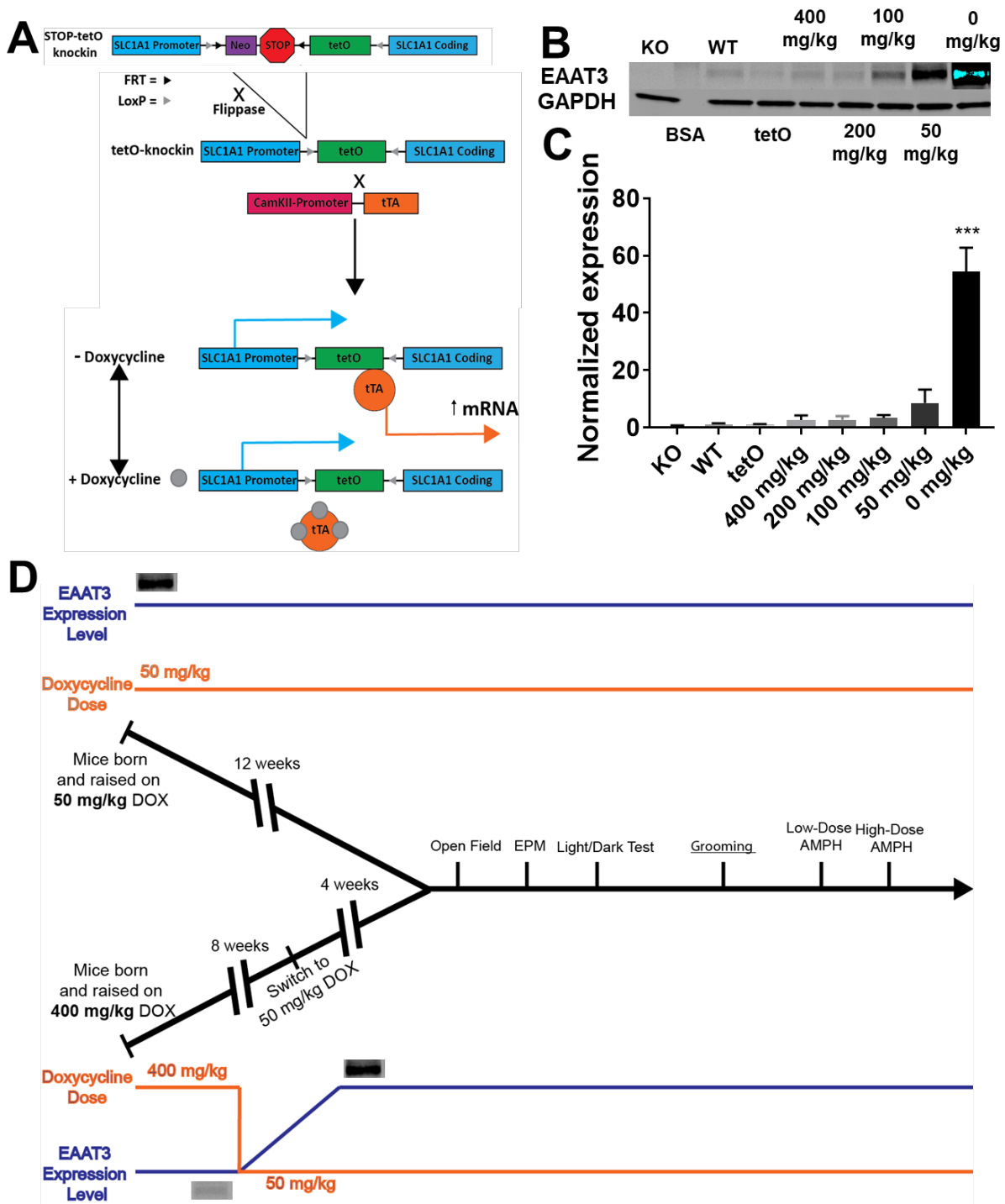


Figure 2-1 *Slc1a1*-OE mice show increased EAAT3 protein expression that can be reversed by doxycycline administration

(A) Schematic of *Slc1a1* overexpression in *Slc1a1*-tetO/*CaMKII*-tTA mice. The neo-STOP cassette is excised by crossing with a mouse line expressing flippase. Crossing to *CaMKII*-tTA results in doxycycline-dependent

overexpression specifically in forebrain neurons. (B) Representative Western blot of EAAT3 expression in *Slc1a1*-knockout (KO), wildtype (WT), *Slc1a1*-tetO, and *Slc1a1*-tetO/*CaMKII*-tTA mice receiving one of five different doses of doxycycline (0 mg/kg, 50 mg/kg, 100 mg/kg, 200 mg/kg, or 400 mg/kg). (C) Quantification of expression in the same groups (one-way ANOVA, $F(7, 16) = 53.81$, $p < 0.001$, $n = 3$ mice/group). (D) Timeline of experiment for cohort I that included both lifetime *Slc1a1*-OE mice (top line) that were born and raised on a low dose of doxycycline, and adult-specific *Slc1a1*-OE mice (bottom-line) that were born and raised on a high dose (400mg/kg) of doxycycline and switched to low dose (50mg/kg) at 8 weeks.

To examine the behavioral effects of *Slc1a1* overexpression, lifetime and adult-specific overexpressers were run through a variety of behavioral tests (Fig. 2-1D). Both lifetime and adult-specific *Slc1a1* overexpression resulted in increased behavioral response to amphetamine. Lifetime overexpressing *Slc1a1*-OE mice showed potentiated hyperlocomotion in response to low dose (3.0 mg/kg) amphetamine (Curve-fit analysis, $F(4, 802) = 3.1$, $p < 0.05$) (Fig. 2-2A) and significantly increased percent time spent in stereotypy at all three timepoints (20, 50, 80 mins) relative to tTA- controls following a high dose (8.0 mg/kg) of amphetamine (repeated measures ANOVA, main effect of genotype; $F(1, 43) = 39.16$, $p < 0.001$) (Fig. 2-2C). The adult-specific overexpression cohort showed similar results, with *Slc1a1*-OE mice showing significantly higher levels of amphetamine-induced hyperlocomotion following a low dose of amphetamine (curve-fit analysis, $F(4, 676) = 3.72$, $p < 0.01$) (Fig. 2-2B), and increased amphetamine-induced stereotypy behavior at all timepoints following a high dose of amphetamine (Repeated measures ANOVA, main effect of genotype; $F(1, 36) = 14.96$, $p < 0.001$) (Fig.2-2D). Observation of the tTA- mice following high dose amphetamine showed that they were engaged in hyperlocomotion when not engaged in stereotypy. While locomotor behavior could not be quantified in these experiments

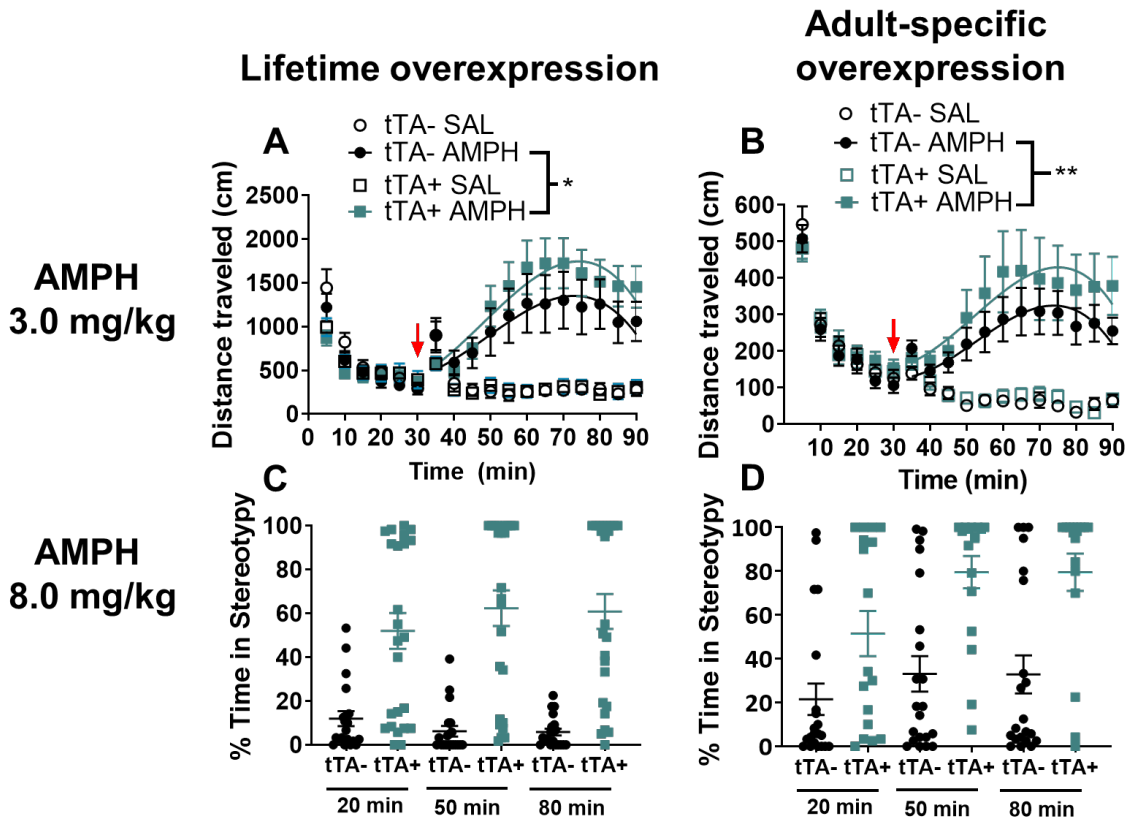


Figure 2-2 *Slc11a1*-OE mice show potentiated behavioral response to both low-dose and high-dose amphetamine

Both lifetime (A) and adult-specific (B) *Slc11a1*-OE mice (tTA+) show significantly higher levels of locomotion following amphetamine administration (3.0 mg/kg) relative to tTA- controls (A, Curve-fit analysis, $F(4, 802) = 3.1$, $p < 0.05$; B, Curve-fit analysis, $F(4, 676) = 3.72$, $p < 0.01$). Red arrow indicates amphetamine injection at $t = 30$. Lifetime (C) and adult-specific (B) *Slc11a1*-OE (tTA+) mice showed significantly higher levels of locomotion relative to tTA- controls following a high dose (8.0 mg/kg) of amphetamine (C, Repeated measures ANOVA, main effect of genotype, $F(1, 43) = 39.16$, $p < 0.001$; D, Repeated measures ANOVA, main effect of genotype, $F(1, 36) = 14.96$, $p < 0.001$, main effect of time, $F(1.37, 49) = 11.87$, $p < 0.001$).

given our side-view recordings, this suggests that *Slc11a1*-OE mice have a potentiated behavioral response to amphetamine, with these mice engaging in more hyperlocomotion at the low dose of amphetamine and engaging in less locomotion and more stereotypy at the high dose relative to tTA- controls.

While we saw a robust increase in the sensitivity to amphetamine-induced repetitive behavior in *Slc1a1*-OE mice, we saw no baseline increases in compulsive-like grooming behavior (Fig. A-1). Both lifetime and adult specific *Slc1a1*-OE mice showed no significant differences in percent time spent grooming relative to tTA- controls. We also measured anxiety-like behavior in *Slc1a1*-OE mice, as anxiety is thought to be a key component of OCD. In cohort I, lifetime *Slc1a1*-OE mice showed a significant reduction in the percent time spent in the center of the OF (unpaired t-test; $t(43) = 2.33, p < 0.05$) and in the percent time spent in the in the open arms of the EPM (unpaired t-test; $t(43) = 2.12, p < 0.05$) (Fig. A-2A, C). There was no significant difference in the percent time spent in the light side of the LD chamber (Fig. A-2B). In contrast, adult-specific *Slc1a1*-OE mice showed no significant differences from tTA- controls in the percent time spent in the center of the OF (Fig. A-2B), the open arms of the EPM (Fig. A-2D), or the light side of the LD chamber (Fig. A-2F). The results from cohort I indicated that there was a significant anxiety-like phenotype in the lifetime overexpression group but not the adult-specific overexpression group. However, several subsequent cohorts failed to replicate these anxiety-like behaviors in the OF test or EPM test in lifetime *Slc1a1*-OE mice (Fig. A-3).

To investigate the neural activity underlying the increased behavioral response to amphetamine in *Slc1a1*-OE mice, we administered a high dose of amphetamine to a separate cohort of mice and measured striatal expression of the immediate early gene cFos. Mice were sacrificed 140 minutes following amphetamine injection to capture cFos expression corresponding to the maximal behavioral response to amphetamine (i.e. 60-90 minutes following the peak AMPH response 50-80 minutes post-injection, Fig. 2-3A). Similar to the previous cohort, *Slc1a1*-OE mice showed a potentiated stereotypy response to amphetamine (three-way repeated measure ANOVA, genotype main effect, $F(1, 28) = 5.35, p < 0.05$, genotype x drug interaction, $F(8, 224) = 5.348, p$

< 0.05), with tTA+ mice treated with amphetamine displaying significantly higher levels of stereotypy than both tTA- controls treated with amphetamine and tTA+ mice receiving vehicle (Fig. 2-3A).

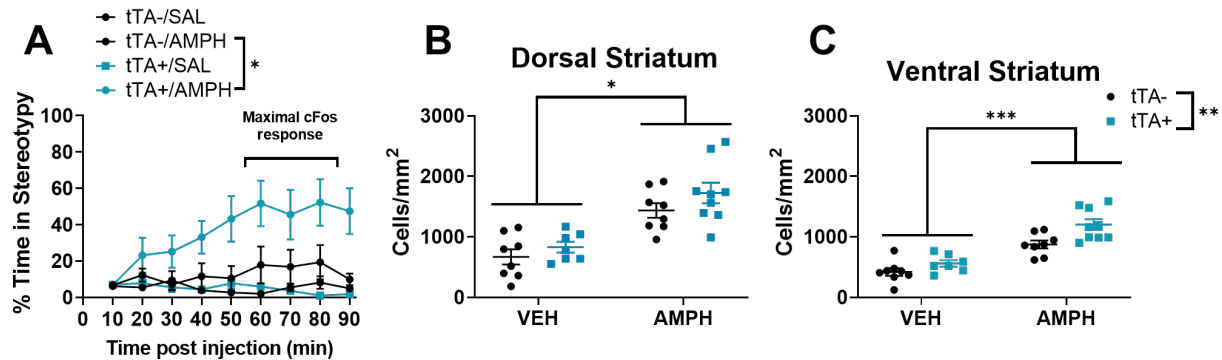


Figure 2-3 *Slc11a1*-OE mice show increased stereotypy behavior following amphetamine and increased cFos expression in the ventral striatum

(A) *Slc11a1*-OE mice show increased stereotypy in response to amphetamine relative to controls (genotype x drug interaction, $F(8,224) = 5.348, p < 0.05$). (B) Amphetamine increased cFos expression in dorsal striatum (drug main effect, Two-way ANOVA, $F(1, 28) = 46.62, p < 0.0001$). (C) Amphetamine increased cFos expression in ventral striatum, and *Slc11a1*-OE mice show increased cFos expression in ventral striatum (genotype main effect, Two-way ANOVA, $F(1, 28) = 56.63, p < 0.0001$; drug main effect, Two-way ANOVA, $F(1, 28) = 10.64, p < 0.01$).

The number of cFos positive cells was quantified in 10 striatal subregions (Fig. A-4). Amphetamine increased cFos in every striatal subregion studied (Fig. A-4; see Table A-1 for statistics). After controlling for multiple comparisons, there was a significant main effect of genotype on cFos in the dorsal medial nucleus accumbens shell (Fig. A-3D). There was no genotype x drug interaction in any subregion after controlling for multiple comparisons, although the ventromedial striatum (VMS) was the region with a genotype x drug effect that was closest to significance (Fig. A-3F; Table A-1). Next, we pooled data from the different subregions into

composite dorsal and ventral striatum cFos responses. There was a main effect of drug on cFos expression in the dorsal striatum (two-way ANOVA, $F(1, 28) = 46.62, p < 0.0001$), but no effect of genotype (Fig. 2-3B). There was a significant effect of both genotype (two-way ANOVA, $F(1, 28) = 56.63, p < 0.0001$) and drug (two-way ANOVA, $F(1, 28) = 10.64, p < 0.01$) on cFos expression in the ventral striatum (Fig. 2-3C). Post-hoc analysis revealed that tTA+ mice had significantly higher cFos expression in the ventral striatum compared to tTA- mice following amphetamine (Sidak's multiple comparison test, $p < 0.01$). We then investigated the correlation between stereotypy behavior and cFos response in dorsal and ventral striatum and each of the ten striatal subregions in amphetamine-treated mice. After correcting for multiple comparisons (Bonferroni correction, $\alpha = 0.0042$), there were no significant correlations (Table A-2). However, the VMS again was the region with a genotype x drug effect that was closest to significance.

Previous research has implicated compartment-specific cFos expression in stereotypy response to amphetamine. In particular, studies have shown that index of striosome to matrix predominance (ISMP) [ratio of cFos expression in the striatal patch/striosome compartment to cFos expression in the striatal matrix compartment] correlates very highly with stereotypy response and predicts the amount of stereotypy (Canales and Graybiel 2000). In the same cohort, we therefore performed double-immunohistochemistry for cFos and μ -opioid receptor (MOR), a marker of striosome compartment (Figure 2-4A). There was also a significant main effect of amphetamine (drug main effect, two-way ANOVA, $F(1,24) = 84.54, p < 0.0001$), as well as a significant main effect of genotype (two-way ANOVA, $F(1,24) = 4.45, p < 0.05$) on cFos

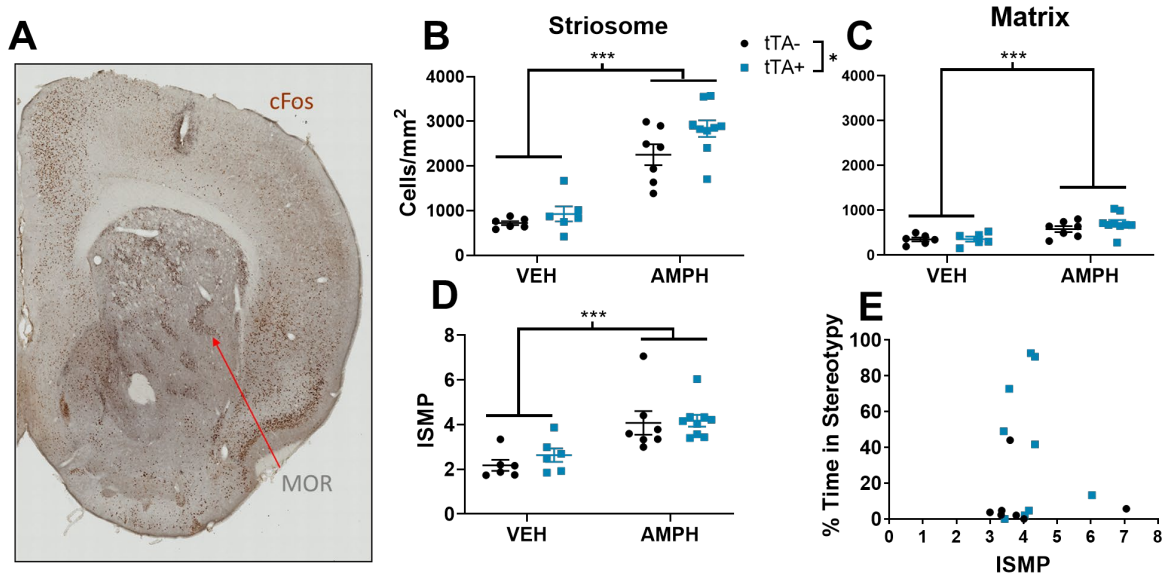


Figure 2-4 Amphetamine increases cFos across striatal subcompartments

(A) Representative section showing cFos and μ -opioid receptor (MOR) staining in striatum. (B) There was a main effect of drug (two-way ANOVA, $F(1,24) = 84.54, p < 0.0001$) and genotype (two-way ANOVA, $F(1,24) = 4.45, p < 0.05$) in the striosome compartment of striatum. (C) There was a main effect of drug in the matrix compartment (two-way ANOVA, $F(1,24) = 19.20, p < 0.0001$). (D) There was a significant effect of drug on index of striosome to matrix predominance (ISMP) (drug main effect, Two-way ANOVA, $F(1,24) = 22.69, p < 0.0001$). (E) There was no significant correlation between ISMP and stereotypy behavior.

expression in the striosomes (Fig. 2-4B). There was a significant main effect of amphetamine on cFos expression in the matrix compartment (drug main effect, Two-way ANOVA, $F(1,24) = 19.20, p < 0.0001$) (Fig. 2-4C), and a main effect of amphetamine on ISMP (drug main effect, two-way ANOVA, $F(1,24) = 22.69, p < 0.0001$). However, there was no genotype or genotype x drug interaction effect on ISMP (Fig. 2-4D), and no significant correlation between ISMP and stereotypy response in amphetamine treated mice (Fig. 2-4E), indicating that this measure did not predict stereotypy behavior in the *Slc1a1*-OE cohort.

To further dissect the mechanism of the effects amphetamine in *Slc1a1*-OE mice, we next examined cFos in D1/D2 cells in the striatum in conjunction with a comprehensive unbiased examination of behavior following amphetamine administration. Mice were injected with either vehicle or amphetamine (3.0 mg/kg or 8.0 mg/kg) with automated scoring of behavior and cFos analysis in D1 and D2 striatal neurons. Videos were analyzed using DeepLabCut (DLC) to track the x- and y-coordinates of the nose, four paws, and tail base for every frame of the video. This information was then analyzed using Behavioral Segmentation of Open Field in DeepLabCut (B-SOID), an unsupervised learning algorithm that discovers and classifies actions based on the inherent statistics of the x- and y-coordinates from the DLC output. This unbiased classification algorithm yielded 12 clusters of behavior for this cohort and classified every frame from each behavioral video as belonging to one of these clusters.

Upon inspection of videos corresponding to each of the clusters, it was determined that several of the clusters overlapped and were indistinguishable. Specifically, six of the clusters represented rest/quiescence, which was highly represented in these videos by all mice during the habituation period and by the vehicle-treated mice throughout the videos. These behavior clusters were therefore pooled, yielding six distinct clusters of behavior. These corresponded to stereotypy (a characteristic rapid head bobbing/sniffing behavior while stationary), rest/quiescence (complete or almost complete lack of motion), locomotion, exploration (stationary back paws with stretching forward), sniffing, and grooming (face and body grooming) (See supplemental video file 1). Behavior was analyzed in 5 minute time bins, and the behavioral trace for all 6 clusters (as well as individuals within each group) is shown in Fig A-5. A summary of this behavioral analysis is shown in pie-chart form in Fig. A-6.

These data were used to test several *a priori* hypotheses regarding the effect of amphetamine on behavior in *Slc1a1*-OE and control mice. Previous results from both low- and high-dose amphetamine experiments led us to the hypothesis that the amphetamine behavioral response was potentiated in *Slc1a1*-OE mice relative to controls, with tTA⁺ mice showing potentiated hyperlocomotion following low dose amphetamine and potentiated stereotypy following high-dose amphetamine, while tTA⁻ mice show lower levels of hyperlocomotion following low dose amphetamine, and a combination of stereotypy and hyperlocomotion at following high dose amphetamine (Fig. 2-2). To test this, we compared tTA⁺ and tTA⁻ mice receiving either 3.0 mg/kg or 8.0 mg/kg amphetamine in their stereotypy and locomotion response. As predicted, at the low dose of amphetamine, tTA⁺ mice show increased locomotion relative to tTA⁻ controls (Fig. 2-5A; non-linear curve-fit analysis, $F(4, 328) = 13.27, p < 0.001$), but no difference in stereotypy behavior (Fig. 2-5C). Following high-dose amphetamine, tTA⁺ mice spend significantly more time engaged in stereotypy (non-linear curve fit analysis, $F(4, 328) = 3.88, p < 0.01$) (Fig. 2-5D), and less time engaged in hyperlocomotion (non-linear curve fit analysis, $F(4, 328) = 9.05, p < 0.001$) (Fig. 2-5B).

There was a significant main effect of drug administration on quiescence, with no difference between groups during the habituation period, but a dose dependent decrease in the amount of quiescence exhibited by both tTA⁺ and tTA⁻ mice following drug injection (Repeated measures ANOVA, Greenhouse Geisser correction, drug X time, $F(15.79, 37) = 5.58, p < 0.001$), with post-hoc tests revealing increased quiescence in the 3.0 mg/kg group compared to vehicle (Bonferroni, $p < 0.001$) and the 8.0 mg/kg group showing a further decrease relative to the 3.0

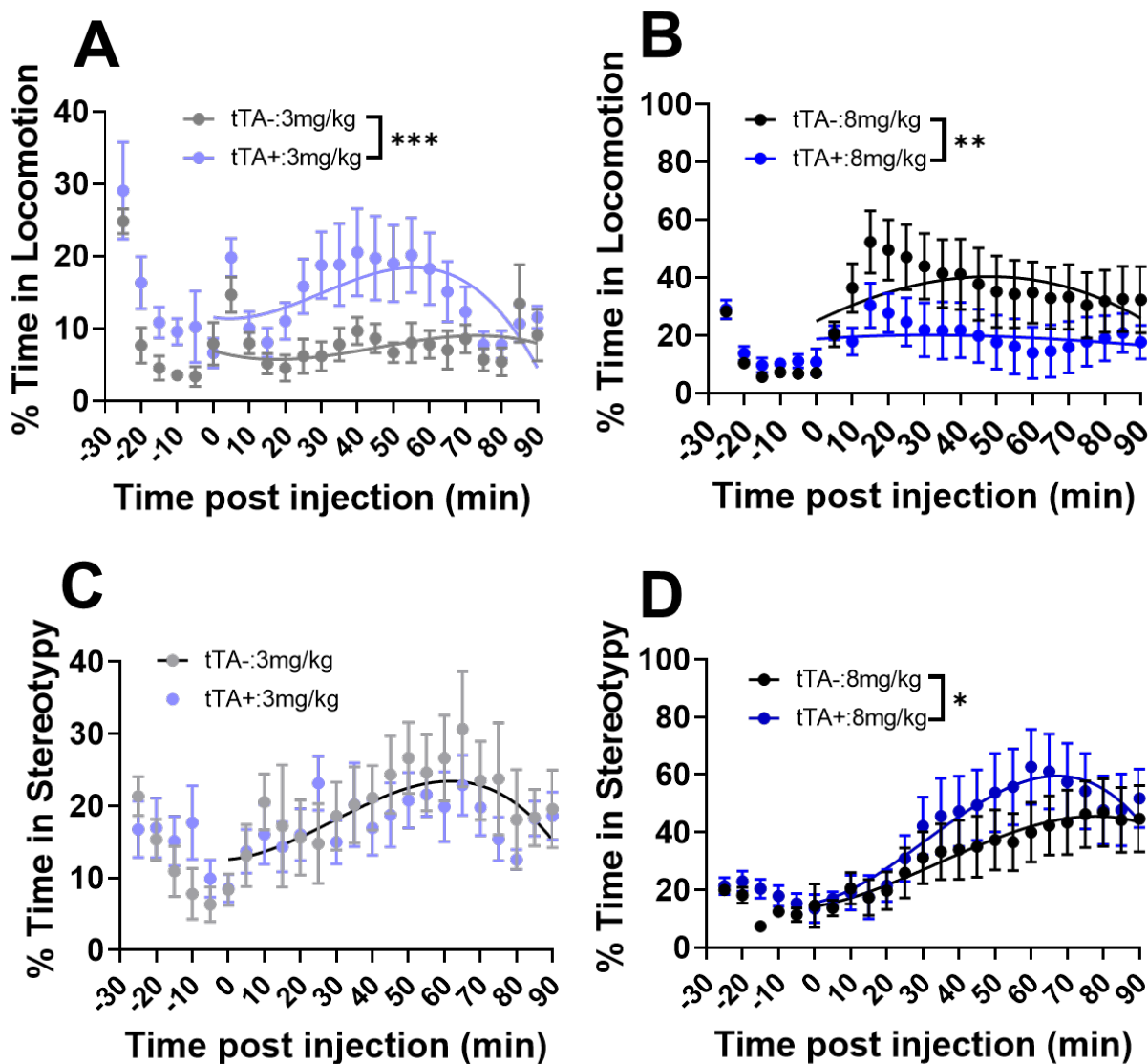


Figure 2-5 *Slc11a1*-OE mice show a potentiated response to amphetamine

(A) Following 3.0 mg/kg amphetamine, *Slc11a1*-OE mice show increased locomotion relative to tTA- controls (non-linear curve-fit analysis, $F(4, 328) = 13.27, p < 0.001$). (B) Following 8.0 mg/kg amphetamine, *Slc11a1*-OE mice show decreased locomotion relative to tTA- controls (non-linear curve fit analysis, $F(4, 328) = 9.05, p < 0.01$). (C) Following 3.0 mg/kg amphetamine, *Slc11a1*-OE mice show no differences in stereotypy behavior. (D) Following high dose amphetamine, *Slc11a1*-OE mice spend significantly more time engaged in stereotypy compared to tTA- controls (non-linear curve fit analysis, $F(4, 328) = 3.88, p < 0.01$).

mg/kg group (Bonferroni, $p < 0.001$) (Fig. A-5). There was also a significant effect of drug administration on grooming behavior (Repeated measures ANOVA, Greenhouse Geisser correction, drug x time, $F(12.01, 37) = 5.18$, $p < 0.001$), with post-hoc tests revealing significantly reduced grooming in 8.0 mg/kg amphetamine-treated mice compared to vehicle-treated mice (Bonferroni, $p = 0.006$), and a trend toward reduced grooming in the 3.0 mg/kg amphetamine group relative to the vehicle group (Bonferroni, $p = 0.073$). There was no effect of drug or genotype on sniffing or exploration behavior.

We also examined cFos expression in D1 and D2 neurons in several subregions of striatum in this cohort of mice (Fig. 2-6A). Based on the results from the previous cFos experiment, we focused on the VMS. We found a significant main effect of amphetamine on the overall number of cFos positive cells in the VMS (drug main effect, $F(2, 31) = 8.29$, $p < 0.05$) (Fig. 2-6B). Furthermore, there was a significant main effect of amphetamine on the number of cFos positive D1 neurons in the VMS (two-way ANOVA, $F(2, 31) = 9.02$, $p < 0.001$), as well as a main effect of genotype (two-way ANOVA, $F(1,31) = 4.35$, $p < 0.05$) on the number of cFos positive D1 neurons in the VMS, with post-hoc tests revealing significantly higher D1 neuron cFos expression in *Slc1a1*-OE mice following high dose amphetamine (Sidak's multiple comparison test, $p < 0.05$). There was no effect of drug or genotype, nor an interaction effect on D2 expression in the VMS. Further analysis revealed a significant effect of amphetamine on overall cFos expression in three other striatal subregions: DMS, DLS, and NAc (Fig. A-7). Again, this increased cFos expression was driven primarily by increased activity of D1 neurons, as there was a significant effect of amphetamine on D1 neuron cFos expression in all three subregions. There was also a significant effect of drug on D2 neuron cFos expression in the NAc, but not in the DMS, DLS, or VMS. This same pattern held true for the composite measures as well, with a significant drug effect on total

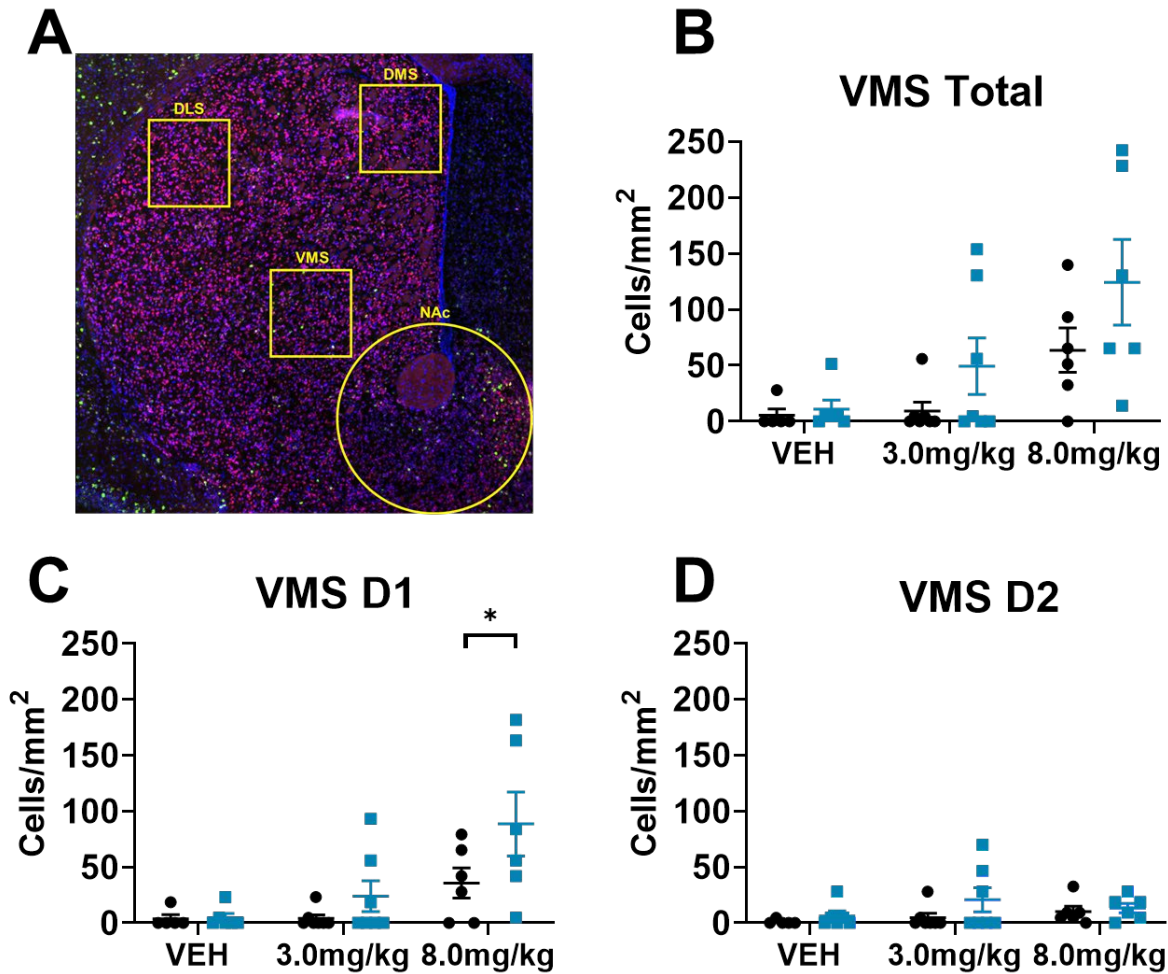


Figure 2-6 *Slc1a1*-OE mice have show increased cFos in D1-neurons following high dose amphetamine.

(A) Representative section showing the fluorescent staining for D1 (Red), D2 (Purple), cFos (Green), and DAPI (blue), as well as the regions where cFos expression was quantified. DLS = dorsolateral striatum, DMS = Dorsomedial striatum, VMS = ventromedial striatum, NAc = nucleus accumbens. (B) Amphetamine increases total cFos expression in VMS (drug main effect, $F(2, 31) = 8.29$, $p < 0.05$). (C) There was a significant main effect of amphetamine (two-way ANOVA, $F(2, 31) = 9.02$, $p < 0.001$) and a main effect of genotype (two-way ANOVA, $F(1,31) = 4.35$, $P 0.05$) on cFos expression in D1 neurons in the VMS, with post-hoc tests revealing a significantly higher cFos expression in *Slc1a1*-OE mice following high dose amphetamine (Sidak's multiple comparison test, $p < 0.05$). (D) There was no effect of drug or genotype, nor an interaction effect on cFos expression in D2 neurons in the VMS.

number of cFos positive cells and D1 neuron cFos positive cells in both dorsal and ventral striatum, and a significant effect of drug on D2 neuron cFos positive cells in the ventral, but not dorsal, striatum (Fig. A-8).

Lastly, we performed correlations between the number of cFos positive cells in dorsal and ventral striatum and B-SOID scored behavior during the last 60 minutes (corresponding to the time course of maximum cFos expression). In amphetamine treated mice, we found a significant positive correlation between the percent time in stereotypy and ventral striatum D1 neuron cFos expression ($R^2 = 0.20$, $p < 0.05$) (Fig. 2-7A). In contrast, there was a significant negative correlation between percent time in rest and ventral striatum D1 neuron expression ($R^2 = 0.17$, $p < 0.05$) (Fig. 2-7B). There was also a significant positive correlation between the percent time in locomotion and dorsal striatum D2 neuron cFos expression ($R^2 = 0.53$, $p < 0.0001$), while there was a significant negative correlation between the percent time in stereotypy and dorsal striatum D2 neuron cFos expression ($R^2 = 0.16$, $p < 0.05$) (Fig. 2-6D). For grooming and exploration, there were no significant correlations with cFos expression in any region.

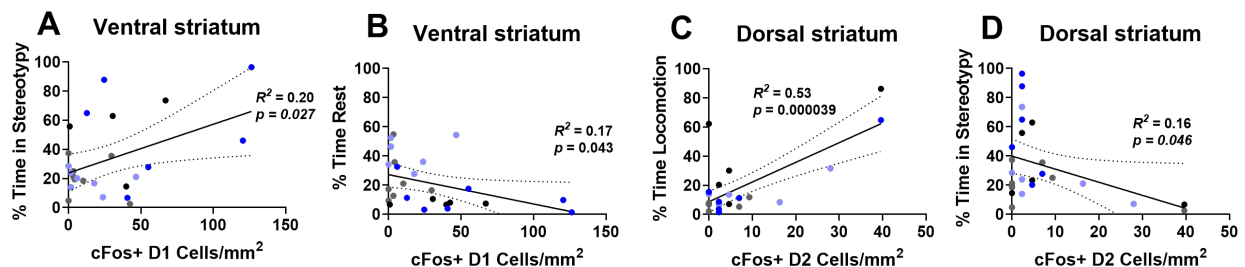


Figure 2-7 Striatal subregion cFos expression in D1 and D2 neurons is significantly correlated with distinct behavioral responses to amphetamine

2.4 Discussion

SLC1A1 is a candidate gene for OCD, and several of its polymorphisms have been associated with the disorder, although none of them have been identified as significant in GWAS studies to date (Mattheisen et al. 2015; Stewart, Yu, et al. 2013). The rs301430 polymorphism, which is highly replicated in association studies of OCD, increases expression of *SLC1A1* in lymphoblastoid cells, human brain tissue, and a luciferase reporter assay, and increases expression and activity of EAAT3, its protein product (Veenstra-VanderWeele et al. 2012; Wendland et al. 2009). In this study, we modeled this change in EAAT3 expression in mice by overexpressing *Slc1a1* in forebrain regions that have been implicated in OCD in humans and OCD-relevant behaviors in mice. We found that overexpression of *Slc1a1* resulted in increased susceptibility to the development of amphetamine-induced repetitive behavior, and that this behavior was associated with altered patterns of cFos expression in striatum. Lastly, we used a novel unbiased machine learning algorithm to cluster behavior following amphetamine and found distinct patterns of amphetamine-induced behavior in *Slc1a1*-overexpressing (OE) mice, behaviors that were again associated with particular patterns of striatal activation.

Relative to control mice, *Slc1a1*-OE mice showed increased hyperlocomotion following a low dose of amphetamine and increased stereotypy following a high dose of amphetamine. While amphetamine-induced behaviors do not model the symptoms of any particular psychiatric disorder *per se*, these are abnormal repetitive behaviors that interfere with adaptive goal-directed behaviors like food-seeking (Wolgin 2012), and may share some of the underlying neural mechanisms with OCD and OCD-related disorders (e.g. tic disorders), such as a hyperdopaminergic state and striatal involvement. In particular, while amphetamine-induced stereotypies appear to be inflexible,

animals can learn to override them, indicating that the urge to perform amphetamine-induced behaviors might share some overlap with obsessions (Wolgin 2012).

Furthermore, we found that this increased amphetamine-induced behavior was associated with particular patterns of striatal activity. We identified increased activation of VMS neurons in *Slc1a1*-OE mice as measured by c-fos, and determined that this was driven by increases in D1 neuron activation within VMS. We also found a significant increase in D1 neuron activation in *Slc1a1*-OE mice following a high dose of amphetamine, indicating the VMS may be particularly important for the behavioral effects of amphetamine in these mice. We also found correlations between cFos expression and behavior following the administration of amphetamine. We found a negative correlation between rest and D1 neuron activation in the ventral striatum. This is perhaps unsurprising, as D1 neurons throughout the striatum have been shown to promote behavioral activation. We also found that stereotypy behavior was positively correlated with cFos expression in D1 neurons in the ventral striatum and negatively correlated with cFos expression in D2 neurons in the dorsal striatum. In contrast, the opposite pattern was found for locomotion, with this behavior showing a significant positive correlation with cFos expression in D2 neurons in the dorsal striatum. This is surprising because activation of D2 neurons in the dorsal striatum have been reported to inhibit locomotion, and because locomotion and stereotypy are both amphetamine induced behaviors with high levels of activity. However, this inconsistency could be explained by the mutually exclusive nature of these two behaviors. Locomotion and stereotypy are the two most common amphetamine-induced behaviors, and these data point toward the possibility that there are separate populations of striatal neurons that drive locomotor and stereotypy behavior and that the relative activation of these two populations determines which behavior the animal expresses. However, the use of cFos is a limitation of this study, and causal experiments and *in vivo* recording

methods will necessary to test this hypothesis and determine what role each of these cell populations plays in amphetamine-induced behavior.

We found no consistent differences in grooming behavior or anxiety-like behavior in *Slc1a1*-OE mice. This is in contrast to the results of a recently published paper that shows significantly increased time spent grooming and anxiety-like behavior in *Slc1a1*-OE mice (Delgado-Acevedo et al. 2019). These differences could be due to several factors, including differences in mouse background, testing conditions, or functional levels of EAAT3 overexpression. Furthermore, while we previously reported no anxiety-like behavioral differences in mice lacking *Slc1a1* (Zike et al. 2017), two previous studies reported increased anxiety-like behavior in *Slc1a1*-knockout mice, with one of these studies reporting an increased number of grooming bouts in *Slc1a1* knockout mice as well (Afshari et al. 2017; Bellini et al. 2018). More research is therefore needed to clarify the role of EAAT3 on OCD-relevant grooming and anxiety-like behavior, and to try to delineate environmental factors that may contribute to these differences in phenotype expression.

To the best of our knowledge, this is the first study to characterize amphetamine-induced behavior using an unbiased clustering approach. Previous analyses of amphetamine-induced behavior have relied on hand-scoring of stereotypy and related behaviors or locomotor chambers for measuring distance traveled (Kelley 2001). There are significant weaknesses to these approaches, and significant advantages to an unbiased approach. Human scorers are subject to fatigue as well as experimenter bias. Furthermore, experimenters must decide *a priori* which behaviors of interest to score. In lengthy behavioral testing sessions, it is usually necessary to score only a subset of the session, which makes it difficult to understand the full time-course of the behavior as the kind of frame-by-frame scoring necessary to fully capture the behavioral time

course is so time-intensive as to be practically impossible for most experiments. In contrast, this new analysis approach allowed us to examine stereotypy behavior and locomotor behavior concurrently in a large cohort of mice, facilitating high throughput screening. Using this technique, we were able to show that mice overexpressing a candidate risk gene for OCD are more susceptible to the development of amphetamine-induced repetitive behavior.

3.0 Examining the therapeutic potential of EAAT3 ablation or inhibition in the *Sapap3*-knockout mouse model of OCD

3.1 Introduction

Obsessive compulsive disorder (OCD) is a common and debilitating neuropsychiatric disorder that affects 2-3% of the population worldwide (Kessler et al. 2005; Robins et al. 1984). It is characterized by thoughts or urges, known as obsessions, and repetitive behaviors, known as compulsions. While OCD is not an anxiety disorder per se, there is evidence that compulsions may be performed to relieve the anxiety associated with obsessions, and OCD has very high comorbidity with anxiety disorders (Pallanti et al. 2011). Current standard of care treatments for OCD include cognitive behavioral therapy and serotonin reuptake inhibitors (SRIs), but only half of the patients treated with these therapies exhibit adequate treatment response, and some have significant side effects (Dougherty et al. 2004; Koran et al. 2007). Some newer experimental therapies for OCD have shown promise, including drugs targeting the dopamine and glutamate systems (Del Casale et al. 2019; Marinova et al. 2017; Pittenger 2015), and deep brain stimulation targeting the ventral capsule/ventral striatum or subthalamic nucleus (Dell’Osso et al. 2018; Graat et al. 2017). However, none of these are first-line therapies and they are not available for most patients. Improved therapies that target the underlying pathology of the disorder are critically needed.

The ultimate causes of OCD are unknown, but twin and family studies have revealed a significant role for genetics in the etiology of the disorder (Grados and Wilcox 2007; Pauls 2008; van Grootheest et al. 2005). Early linkage studies identified association of chromosome 9p24 with

OCD (Hanna, Piacentini, et al. 2002; Willour et al. 2004) This region contains the gene *Slc1a1*, and multiple studies since have identified association of *SLC1A1* polymorphisms with OCD (Arnold et al. 2006; Cai et al. 2013; Dickel et al. 2006; Samuels et al. 2011; Shugart et al. 2009; Stewart et al. 2007; Veenstra-VanderWeele et al. 2012; Wendland et al. 2009), although see also (Stewart, Mayerfeld, et al. 2013). The rs301430 polymorphism is the most commonly implicated (Veenstra-VanderWeele et al. 2012). Importantly, this polymorphism increases expression of the encoded protein – the neuronal glutamate transporter, excitatory amino acid transporter-3 (EAAT3). The OCD-linked C allele is associated with increased *SLC1A1* expression in lymphoblastoid cells, human postmortem brain, a luciferase reporter assay, and transfected HEK cells, where there is also a functional increase in EAAT3 protein, as evidenced by increased glutamate uptake (Veenstra-VanderWeele et al., 2012; Wendland et al., 2009). EAAT3 is expressed throughout the brain, but is enriched in cortex and striatum, both regions heavily implicated in OCD by human imaging studies (Parmar and Sarkar 2016).

Several previous studies have investigated the role of *Slc1a1* in behavior and neural activity relevant to OCD. A recent paper by Delgado-Acevedo showed evidence that EAAT3 may play a role in the development of OCD-relevant behaviors (Delgado-Acevedo et al. 2019). This study showed that overexpression of *Slc1a1* in the forebrain of mice resulted in increased anxiety- and compulsive-like behavior that could be normalized with administration of the SRI fluoxetine. These mice also have differences in signaling at striatal synapses, including slower NMDA-receptor kinetics and altered NMDA-receptor subunit composition, things that have been found in other models of compulsive-like behavior as well (Nagarajan et al. 2018; Welch et al. 2007).

To test the effects of EAAT3 ablation on compulsive-like behavior, we previously created an *Slc1a1*-STOP knock-in mouse that has ablated EAAT3 protein expression and function (Zike

et al. 2017). Because these mice lack *Slc1a1* expression, we predicted that they would have reduced susceptibility to repetitive behaviors. To investigate repetitive behavior in these mice, we tested their response to pharmacologic agents that generate striatum-dependent repetitive behaviors. As predicted, *Slc1a1*-STOP mice had attenuated increases in stereotypy and hyperlocomotion in response to amphetamine, and attenuated increases in grooming in response to the dopamine D1 receptor agonist SKF-38393. This indicates that ablation of EAAT3 might be protective against the development of repetitive behavior. This behavioral phenotype was partially rescued by re-introduction of *Slc1a1* into the midbrain, indicating that knockout of EAAT3 in this region may be at least partially responsible for the observed behavioral abnormalities.

Mice with global knockout of *Sapap3* (*Sapap3*-KO mice) have previously been used as a model of OCD-relevant behavior (Welch et al. 2007). These mice show anxiety-like behavior and a compulsive grooming phenotype that causes them to overgroom to the point of developing skin lesions. These phenotypes can be reversed by administration of chronic fluoxetine, or by re-introduction of *Sapap3* into the striatum via lentiviral injection. *Sapap3*-KO mice also show reduced fEPSP amplitudes and increased NMDA-receptor NR2B subunit expression relative to controls, and follow-up studies demonstrated increased dopamine turnover (Wood et al. 2018). Our preliminary data also show increased EAAT3 protein expression in the striatum of *Sapap3*-KO mice (Fig. A-10). This suggests that increased *SLC1A1* expression may contribute to the generation of abnormal repetitive behaviors, and lead to the prediction that reducing EAAT3 activation may reduce compulsive behavior.

To test this hypothesis, we conducted two sets of experiments. The first of these examined compulsive grooming in *Sapap3*-KO mice given two different doses of an EAAT3 inhibitor. This drug, developed and provided to us by Roche, was previously shown to reduce overgrooming in

Shank3-KO mice, a model of autism-like behavior (Fig. A-11). The second set of experiments investigated the effects of genetic ablation of *Slc1a1* on anxiety-like behavior and compulsive grooming in *Sapap3*-KO mice.

3.2 Methods

3.2.1 Mice

All procedures were carried out in accordance with the guidelines set out by the NIH in the Guide for the Care and Use of Laboratory (Guide for the Care and Use of Laboratory Animals, 1996) and were approved by the University of Pittsburgh Institutional Animal Care and Use Committee (IACUC). All mice were housed in cages of 3-5 mice/cage with free access to water and rodent chow. Mice were on a 12hr:12hr light/dark cycle, with lights on at 7:00AM and lights off at 7:00PM.

3.2.1.1 *Sapap3* mice

Sapap3-KO mice were derived from the colony originally generated at MIT by Dr. Guoping Feng. To generate *Sapap3*-KOs and wild-type (WT) littermates on a mixed C57 and 129s background, *Sapap3*-heterozygous (*Sapap3*-Het) mice on a 100% C57BL/6 background were crossed with mice on a 100% 129S1/SvImJ background. The resulting *Sapap3*-Het progeny were mated, resulting in *Sapap3*-KO and littermate *Sapap3*-WT mice on a mixed background that was ~50% C57BL/6 ~50% 129S1/SvImJ. Mice were 3-6 months old at time of testing.

3.2.1.2 *Slc1a1*-STOP mice

Slc1a1-STOP mice were generated as previously described (Tanaka et al. 2010; Zike et al. 2017). Briefly, BAC recombineering was used to construct a NeoSTOP-tetO plasmid, and the STOP-tetO cassette was inserted just upstream of the *Slc1a1* translation initiation start site (Figure 1). The NeoSTOPtetO was located between two homologous arms and consisted of a multicloning site 1, loxP, FRT, HSV thymidine kinase poly(A) minigene, STOP sequence, FRT, tetO sequence, loxP, and minicloning site 2. The linearized NeoSTOP-tetO cassette was transferred into bacteria. The targeting vector was isolated from the recombined kanamycin-resistant clone using a retrieving technique and inserted into the plasmid. Eight colonies were found to be kanamycin resistant, and two of the eight were found to contain the NeoSTOP-tetO cassette via direct PCR. The targeting vector was electroporated into a 129SvEvTac mouse ES cell line in the Duke Embryonic Stem Cell Core. Homologous recombinants were detected using PCR, an dtransgene incorporation was verified using Southern blot. Positive ES clones were injected into C57BL/6J blastocysts to obtain chimeric mice, which were crossed to 129S6/SvEvTac females to obtain germline transmission. Offspring were then established as *Slc1a1*-STOPtetO heterozygous knockins on a pure 129S6/SvEvTac background.

3.2.1.3 *Sapap3/Slc1a1* mice

Sapap3-het mice were bred with *Slc1a1*-Heterozygous (*Slc1a1*-Het) mice to create *Sapap3*-het//*Slc1a1*-het mice. These mice were then bred to create experimental mice that were either *Sapap3*-WT//*Slc1a1*-STOP, *Sapap3*-WT//*Slc1a1*-Het, or *Sapap3*-KO//*Slc1a1*-WT littermates. Only *Sapap3*-KO mice were used for these experiments; however, to obtain sufficient experimental animals, *Sapap3*-Het mice were used as breeders, as *Sapap3*-KO mice have small litter size and poor litter survival to adulthood.

3.2.2 Behavioral testing

All testing was conducted between the hours of 8:00AM and 6:00PM. Mice were habituated in their home cages to the testing room for 20-40 minutes prior to testing. Each behavioral apparatus was washed with 70% EtOH and allowed to dry completely between mice.

3.2.2.1 Anxiety tests

Anxiety testing occurred in unhandled, naïve mice prior to any other testing. The tests were conducted in the following order: open field (OF) test, elevated plus maze (EPM) test, and light dark (LD) test, with one day between tests.

3.2.2.1.1 Open field test

Mice were placed into the center of a 41 cm X 41cm Plexiglas open field chamber under room lights for 30 minutes. Locomotor activity was scored by detecting interruptions of infrared beams by the body of the mouse; data was collected and analyzed using Motor Monitor (Kinder Scientific). The total distance as well as the time and distance in the center (10 cm X 10 cm) of the chamber was recorded.

3.2.2.1.2 Elevated plus maze test

The elevated-plus maze is a cross maze that consists of two open and two closed 30×5 cm arms. Top-view video was recorded using an Any Maze video camera, and automated tracking of the mouse (Any Maze). Time spent in the open arms, distance traveled in the open arms, and total distance traveled was recorded for 5 minutes.

3.2.2.1.3 Light dark test

The light dark chamber consists of two equally sized chambers (24cm x 24cm), one enclosed and dark and one brightly lit (~300lux). Mice are placed in the dark side of the chamber and allowed to freely explore both sides for 10 minutes. Locomotor activity was scored by detecting interruptions of infrared beams by the body of the mouse; data was collected and analyzed using Motor Monitor (Kinder Scientific). The total distance as well as the time and distance in the light and dark sides of the chamber was recorded.

3.2.2.1.4 Grooming assessment

For assessment of grooming behavior, mice were placed in a plexiglass chamber (20 cm x 20cm) and video recorded (Cannon) for 30 minutes. A trained experimenter blind to group then scored the amount of time spent grooming during the three sessions.

3.2.3 EAAT3i delivery

The EAAT3 inhibitor (EAAT3i) was provided to us by Roche. Due to high mortality in the Sapap3-KO mice after gavage administration of the drug, it was administered to subsequent cohorts in sweetened condensed milk. Mice were scruffed and trained to consume sweetened condensed milk for 2 days prior to the experiment. On the day of the experiment, mice were weighted and fed the appropriate amount of sweetened condensed milk with drug or vehicle 1 hour prior to grooming assessment.

3.2.4 Western Blot

Western blot was performed according to Zike et al. (2017). Briefly, brains were extracted from mice after rapid decapitation and immediately frozen on an ice-cold metal platform. Sections were cut on a microtome and the whole striatum was dissected and homogenized. Protein concentrations of all samples were determined by a bicinchoninic acid (BCA) protein assay (Thermo Fisher Scientific). Equal amounts of protein were incubated with a Laemmi sample buffer for 5 minutes at room temperature. Samples were analyzed by SDS/PAGE followed by Western blotting. EAAT3 protein was visualized using a rabbit anti-EAAC1/EAAT3 antibody (1:1,000 dilution; EAAC110A, Alpha Diagnostics).

3.2.5 In situ

In situ hybridization was performed based on the Allen Brain Atlas Protocol using a digoxigenin (DIG)-labeled *Slc1a1* cRNA probe previously described (Tanaka et al., 2012). Mice were rapidly decapitated and brains immediately frozen on dry ice. Sections were sliced at 14 μ m on a cryostat and mounted on directly to slides. Slide-mounted sections were treated with 4% paraformaldehyde in 1 X phosphate buffered saline (PBS) for 20 min, washed in 1X PBS for 5 min, treated with 0.2M HCL, washed in 1X PBS for 5 min, and then treated with 40 μ g/mL of Proteinase K (Roche, Basel, Switzerland) for 20 min. Slides were again washed in 1X PBS and fixed again in 4% PFA in 1X PBS for 20 min, washed in 1X PBS, and acetylated with 0.25% acetic anhydride (Sigma-Aldrich) in 1% triethanolamine (Sigma-Aldrich) for 10 min. Sections were pre-hybridized for 3 hr at room temperature in hybridization buffer, made up of 50% formamide (Roche), 5X saline sodium citrate buffer (SCC), 5X Denhardtts (Sigma-Aldrich), 0.25 mg/mL yeast

tRNA (Ambion, Carlsbad, CA), and 0.4 mg/mL Salmon Sperm DNA (Stratagene, La Jolla, CA). Sections were then hybridized for 16 hr at 65°C in the hybridization buffer with 2% dextran sulfate and the DIG-labeled *Slc1a1* probe (created using a probe labeling kit, Roche). After hybridization, sections were washed with dilutions of 5X SSC for 5 min 65°C, 2X SSC for 5 min 65°C, and 0.2X SSC/50% formamide for 30 min room temperature. Slides were then incubated in blocking buffer (1% blocking reagent: Roche) for 30 mins and incubated with anti-DIG phosphatase-conjugated antibody (1:5000, Roche) for 90 mins at room temperature. They were then washed with MABT (100 mM Maleic Acid, 150 mM NaCl, 0.1% Tween-20, pH 7.5) followed by an incubation with nitroblue tetrazolium chloride/5-bromo-4-chloro-3-indolyphosphate p-toluidine salt (NBT/BCIP) color substrate (Roche) in the dark for 24hrs at 32°C. The color reaction was stopped with Tris-EDTA washes, and sections coverslipped with Aqua Poly/Mount (Polysciences, Warrington, PA). Sections were imaged with an Olympus 120VS Slide-scanning scope. Cell counts were conducted using Image-J (NIH, Bethesda, MD).

3.2.6 Statistical analysis

Data were analyzed using Prism (GraphPad, La Jolla, CA, USA). Two-tailed, unpaired Student t-test or two-way ANOVA were used to analyze the primary data. Specific statistical analyses for each data set are described in results and in the figure legends. All data are reported as the mean \pm standard error of the mean. Geisser-Greenhouse corrections were used for ANOVA where appropriate.

3.3 Results

The initial characterization of *Sapap3*-KO mice on a 129S background showed increased anxiety-like behavior (Welch et al. 2007). However, previous experiments in our lab failed to find a robust anxiety-like behavioral phenotype in *Sapap3*-KO mice on a C57Bl/6 background (Fig. A-12). In order to investigate the effect of background on anxiety-like behavior in *Sapap3*-KO mice and to see baseline behavior in *Sapap3*-KO prior to EAAT3 ablation, we crossed *Sapap3*-KO mice on a C57Bl/6 background with 129S mice for 1 generation. The resulting offspring were tested for anxiety-like behavior in the open-field (OF), elevated-plus maze (EPM), light/dark (L/D), and elevated zero maze (EZM) tests. *Sapap3*-KO mice showed a reduction in both the percent time (repeated measures two-way ANOVA; genotype main effect, $F(1, 51) = 6.04$, $p < 0.05$) and percent distance (repeated measures two-way ANOVA; genotype main effect, $F(1, 51) = 15.04$, $p < 0.001$) spent in the anxiogenic center of the OF relative to *Sapap3*-WT controls (Figure 3-1A, B). Similarly, they showed a reduction in both the percent time (unpaired t-test, $t(51) = 5.57$, $p < 0.001$) and percent distance (unpaired t-test, $t(51) = 6.271$, $p < 0.001$) in the anxiogenic light side of the LD chamber (Figure 3-1C, D). *Sapap3*-KO showed a reduction in the percent time in the anxiogenic open track of the EZM (Unpaired t-test, $t(51) = 2.91$, $p < 0.01$) compared to *Sapap3*-WT mice (Figure 3-1F), but no difference in time spent in the anxiogenic open arms of the EPM (Unpaired t-test, $t(51) = 0.81$, $p = 0.42$; Figure 3-1E). In addition to increased anxiety-like behavior seen in *Sapap3*-KO mice, there was also a decrease in locomotion in these mice compared to *Sapap3*-WT mice. In both the OF and LD tests, *Sapap3*-KO mice showed significantly reduced distance traveled compared to *Sapap3*-WT mice, similar to *Sapap3*-KO mice on a C57Bl/6 background (Fig. A-12).

To test whether EAAT3 activity is necessary for the compulsive overgrooming seen in *Sapap3*-KO mice, we administered two doses (30mg/kg and 100mg/kg) of an EAAT3 inhibitor (EAAT3i) or vehicle (VEH) to *Sapap3*-KO mice and *Sapap3*-WT controls via gavage prior to a grooming assessment. In the initial cohort of mice, there was significantly increased mortality in the *Sapap3*-KO mice relative to controls following gavage feeding (data not shown), which prevented us from determining if EAAT3i reduced compulsive overgrooming behavior. Therefore, we dissolved the EAAT3i in sweetened condensed milk and trained mice to consume this mixture from a needle prior to the experiment. Mice were then administered one of two doses of EAAT3i or VEH 1 hour prior to a 15 minute grooming assessment. One week later, mice were administered VEH or EAAT3i in a crossover design. There was a main effect of genotype, with *Sapap3*-KO mice showing increased grooming time relative to *Sapap3*-WT controls (Two-way ANOVA genotype main-effect, $F(1, 124) = 16.53, P < 0.001$). However, there was no drug effect, with vehicle, low dose, and high dose EAAT3i producing similar levels of grooming in both *Sapap3*-KO and *Sapap3*-WT mice (Figure 3-2).

EAAT3 activity has been shown to be necessary for amphetamine-induced decreases in firing rate of midbrain dopamine cells (Underhill et al. 2014). We took advantage of this to confirm activity of the EAAT3i and ensure that our results could not be attributed to a lack of drug activity. We administered EAAT3i to anesthetized mice 1 hour following administration of amphetamine (3 mg/kg). As previously seen, amphetamine administration significantly reduced the firing rate of dopamine cells, a result which was blunted by the administration of 30 mg/kg EAAT3i (repeated measures ANOVA, time x drug interaction, $F(29, 163) = 2.21, p < 0.01$) (Fig. A-13).

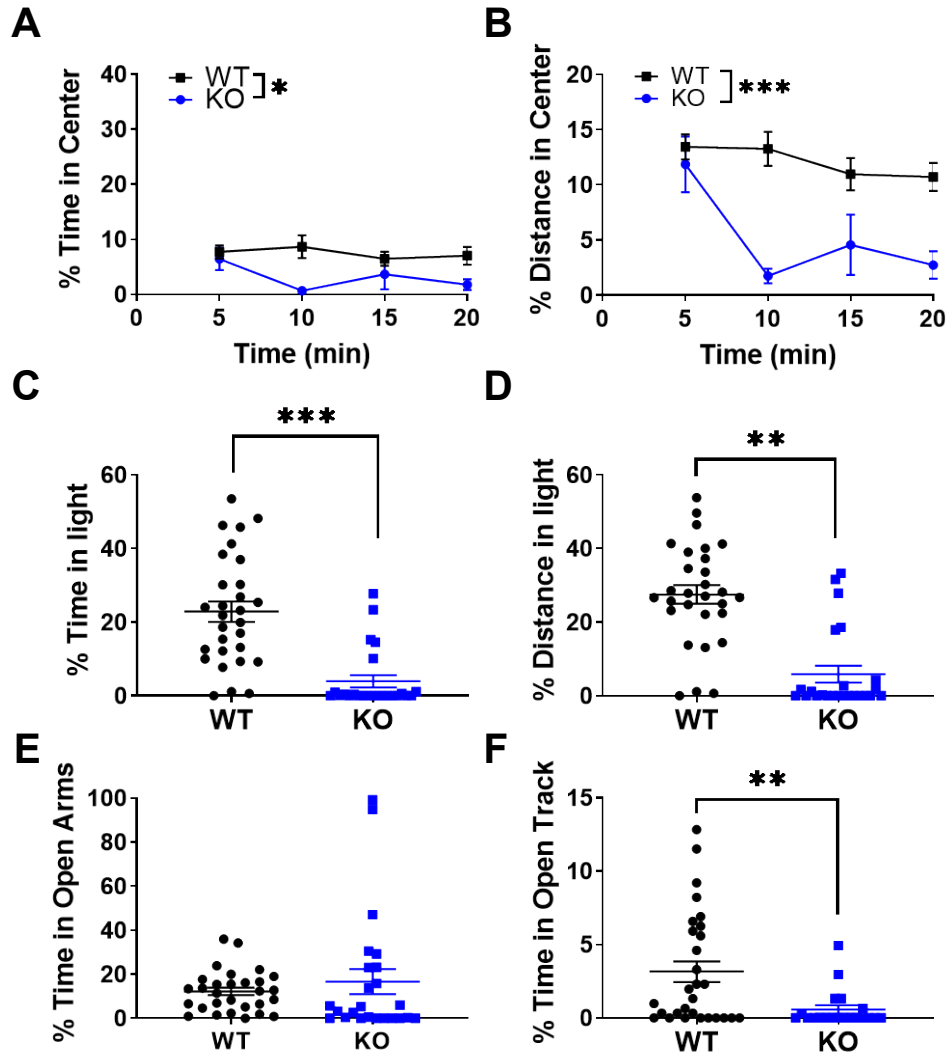


Figure 3-1 *Sapap3*-KO mice on a 129s background show a robust anxiety-like behavioral phenotype

(A, B) *Sapap3*-KO mice show a significant decrease in percent time (two-way repeated measures ANOVA; genotype main effect, $F(1, 51) = 6.04, p < 0.05$) and percent distance (two-way repeated measures ANOVA; genotype main effect, $F(1, 51) = 15.04, p < 0.001$) spent in the center of the OF arena compared to *Sapap3*-WT controls. (C, D) *Sapap3*-KO mice show a significant decrease in percent time (unpaired t-test, $t(51) = 5.57, p < 0.001$) and percent distance (unpaired t-test, $t(51) = 6.271, p < 0.001$) in the light side of the LD chamber compared to *Sapap3*-WT controls. (E) *Sapap3*-KO mice show no significant difference in the percent time spent in the open arms of the EPM compared to *Sapap3*-WT mice. (F) *Sapap3*-KO show a significant decrease in the time spent in the open track of the EZM relative to *Sapap3*-WT controls (unpaired t-test, $t(51) = 2.91, p < 0.01$).

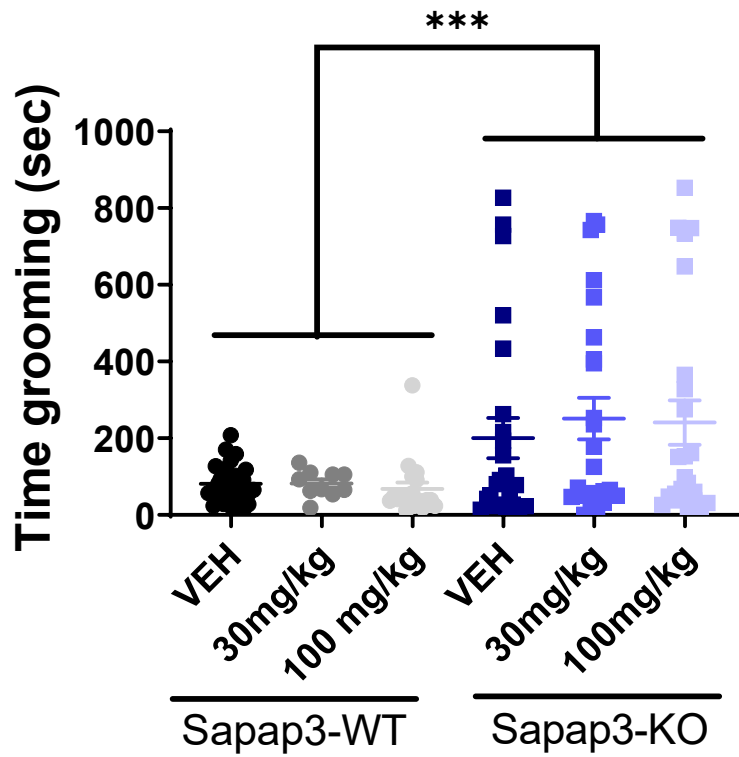


Figure 3-2 Administration of an EAAT3 inhibitor does not normalize compulsive grooming behavior in *Sapap3*-KO mice

Sapap3-KO mice show a significant increase in grooming time relative to *Sapap3*-WT mice, across all three drug dose (two-way ANOVA genotype main-effect, $F(1, 124) = 16.53$, $P < 0.001$). There was no significant effect of drug on grooming time in *Sapap3*-KO or *Sapap3*-WT mice, and no interaction of genotype X drug.

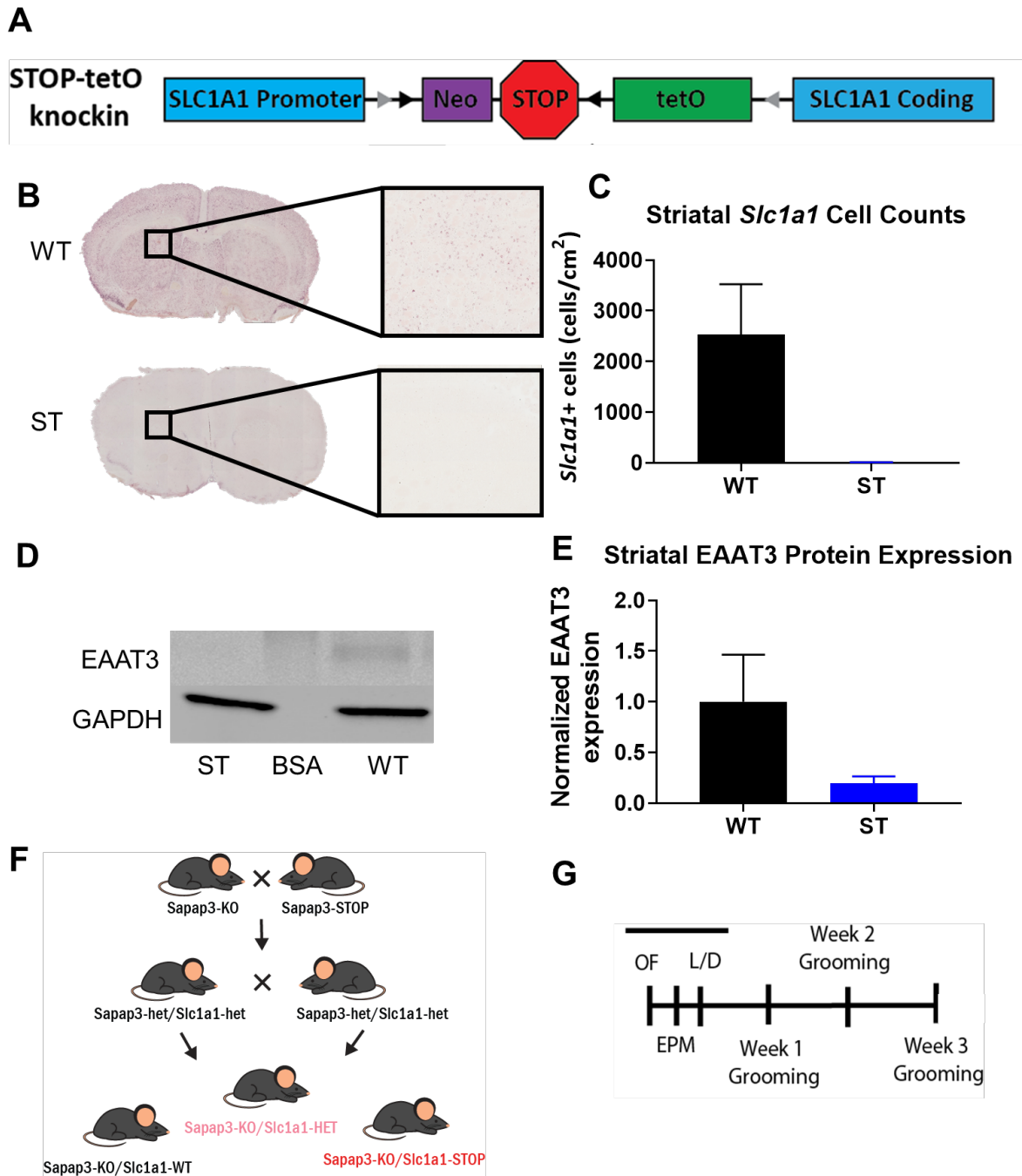


Figure 3-3 *Slc1a1*-STOP mice show ablated *Slc1a1* mRNA and EAAT3 protein expression

(A) Schematic of the *Slc1a1*-STOP construct. Black triangles represent flippase recognition target sequences, and grey triangles represent LoxP sites. Neo: PGK-EM7-NEO minigene, STOP; Stop signal, tetO: tetracycline operon. (B, C) *Slc1a1*-STOP mice have reduced *Slc1a1* mRNA as measured by *in situ* hybridization (Unpaired t-test, $t(2) = 2.54, p < 0.05$). (D, E) *Slc1a1*-STOP mice have reduced EAAT3 expression measured by Western blot (Paired t-test, $t(2) = 2.16, p < 0.05$). (F) Schematic of *Sapap3*-KO/*Slc1a1*-STOP breeding strategy. (G) Timeline of behavioral experiments in *Sapap3*-KO/*Slc1a1*-STOP.

We next turned to lifetime genetic ablation of EAAT3 activity to test the role of this protein in behavior in *Sapap3*-KO mice (Fig. 3-3A). To validate the efficacy of our *Slc1a1*-STOP mouse model of ablated EAAT3 expression, we quantified *Slc1a1* mRNA and EAAT3 protein in these mice. As predicted, *Slc1a1*-WT mice show *Slc1a1* mRNA expression throughout the whole brain, as measured by *in situ* hybridization (Fig A-14). In particular, *Slc1a1*-WT mice show high levels of *Slc1a1* mRNA expression in the striatum. In contrast, *Slc1a1*-STOP mice have undetectable levels of *Slc1a1* mRNA in these regions (unpaired t-test, $t(2) = 2.54$, $p < 0.05$) (Fig.3-3A, B). Furthermore, immunoblots of whole striatal punches similarly show ablated EAAT3 expression in *Slc1a1*-STOP mice compared to controls (Fig. 3-3B, C; Paired t-test, $t(2) = 2.16$, $p < 0.05$). *Sapap3*-KO mice with full (*Slc1a1*-STOP) or partial (*Slc1a1*-Het) EAAT3 ablation and *Sapap3*-KO mice with normal levels of EAAT3 expression (*Slc1a1*-WT) were tested for OCD-relevant behaviors. These mice underwent anxiety- like behavioral testing at 4 weeks of age – specifically - they were run through the OF, EPM, and LD test with one day between testing sessions. Following the completion of anxiety testing, mice underwent grooming assessment once per week for 3 weeks, beginning at 4 months of age (Fig. 3-3F, G).

In the OF test there was no significant difference between groups in the percent time or percent distance spent in the center of the open field (Fig. 3-4A, B). In the EPM test, there was no significant difference between groups in the percent time or percent distance spent in the open arms, and there was no difference in percent entries into the open arms (Fig. 3-4C, D). In the LD test, there was no significant difference in the percent time or percent distance spent in the light side of the chamber (Fig. 3-4E, F). In addition to these measures of anxiety-like behavior, there

was no difference in locomotion on any of these tests, with all three groups having similar total distance traveled in the OF, EPM, and LD tests (data not shown).

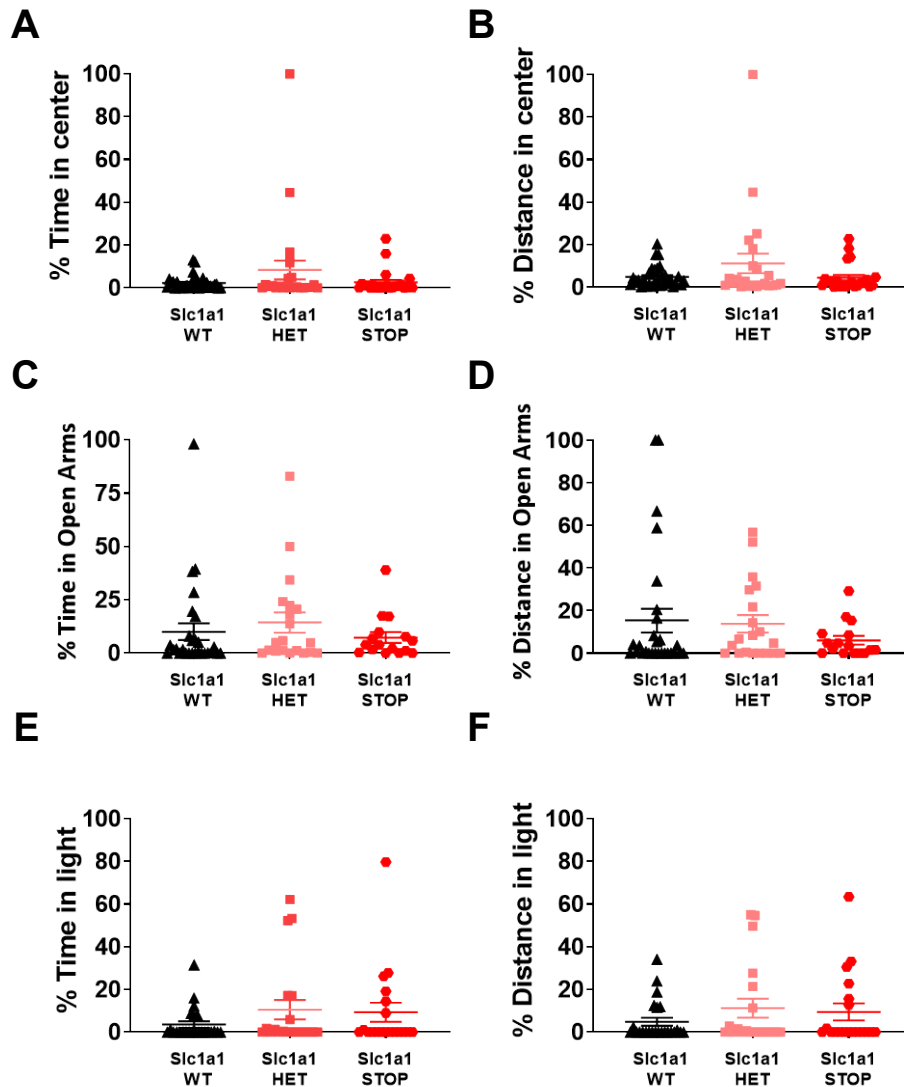


Figure 3-4 *Slc1a1* ablation does not rescue anxiety-like behavior in *Sapap3*-KO mice

(A, B) *Sapap3*-KO mice with normal (*Slc1a1*-WT), reduced (*Slc1a1*-HET), or ablated levels of *Slc1a1* expression show no differences in percent time (one-way ANOVA; $F(2, 76) = 1.934, p = 0.15$) or percent distance (one-way ANOVA; $F(2, 76) = 0.05, p = 0.94$) in the center of the OF. (C, D) *Sapap3*-KO mice with varying levels of *Slc1a1* expression show no differences in percent time (one-way ANOVA; $F(2, 76) = 0.66, p = 0.52$) or percent distance (one-way ANOVA; $F(2, 76) = 0.92, p = 0.41$) in the open arms of the EPM. (E, F) *Sapap3*-KO mice with varying levels of *Slc1a1* expression show no differences in percent time (one-way ANOVA; $F(2, 76) = 0.117, p = 0.32$) or percent distance (one-way ANOVA; $F(2, 76) = 1.0, p = 0.48$) in the light side of the LD chamber.

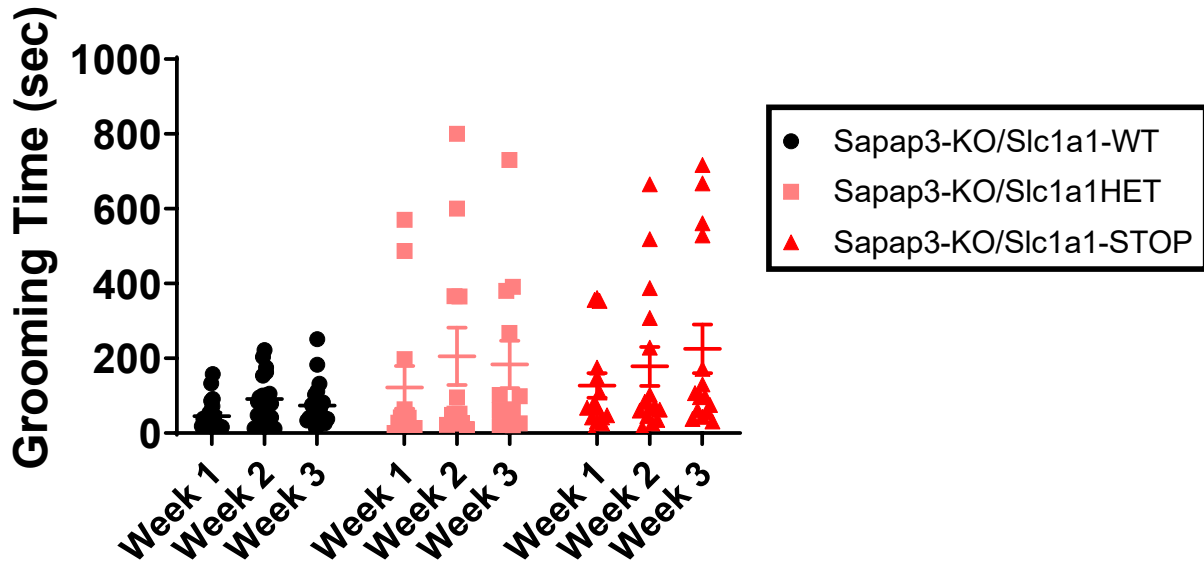


Figure 3-5 *Slc1a1* ablation does not normalize grooming in *Sapap3*-KO mice

Sapap-KO mice with normal (*Slc1a1*-WT), reduced (*Slc1a1*-HET), or ablated (*Slc1a1*-STOP) *Slc1a1* expression show no differences in grooming time across week. There is a main effect of time, with grooming increasing over subsequent (repeated measures two-way ANOVA; $F(1.72, 77.26) = 7.44, p < 0.01$). There was a trend toward a genotype main effect (repeated measures two-way ANOVA; $F(2, 45) = 2.96, p = 0.062$), with a paradoxical increase in grooming time in the mice with lower levels of *Slc1a1* expression. There was no significant interaction between time and genotype.

3.4 Discussion

OCD, like other psychiatric illnesses, is a tremendously complex disorder with a multifaceted etiology and heterogenous presentation. Unlike diseases in almost every other area of medicine, there are no biologic markers or diagnostic tests for OCD. This lack of markers has hindered the development of rationally designed therapies, as the underlying biological pathways that could be targeted to affect symptom improvement are largely unknown. Partially as a result

of this, classes of medication for the treatment of OCD have been approved for decades. Some of the most consistent findings in OCD involve dysfunction of the glutamatergic system, including genetic evidence from a variety of association studies implicating polymorphisms in *SLC1A1* in OCD (Arnold et al. 2006; Cai et al. 2013; Dickel et al. 2006; Samuels et al. 2011; Shugart et al. 2009; Stewart et al. 2007; Veenstra-VanderWeele et al. 2012; Wendland et al. 2009). In this chapter, we attempt to therapeutically target, both genetically and pharmacologically, EAAT3/*Slc1a1*, one of the most promising early findings from genetic studies of OCD. First, we blocked EAAT3 pharmacologically by administering a novel EAAT3 inhibitor to *Sapap3*-KO mice. Second, we ablated EAAT3 throughout development by crossing *Sapap3*-KO mice with mice from our *Slc1a1*-STOP line. We then examined the impact of these interventions on OCD-relevant behavior, including grooming behavior and anxiety-like behavior.

Sapap3-KO mice are the most well-validated and well-characterized transgenic model of OCD-relevant behavior and associated abnormalities in neural activity. These mice show compulsive overgrooming, a pathological repetitive behavior with direct correlates to human OCD symptoms, and anxiety-like behavior, which is often seen in OCD patients. The overgrooming and anxiety-like behavior can be rescued with administration of an SRI, the first-line pharmacologic treatment for OCD patients (Welch et al. 2007), and the overgrooming can be rescued with re-introduction of *Sapap3* into the striatum, a region consistently implicated in human OCD. These mice also display a variety of specific abnormalities in glutamatergic signaling within CTSC circuitry, including decreased cortico-striatal fEPSPs, increased NR1 and NR2B and decreased NR2A expression in striatum, increased AMPAR activation and mGluR5 activity in striatum, and strengthened inputs from secondary motor cortex to striatum (Ade et al. 2016; Corbit et al. 2019; Welch et al. 2007). SAPAP3 is expressed in the postsynaptic density at excitatory synapses.

EAAT3 is also expressed post-synaptically at excitatory synapses, and there are many potential pathways upon which the activity of these two proteins could converge, including activation of glutamate receptors and trafficking glutamate receptors to the cell surface. Lastly, *Sapap3*-KO mice show increased *Slc1a1*-expression (Fig. A-10) making EAAT3 an encouraging target for investigation in this preclinical model.

Contrary to our predictions, *Sapap3*-KO mice treated with two doses (30 mg/kg and 100mg/kg) of an EAAT3 inhibitor showed no differences in grooming behavior 1 hour following treatment (Figure 3-2). This is in contrast with findings in *Shank3B*-KO mice, a model of autism-like behavior that also shows increased grooming compared to *Shank3B*-WT mice. In *Shank3B*-Kos, overgrooming was significantly reduced by pretreatment with 30 mg/kg EAAT3i 1 hr prior (Fig. A-9). This indicates that the mechanism underlying overgrooming in these two models likely differs, which may be consistent with the fact that they are attempting to model symptoms of distinct psychiatric disorders.

There are many possible explanations for the lack of effect of the EAAT3i on grooming in *Sapap3*-KOs. The pharmacology and pharmacodynamics of this novel drug are unknown. Therefore, the dose and time course of the drug administration we chose might have been incorrect, and it is possible that sufficient drug was not present at the relevant synapses to affect EAAT3 activity and therefore grooming at the time of testing, either because of insufficient blood brain barrier penetration or rapid metabolism. However, this is unlikely to be the case, both because of behavioral effects seen in the *Shank3B*-KO mice using this same time-course and dose as well as the *in vivo* effects of EAAT3i on dopamine neuron firing rate (Figure A-3). Furthermore, our results from studies utilizing genetic ablation of EAAT3 (see below) support the idea that activity of EAAT3 is not necessary for overgrooming in *Sapap3*-KO mice. While EAAT3 protein was

increased in *Sapap3*-KOs, activity of EAAT3, measured by cysteine uptake, was unaffected (Figure A-5). Specific EAAT3 inhibitors have not been widely available, and most of the evidence we have for the glutamatergic activity of EAAT3 comes from studies using non-specific inhibitors that also target other EAATs, genetic knockout of *Slc1a1*, or cysteine reuptake. All of these approaches have significant weaknesses, and future studies investigating the use of specific EAAT3 inhibitors on the glutamatergic system both *in vivo* and in slice have great potential to improve our understanding of the role of EAAT3 in both health and disease.

Genetic ablation of EAAT3 had no significant effect on anxiety-like behavior (Figure 3-4) or grooming behavior (Figure 3-5) in *Sapap3*-KO mice (Figure 3-4). There could be several explanations for this. Lifetime knockout of a protein can have extreme effects on normal development, and there may be compensatory changes that prevent normalization of behavior in *Sapap3*-KO mice. Furthermore, SAPAP3 might be downstream of EAAT3 signaling, meaning that changing EAAT3 levels would have no behavioral effects on *Sapap3*-KO mice. In addition, baseline levels of behavior in the *Sapap3/Slc1a1* cross are different from those we would normally expect in *Sapap3*-KO mice. In particular, the baseline levels of grooming seen in these mice resemble the *Sapap3*-WT grooming levels seen previously (Fig. 3-2). Lack of littermate control *Sapap3*-WT mice for comparison is a weakness of this study, but was not possible due to the breeding scheme required to produce the double transgenic mice. Lastly, EAAT3 signaling may be unrelated to behavior in *Sapap3*-KO mice, or to behavioral abnormalities seen in OCD patients. More research is necessary to clarify the exact role of EAAT3/*Slc1a1* in OCD-relevant behaviors.

4.0 Conclusions

4.1 Dissertation background

OCD is a serious neuropsychiatric illness with a significant negative impact on the quality of life of both patients and family members of patients (Koran et al. 2007; Koran, Thienemann, and Davenport 1996), and it is a large economic burden on society as a whole (DuPont et al. 1995). Up to 50% of OCD patients do not show adequate response to current standard-of-care treatments, and new therapeutics for the disorder are clearly needed. Useful preclinical models of OCD are an important step on this pathway. To date, there are no biological markers routinely used to diagnose any psychiatric disorder in the clinical setting; in fact, in certain situations, biological markers are used to rule out general medical causes of psychiatric symptoms and therefore confirm a psychiatric diagnosis. This lack of markers, and a general inaccessibility of/inability to directly measure from the organ system involved (i.e. the brain) in most patients has made preclinical animal modeling of psychiatric disorders instrumental as a bridge from the pathology of a disorder to its behavioral symptoms.

Rodent models have taught us a tremendous amount about the biology of mental illness, and this progress has only accelerated in recent years, with the development of powerful techniques for monitoring and manipulating specific cell populations (Fenno et al 2019) and analyzing large data sets (Glaser et al 2019). However, this improved understanding of the brain and behavior is yet to be accompanied by a widespread improvement in the way psychiatric disorders are treated or a meaningful increase in the approval of novel medications for psychiatric disorders (the recent approval of esketamine for the treatment of depression and brexanolone for the treatment of post-

partum depression being notable exceptions). Part of this has likely stemmed from a lack of construct validity of the animal models used (Bale et al 2019). While understanding behavior and neurobiology in rodents is necessary and interesting in its own right, this understanding likely needs a clear and valid connection to the human disorder to lead to novel treatments. To this end, genetic studies have proved fruitful for providing us with “bedside-to-bench” input upon which to base animal models.

Unfortunately, genetic studies of OCD have yet to find consistently reproducible genes of interest. First, genome-wide association studies (GWAS) have yet to identify significant variants for OCD (Fernandez et al 2018). It is still early in the search for OCD risk genes. The sample sizes for the GWAS studies are likely still too small to reliably identify genes with the small effect size thought to be involved in OCD. To date, GWAS studies of OCD have included 2688 OCD cases and 7037 controls. For comparison, the GWAS study of schizophrenia that found 108 significant risk genes included 36,989 cases and 113,075 controls.

Rare variants with large effect size have been tremendously useful for modeling other disorders; however, only two such variants have been recently identified in OCD to date, and still have not been formally translated into animal models to study OCD. These two variants are SCUBE1 and CHD8 (Cappi et al. 2020). SCUBE1 is a relatively understudied gene. It is expressed in the developing brain, but has mostly been studied in the context of platelet activation and adhesion (Wu et al. 2014). De novo variants of CHD have previously been associated with autism spectrum disorders (Sanders et al. 2012), with some reports indicating that this gene may be associated with repetitive behaviors in autism spectrum disorders (Bernier et al. 2014). Work to model these genetic findings in rodents is currently underway, as are large scale coordinated searches for other rare variants of large effect size.

At the beginning of the work for this dissertation, *SLC1A1* was the most promising genetic target in OCD, with a variety of gene association studies suggesting a link between polymorphisms of this gene and OCD (Arnold et al. 2006; Cai et al. 2013; Dickel et al. 2006; Samuels et al. 2011; Shugart et al. 2009; Stewart et al. 2007; Veenstra-VanderWeele et al. 2012; Wendland et al. 2009). Knockout of this gene had been done prior (by our group in collaboration with a group at Columbia University). The findings showed that ablation of this gene was protective against the development of pharmacologically-induced repetitive behavior (Zike et al. 2017). This fit with what was known about the role of the most common *SLC1A1* polymorphism in OCD, which was increases expression of *SLC1A1* and its protein product. Therefore, the goal of this dissertation was twofold: (1) Determine whether overexpression of *Slc1a1* in a rodent model would result in the development of OCD-relevant behaviors and neural activity, and (2) Follow up on the initial *Slc1a1* ablation results to further investigate the therapeutic potential of blocking this gene or its protein product in a mouse model of OCD-relevant behavior.

4.2 Summary of findings

4.2.1 Chapter 2: EAAT3 overexpression increases susceptibility to the development of amphetamine-induced repetitive behaviors

In Chapter 2, I investigated the effect of EAAT3 overexpression on OCD-relevant behavior and neural activity. To overexpress EAAT3 in forebrain neurons, I crossed *Slc1a1*-NeoSTOP-tetO mice with a flippase mouse line to excise the Neo-STOP cassette (Fig. 2-1A). I then crossed these *Slc1a1*-tetO mice with CaMKII-tTA mice to obtain *Slc1a1*-tetO/CaMKII-tTA mice and tTA-

littermate controls. These mice overexpress EAAT3 at extremely high levels at baseline, and this overexpression can be reversed in a dose-dependent manner by the administration of doxycycline (Fig. 2-1B, C). Mice were either born and raised on a low dose of doxycycline (lifetime overexpression) or born and raised on a high dose of doxycycline and switched to a low dose at 8 weeks of age (adult-specific overexpression). Both groups were then tested for a variety of OCD-relevant behaviors, including anxiety-like behaviors, grooming behavior, and repetitive behavioral response to amphetamine (Fig. 2-1D).

I showed that both lifetime and adult-specific EAAT3 overexpression results in a significant increase in behavioral response to amphetamine. Both lifetime and adult-specific *Slc1a1*-OE mice show a significantly potentiated locomotor response to a low dose (3mg/kg) of amphetamine and a significantly potentiated stereotypy response to a high dose (8mg/kg) of amphetamine compared to tTA- controls (Fig. 2-2). In contrast, I found no significant effect of EAAT3 overexpression on grooming behavior (Fig. A-1). In addition, I observed conflicting findings on tests of anxiety-related behavior. The initial cohort of lifetime *Slc1a1*-OE mice (Cohort 1) showed a significant increase in anxiety-like behavior relative to tTA- controls, while adult-specific *Slc1a1*-OE mice showed no such differences. Specifically, lifetime *Slc1a1*-OE mice showed significantly increased time spent in the center of the open field (OF) and time spent in the open arms of the elevated plus maze (EPM) compared to tTA+ mice (Fig. A-2). However, these findings were not replicated in subsequent cohorts. Potential reasons for this include genetic drift of the background strain in subsequent cohorts as well as changes in level of stress within the animal housing facility.

To begin to dissect the neural circuits involved in this increase in amphetamine-responsivity, I next examined the cFos response to high-dose amphetamine in a separate cohort of

Slc1a1-OE mice. I found that EAAT3 overexpression again produced a robust increase in the amount of stereotypy, with *Slc1a1*-OE mice engaging in stereotypy at significantly higher levels than tTA- littermate controls and vehicle treated mice (Fig. 2-3A). I found a significant effect of amphetamine on cFos expression in every striatal subregion examined (Fig. A-3), as well as on cFos expression in the composite dorsal and ventral striatum (Fig. 2-3B, C). Though I also found a significant effect of genotype on cFos expression in the ventral striatum, with *Slc1a1*-OE mice showing increased cFos expression relative to tTA- controls, there was no significant effect of genotype or genotype x drug interaction on cFos expression in any striatal subregion after correcting for multiple comparisons. However, the VMS was the region that was closest to significance, for both a genotype main effect and a genotype x drug effect (Fig. A-3F).

In this same cohort of mice, I also examined cFos expression in the striosome and matrix subcompartments of the striatum (Fig. 2-4A). Amphetamine significantly increased striosome cFos expression, as did *Slc1a1*-OE, but there was no significant genotype x drug interaction effect. Amphetamine also increased both matrix cFos expression and the index of striosome to matrix predominance (ISMP) [ratio of cFos expression in the striatal striosome compartment to cFos expression in the striatal matrix compartment], but there was no main effect of genotype, and no genotype x drug interaction effect on either of these measures. Furthermore, ISMP showed no significant interaction with stereotypy behavior, indicating that this measure is not driving stereotypy behavior in the *Slc1a1*-OE mice.

I next administered low dose amphetamine, high dose amphetamine, or vehicle to a third cohort of *Slc1a1*-OE mice and controls, with time-locked sacrifice to measure cFos in D1 and D2 neurons in the striatum using RNAScope *in situ* hybridization. To perform a more thorough behavioral characterization of AMPH-induced behavior, I recorded videos from below and

analyzed the videos using DeepLabCut (DLC) and Behavioral Segmentation of Open Field in DeepLabCut (B-SOID) to analyze the behavior in an unbiased fashion. This analysis revealed 6 distinct clusters of behaviors following amphetamine-administration, corresponding to stereotypy, locomotion, rest, sniffing, exploration, and grooming (Fig. A-4). The composition of behaviors varied by genotype and drug administration, with clear effects of amphetamine on quiescence, locomotion, and stereotypy behavior, as is seen from the pie charts describing each group (Fig. A-5).

This analysis of stereotypy and locomotion in the same data set allowed me to test the hypothesis that *Slc1a1*-OE mice have a potentiated response to amphetamine relative to tTA- mice. The automated behavioral analysis showed that *Slc1a1*-OE mice show increased locomotion in response to low dose amphetamine (Fig. 2-5A) and increased stereotypy in response to high dose amphetamine (Fig. 2-5B), as previously shown with manual behavior scoring (Fig. 2-2). This analysis also revealed that *Slc1a1*-OE mice show significantly lower levels of locomotion following high dose amphetamine, indicating that the behavioral response to amphetamine is indeed potentiated in these mice.

I also analyzed the cFos expression in D1, D2, and all cells in several striatal subregions in these mice (Fig. 2-5A). I found amphetamine significantly increased the number of cFos positive D1 neurons in all four subregions studied (DLS, DMS, VMS, and NAc), as well as in composite dorsal and ventral striatum (Fig. A-6). Furthermore, in VMS only there was a significant increase in cFos positive D1 neurons in *Slc1a1*-OE mice relative to controls, with post-hoc testing revealing a significant increase in cFos expression in D1 neurons of VMS in *Slc1a1*-OE mice relative to and tTA- controls at the high dose of amphetamine (Fig. 2-5C).

In addition to these changes in both behavior and cFos expression in *Slc1a1*-OE mice relative to controls, I also found a significant correlation between cFos expression in striatal subregions and stereotypy, locomotion, and rest. Specifically, I found that cFos in the D1 neurons in the ventral striatum was positively correlated with stereotypy behavior, while this same population of neurons was negatively correlated with rest behavior. Furthermore, I found that D2 neurons in the dorsal striatum were negatively correlated with stereotypy behavior, while this same cell population was positively correlated with locomotion.

4.2.2 Chapter 3: Examining the therapeutic potential of EAAT3 in the *Sapap3*-knockout mouse model of OCD

In Chapter 3, I investigated the role of *Slc1a1*/EAAT3 in behavior in *Sapap3*-KO mice. *Sapap3*-KO mice were chosen because they are a model of OCD-relevant behavior that display compulsive grooming, anxiety-like behavior, and abnormalities in cognitive tests that parallel those seen in OCD patients (Ade et al. 2016; Corbit et al. 2019; Welch et al. 2007). They also show reversal of behavioral abnormalities following treatment with an SRI, the first-line medication for OCD patients. The phenotype also has been shown to depend on abnormal activity in cortico-striatal-thalamo-cortical (CSTC) circuits, which are thought to underlie the symptoms of OCD in patients. Furthermore, our preliminary data show that these mice have increased EAAT3 expression in the striatum (Fig. A-9), pointing to a possible role for this protein in the behavioral and neural abnormalities displayed by *Sapap3*-KO mice.

I first showed that *Sapap3*-KO mice that are backcrossed to a 129S background display a robust anxiety-like behavioral phenotype (Fig. 3-1), a phenotype which seemed to be lost in *Sapap3*-KO mice on a pure C57Bl/6 background (Fig. A-10). Mice on a 129S background showed

a significant decrease in time and distance traveled in the anxiogenic center of the open field (OF), a significant decrease in the time and distance traveled in the anxiogenic light side of the light dark (LD) chamber, and a significant decrease in the distance traveled in the open track of the elevated zero maze (EZM). In contrast, *Sapap3*-KO mice on a C57Bl/6 background showed no differences in time or distance traveled in the center of the OF and no differences in time or distance traveled in the light side of the LD chamber, but a significant decrease in the time spent in the open track.

Next, I administered one of two doses of a novel EAAT3 inhibitor (EAAT3I) or vehicle to *Sapap3*-KO and *Sapap3*-WT controls one hour prior to grooming assessment. Our preliminary data showed that this compound reduced compulsive-like grooming behavior in a mouse model of autism-like behavior (*Shank3*-KO mice) using this same dose and time course (Fig. A-10). EAAT3I administration had no significant effect on time spent grooming in either *Sapap3*-KO or *Sapap3*-WT mice in this cohort (Fig. 3-2). While *Sapap3*-KO mice did show increased time spent grooming relative to controls as expected, neither dose of EAAT3I reduced this grooming time. To confirm activity of the EAAT3I, we administered this compound to a separate cohort of mice and monitored the firing rate of midbrain dopamine neurons following amphetamine. EAAT3I showed the expected inhibition of amphetamine-induced decreases in firing rate, indicating that this compound was active (Fig. A11)

Next, I ablated expression of *Slc1a1*/EAAT3 in *Sapap3*-KO mice in order to determine whether lifetime genetic ablation of this gene could rescue the behavioral deficits seen in *Sapap3*-KO mice. To accomplish this, I used *Slc1a1*-STOP mice that have a Neo-STOP cassette between the promotor and coding region of the *Slc1a1* gene (Fig. 3-3A). These mice show reduced *Slc1a1* mRNA expression (Fig. 3-3B, C) and reduced EAAT3 protein expression (Fig. 3-3D, F). I crossed these mice with *Sapap3*-KO mice to generate *Sapap3*-KO//*Slc1a1*-STOP, *Sapap3*-KO//*Slc1a1*-

HET, and *Sapap3*-KO//*Slc1a1*-WT mice (Fig. 3-3F). We then ran these mice through anxiety-like behavioral testing and three weeks of grooming testing (Fig. 3-3G).

There was no significant effect of EAAT3 ablation on anxiety-like behavior in *Sapap3*-KO mice. *Sapap3*-KO mice that were *Slc1a1*-STOP, *Slc1a1*-HET, and *Slc1a1*-WT showed no significant differences in the time or distance traveled in the center of the OF (Fig. 3-4A, B), no significant differences in the time or distance traveled in the open arms of the EPM (Fig. 3-4C, D), and no significant differences in the time or distance in the light side of the LD chamber (Fig. 3-4E, F). There was also no effect of EAAT3 ablation on total distance traveled in the OF or LD tests (Fig. A-12). Furthermore, there was no significant effect of EAAT3 ablation on grooming behavior in *Sapap3*-KO mice, with all 3 genotypes of *Slc1a1* showing similar levels of grooming; however, there was an unexpected trend towards increased grooming in the *Slc1a1*-HET and *Slc1a1*-STOP mice (Fig 3-5).

4.3 Grooming/ anxiety-like behaviors in *Slc1a1*-OE mice

In this dissertation, I showed that EAAT3 overexpression has significant effects on amphetamine-induced repetitive behaviors. However, there were no significant effects of EAAT3 overexpression on grooming behavior, and no consistent effects of EAAT3 overexpression on anxiety-like behavior. This is in contrast with a recent paper on EAAT3 overexpression that reported significant increases in grooming behavior and anxiety-like behavior in *Slc1a1*-OE mice relative to controls (Delgado-Acevedo et al 2019). There are several explanations for this discrepancy. One of them is related to mouse background. As I showed in chapter 3 regarding *Sapap3*-KO mice and anxiety, mice with identical mutations can show different behavioral

manifestations depending on background strain. In a comprehensive investigation of this phenomenon, a previous paper found that F1 crosses of C57Bl/6 mice with 30 other laboratory strains resulted in different, and sometimes diametrically opposite, conclusions regarding the effect of single gene mutations (Sittig et al 2016). Therefore, reporting mouse strain, and taking it into consideration when interpreting results, is essential.

Another possible explanation for the differences in behavior between my model of *Slc1a1*-OE and that of Delgado-Acevedo et al (2019) is potential differences in the absolute levels of EAAT3 overexpression. Our mice overexpress EAAT3 at 4-6 times the WT levels, while Delgado-Acevedo et al reported overexpression of EAAT3 at 2-3 times WT levels. While we would predict that higher levels of overexpression would result in a more robust behavioral phenotype, it is possible that the dose response is non-linear or even U-shaped and that higher levels of overexpression do not have an effect while lower levels do. To test this hypothesis, we could investigate behavior in *Slc1a1*-OE mice given 100 mg/kg of doxycycline, as these mice show lower levels of overexpression closer to 2-3 times WT levels (Fig. 2-1B, C). The use of doxycycline in our mice could also have had an effect on baseline levels of anxiety-like or grooming behavior. A recent report in humans showed that administration of the antibiotic doxycycline results in a disruption in fear memory, hypothesized to be dependent upon disruption of the extracellular enzyme matrix metalloproteinase (MMP)-9 (Bach et al 2018). While both tTA⁺ and tTA⁻ mice in each experiment received the same dose of doxycycline in their chow, there could be an effect of this drug to prevent the expression of anxiety-like or grooming behavior. Lastly, the behavioral differences seen between the two studies could be due to differences in the way in which the tests were conducted, as these tests have been shown to be sensitive to variables

such as baseline levels of rodent stress, lighting conditions in the test room, habituation conditions prior to testing, and even experimenter sex (Sorge et al. 2014).

4.4 Mechanisms of amphetamine-induced behaviors

Our results provide evidence for a role of particular neuronal populations in distinct amphetamine-induced behaviors. We found that cFos in D1 neurons in the ventral striatum was positively correlated with stereotypy behavior. A previous report found that D1 activation in a similar subregion of the striatum was necessary for stereotypy behavior following L-DOPA administration (Chartoff et al 2001), further supporting a role for this cell population in stereotypy. We also found a positive correlation between cFos expression in D2 neurons in the dorsal striatum and locomotor behavior, and a negative correlation between cFos expression in this population and stereotypy behavior. This result is unexpected and raises the possibility that there are separate populations of striatal neurons that drive locomotor and stereotypy behavior, and that the relative activation of these two populations determines which behavior the animal expresses. More work is necessary to test this intriguing possibility.

Other recent work focusing on stereotypy behavior in particular has found that the stereotypy-inducing effects of amphetamine (and other drugs) are highly correlated with cFos expression (and presumed activation) of the striosome region of the striatum relative to the matrix (Canales et al 2000). In addition, ablation of neurons within striosomes blocked induction of stereotypy in response to the amphetamine-related drug methamphetamine (Horner et al 2014). However, we found that there was no correlation between ISMP and stereotypy. It is possible that

this discrepancy in results may be explained by the definitions we used to score stereotypy. Canales and Graybiel (2000) used a measure of stereotypy based on estimates of four behavioral dimensions (repetitiveness/flexibility, frequency, duration, and spatial distribution). In contrast, we used a binary scoring of stereotypy behavior, with a trained experimenter scoring the amount of time a mouse was engaged in stereotypy for the striosome/matrix study.

4.5 Possible mechanisms underlying effect of EAAT3 on amphetamine-induced behavior and neural activity

The role of EAAT3 in signaling at striatal synapses is relatively understudied. Lack of specific EAAT3 inhibitors has made studying its effects at the synapse difficult, and so studies have relied on genetic knockdown or knockout. EAAT3 knockdown in the striatum results in minimal elevation of extracellular glutamate levels, in contrast to knockout of EAAT1 or EAAT2 (Rothstein et al, 1996). Rather, EAAT3 appears to be more involved in regulating local levels of glutamate, for example by limiting activation of group I metabotropic glutamate receptors (mGluRIs) (Bellini et al, 2018). This study found that global knockout of *Slc1a1* increased mGluRI activation and, through an intracellular signaling cascade, led to reduced D1 receptor expression. The inverse could be happening in EAAT3 overexpressers, which could be consistent with our findings. While the one study that has previously examined striatal physiology in EAAT3 overexpressers only reported differences in NMDA receptor activation and subunit expression, they did not rule out changes in mGluR activation or expression (Delgado-Acevedo et al 2019). Therefore, EAAT3 overexpression could reduce mGluRI activation, which could in turn lead to increased D1-receptor expression on striatal neurons. Because amphetamine is a dopamine-

releasing agent that increases dopamine throughout the striatum and D1-receptors are excitatory receptors coupled to Gs/a, this increased D1 expression could lead to increased activation of D1 neurons and therefore increased amphetamine-induced behavior. Future studies could test this hypothesis by measuring D1 receptor expression and/or binding in the striatum of *Slc1a1*-OE mice, or by site-specific microinfusion of a D1 receptor blocker into the VMS.

4.6 Automated scoring of amphetamine-induced behavior

This dissertation represents the first use of an unbiased classifier algorithm to understand amphetamine-induced behavior. Previous studies have relied on hand-scoring of stereotypy and other behaviors, or locomotor chamber scoring of distance traveled. These are blunt measures of mouse behavior that rely on *a priori* decisions about which aspects of the amphetamine response are important. In contrast, my use of DLC and B-SOID to score amphetamine-induced behaviors provides us with an unbiased classification of behavior based only on the structure of the input data. This approach yields a behavioral output for every given moment, a high-throughput, comprehensive examination of behavior that would be prohibitively time consuming using traditional hand-scoring methods. Furthermore, the classification of every individual frame into a behavioral cluster will be tremendously useful for *in vivo* electrophysiology and imaging studies in the future.

My results show clear effects of amphetamine on the composite behavior of mice. There are increases in stereotypy and locomotion that are dose-dependent and replicate previous reports of amphetamine's effect on these behaviors (Fig A-5). Furthermore, there is also an effect of amphetamine on grooming behavior. This is most pronounced and most striking in the high dose

amphetamine group, which has an almost complete lack of grooming behavior several minutes following the administration of amphetamine. In addition, there is a dose dependent effect of amphetamine on rest/quiescence behavior. While locomotor chambers or locomotion tracking software will show a dose-dependent effect of amphetamine on inactivity, high dose amphetamine treatment that results in stereotypy will result in high inactivity scores, something not seen in this unbiased automated analysis of behavior. Adopting this approach for the scoring of drug induced behaviors in the future will streamline analysis and has the potential provide novel insights into the effect of drugs.

4.7 Future directions

While follow up experiments are discussed throughout this chapter as well as in the discussion sections of Chapters 2 and 3, it is worth reiterating and expanding upon several of them here. While I have shown association of amphetamine-induced behaviors with cFos expression in striatal subregions, there is no causal testing of this association in this dissertation. Future studies could therefore investigate the effect of increasing activity in D2 dorsal striatal neurons and/or D1 ventral striatal neurons during amphetamine administration and seeing if this results in increased locomotion or increased stereotypy, respectively. This could be done using DREADDs a similar genetic based manipulation of the specific cell population. Furthermore, future studies could utilize the FAST-system upon which this overexpression is based to rescue overexpression in specific striatal subregions. In particular, EAAT3 overexpression seems to increase activity in the VMS. The *Slc1a1*-tetO construct has flanking loxP sites (Fig. 2-1A), and we could therefore test whether

injection of a cre-expressing virus into the VMS to rescue expression in this subregion would result in a rescue of the behavioral effects seen in these mice.

My experiments investigating the role of EAAT3 in *Sapap3*-KO mice showed no significant behavioral effects of either genetic ablation or pharmacological inhibition of EAAT3 on OCD-relevant behaviors. Future studies could use different EAAT3 inhibitors in preclinical animal models, as well as follow up on the results of this EAAT3 inhibitor on behavior in *Shank3*-KO mice. In particular, investigating the differences in the mechanisms underlying grooming in the *Shank3*-KO mice (which show a decrease in grooming in response to EAAT3I) and the *Sapap3*-KO mice (which show no change in grooming in response to EAAT3I) could help shed light on this complex behavior. Lastly, use of this and other specific EAAT3 inhibitors to study the role of EAAT3 in striatal synaptic physiology could provide us with a wealth of information about the role of this transporter in OCD-relevant circuits.

Appendix A Supplemental Data

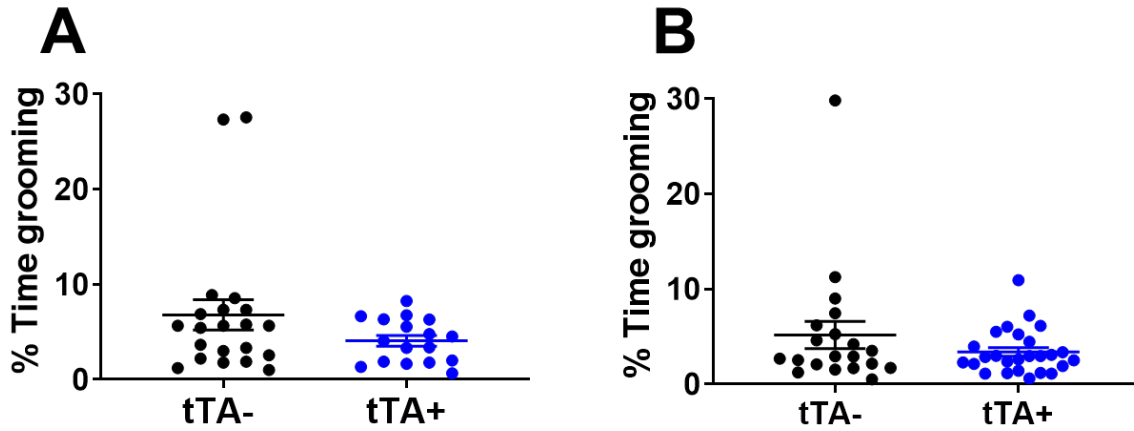


Figure A-1 *Slc1a1*-OE mice show no differences in grooming levels compared to controls

(A) No significant differences in the percent time grooming between lifetime *Slc1a1*-OE (tTA+) mice and tTA- controls. (B) No significant differences in the percent time grooming between adult-specific *Slc1a1*-OE (tTA+) mice and tTA- controls.

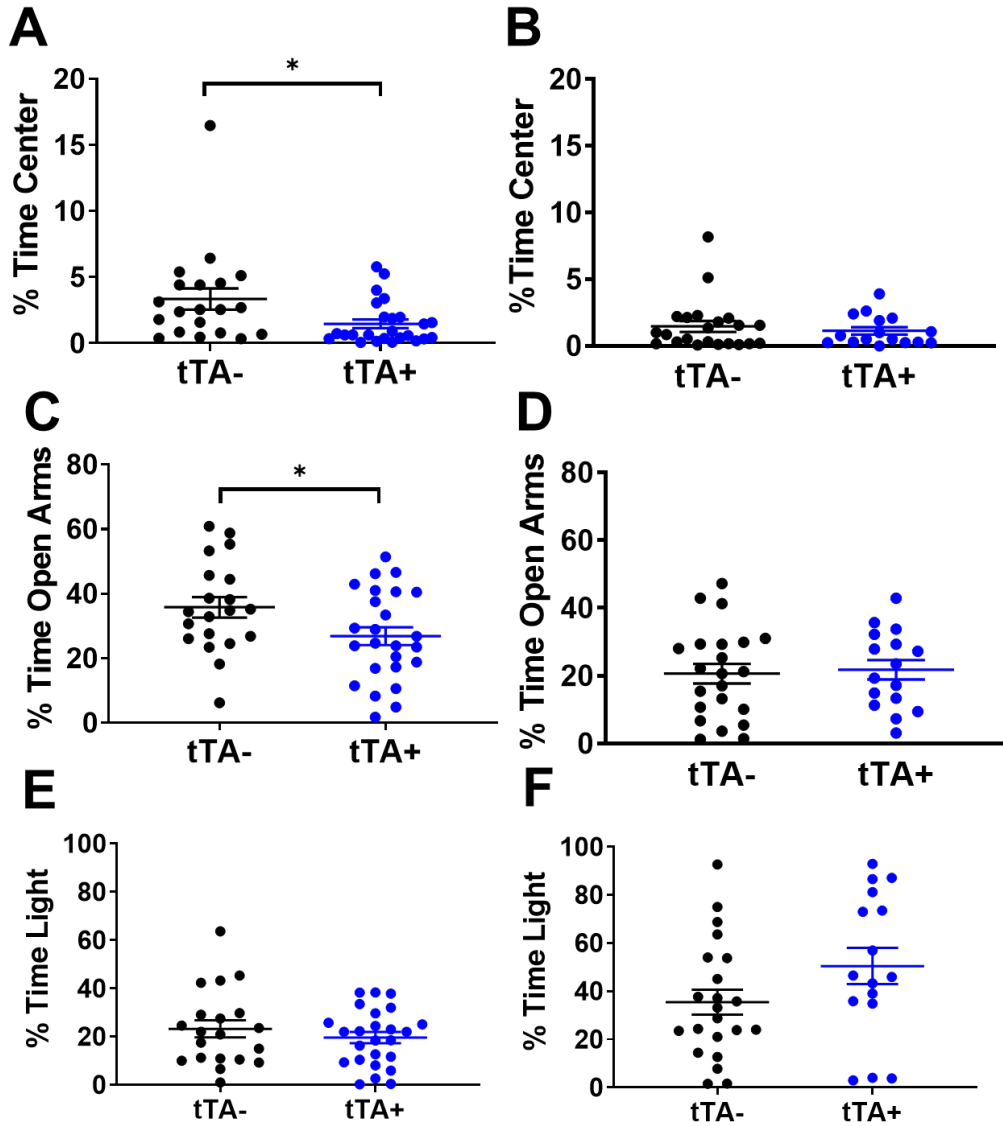


Figure A-2 Anxiety-like behavior in lifetime and adult-specific *Slc1a1*-OE mice

(A) In cohort I, mice overexpressing *Slc1a1* throughout life (tTA+) showed a significant decrease in the percent time spent in the center of the open field relative to controls (tTA-; t-test, $t(43) = 2.33, p < 0.05$), while (B) there was no significant difference in the percent time spent in the center of the open field in adult-specific *Slc1a1*-OE mice relative to controls. (C) Mice overexpressing *Slc1a1* throughout life (tTA+) showed a significant decrease in the percent time spent in the open arms of the elevated plus maze relative to controls (tTA-; t-test, $t(43) = 2.12, p < 0.05$), while (D) there was no significant difference in the percent time spent in the open arms of the elevated plus maze in adult-specific *Slc1a1*-OE mice relative to controls. There was no significant difference in the percent time spent in the light side during the light dark test for either lifetime (E) or adult-specific (F) *Slc1a1*-OE mice.

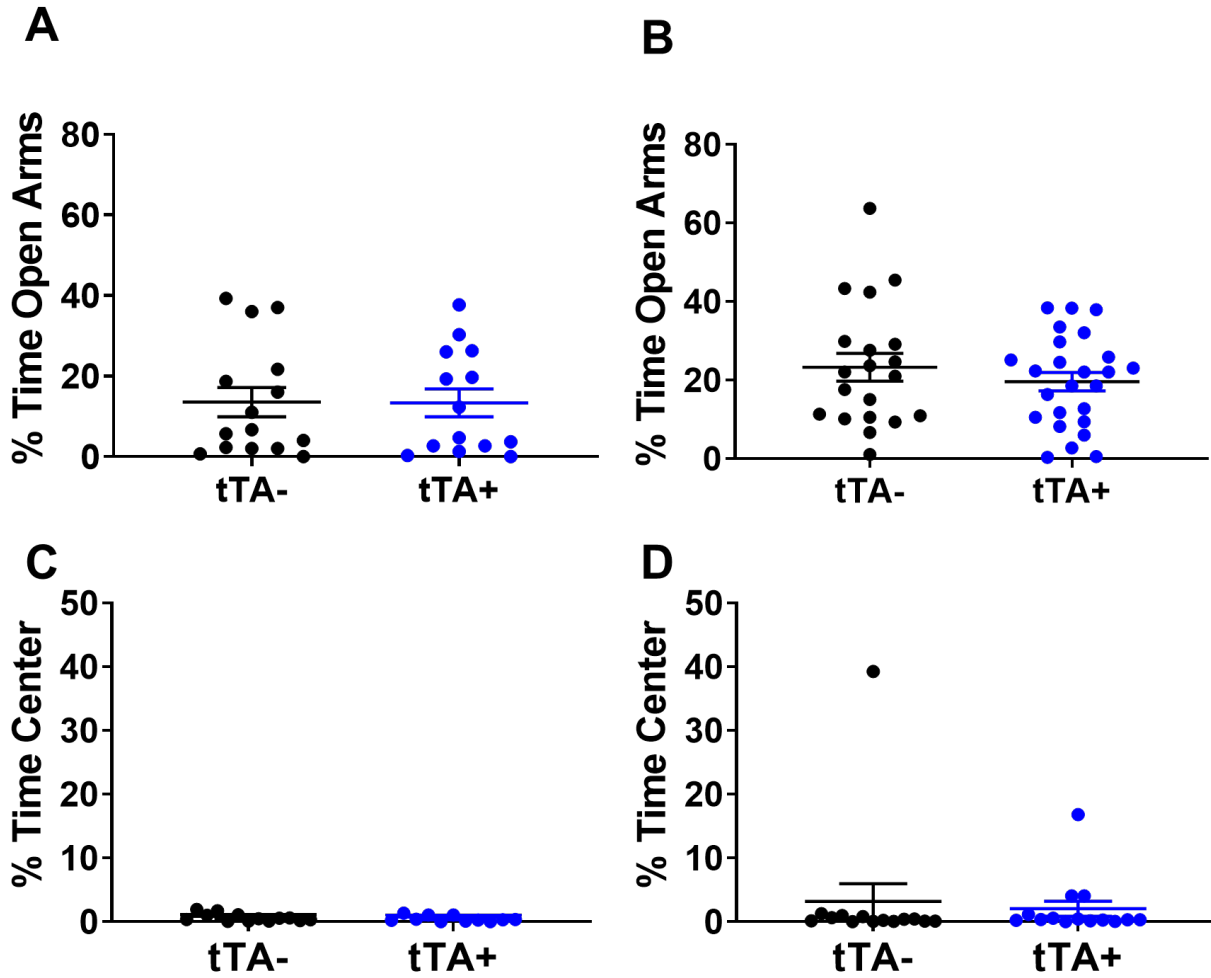


Figure A-3 *Slc1a1*-OE mice show no consistent anxiety-like behavioral phenotype

Two separate replication cohorts of *Slc1a1*-OE mice show no significant differences in behavior in the EPM (A, B) or Open field (C, D)

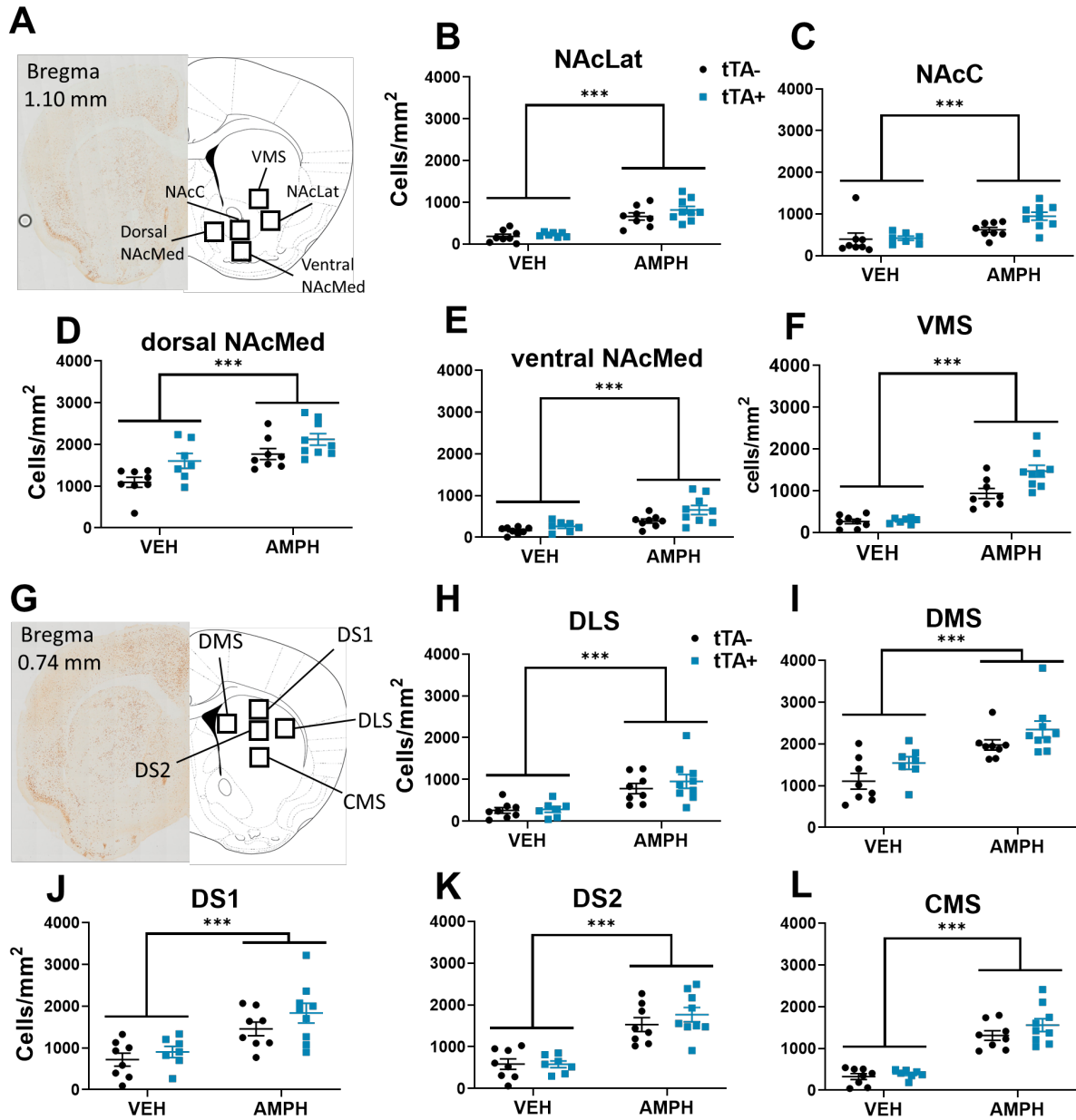


Figure A-4 Amphetamine significantly increases cFos in subregions throughout dorsal and ventral striatum

NAcLat = lateral nucleus accumbens shell, NAcC = nucleus accumbens core, dorsal NAcMed = dorsal medial nucleus accumbens shell, ventral NAcMed = ventral medial NAc shell, VMS = ventromedial striatum, DLS = dorsolateral striatum, DMS = dorsomedial striatum, DS1 = dorsal striatum-1, DS2 = dorsal striatum-2, CMS = centromedial striatum

Table A-1 Table of statistics for two-way repeated measures analysis of cFos in striatal subregions.

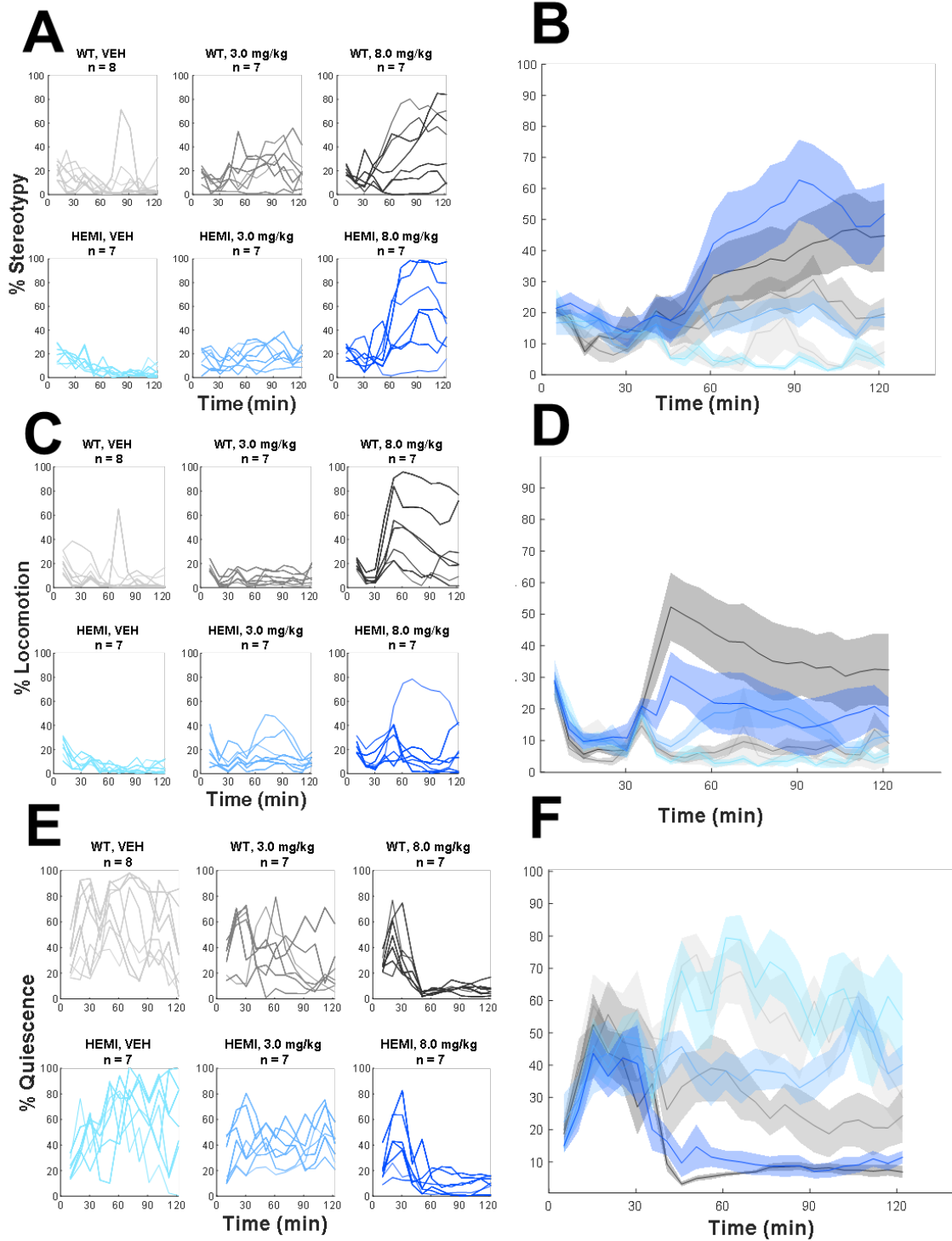
	Drug main effect	Genotype main effect	drug x genotype interaction
DLS	$F(1, 28) = 23.84$	$F(1, 28) = 0.65$	$F(1, 28) = 0.36$
	$p < 0.0001$	$p = 0.42$	$p = 0.56$
DS1	$F(1, 28) = 19.99$	$F(1, 28) = 2.28$	$F(1, 28) = 0.27$
	$p < 0.0001$	$p = 0.6$	$p = 0.14$
DS2	$F(1, 28) = 52.34$	$F(1, 28) = 0.62$	$F(1, 28) = 0.69$
	$p < 0.0001$	$p = 0.44$	$p = 0.41$
DMS	$F(1, 28) = 39.68$	$F(1, 28) = 5.35$	$F(1, 28) = 0.036$
	$p < 0.0001$	0.028	0.85
CS	$F(1, 28) = 91.78$	$F(1, 28) = 1.95$	$F(1, 28) = 0.67$
	$p < 0.0001$	$p = 0.17$	$p = 0.42$
VMS	$F(1, 28) = 80.88$	$F(1, 28) = 7.174$	$F(1, 28) = 6.164$
	$p < 0.0001$	$p = 0.012$	$p = 0.019$
NAcC	$F(1, 28) = 14.68$	$F(1, 28) = 3.12$	$F(1, 28) = 2.35$
	$p < 0.0001$	$p = 0.088$	$p = 0.14$
Dorsal NAcMed	$F(1, 28) = 17.63$	$F(1, 28) = 9.73$	$F(1, 28) = 0.33$
	$p < 0.0001$	$p = 0.0049$	$p = 0.57$
ventral NAcMed	$F(1, 28) = 18.46$	$F(1, 28) = 6.50$	$F(1, 28) = 1.34$
	$p = 0.0002$	$p = 0.017$	$p = 0.25$
NAcLat	$F(1, 28) = 55.14$	$F(1, 28) = 1.97$	$F(1, 28) = 0.62$
	$p < 0.0001$	$p = 0.17$	$p = 0.044$

Bonferroni corrected $\alpha = 0.005$, significant p-values in bold. NAcLat = lateral nucleus accumbens shell, NAcC = nucleus accumbens core, dorsal NAcMed = dorsal medial nucleus accumbens shell, ventral NAcMed = ventral medial NAc shell, VMS = ventromedial striatum, DLS = dorsolateral striatum, DMS = dorsomedial striatum, DS1 = dorsal striatum-1, DS2 = dorsal striatum-2, CMS = centromedial striatum

Table A-2 Correlation between stereotypy behavior and cFos expression in striatal subregions

		All cells
Dorsal striatum	R ²	0.056
	p	0.36
Ventral striatum	R ²	0.19
	p	0.083
DLS	R ²	0.0076
	p	0.74
DS1	R ²	0.040
	p	0.44
DS2	R ²	0.080
	p	0.027
DMS	R ²	0.018
	p	0.61
CS	R ²	0.12
	p	0.168
VMS	R ²	0.34
	p	0.014
NAcC	R ²	0.19
	p	0.08
Dorsal NAcMed	R ²	0.12
	p	0.18
ventral NAcMed	R ²	0.00041
	p	0.94
NAcLat	R ²	0.075
	p	0.29

Bonferroni corrected $\alpha = 0.0042$, NAcLat = lateral nucleus accumbens shell, NAcC = nucleus accumbens core, dorsal NAcMed = dorsal medial nucleus accumbens shell, ventral NAcMed = ventral medial NAc shell, VMS = ventromedial striatum, DLS = dorsolateral striatum, DMS = dorsomedial striatum, DS1 = dorsal striatum-1, DS2 = dorsal striatum-2, CMS = centromedial striatum



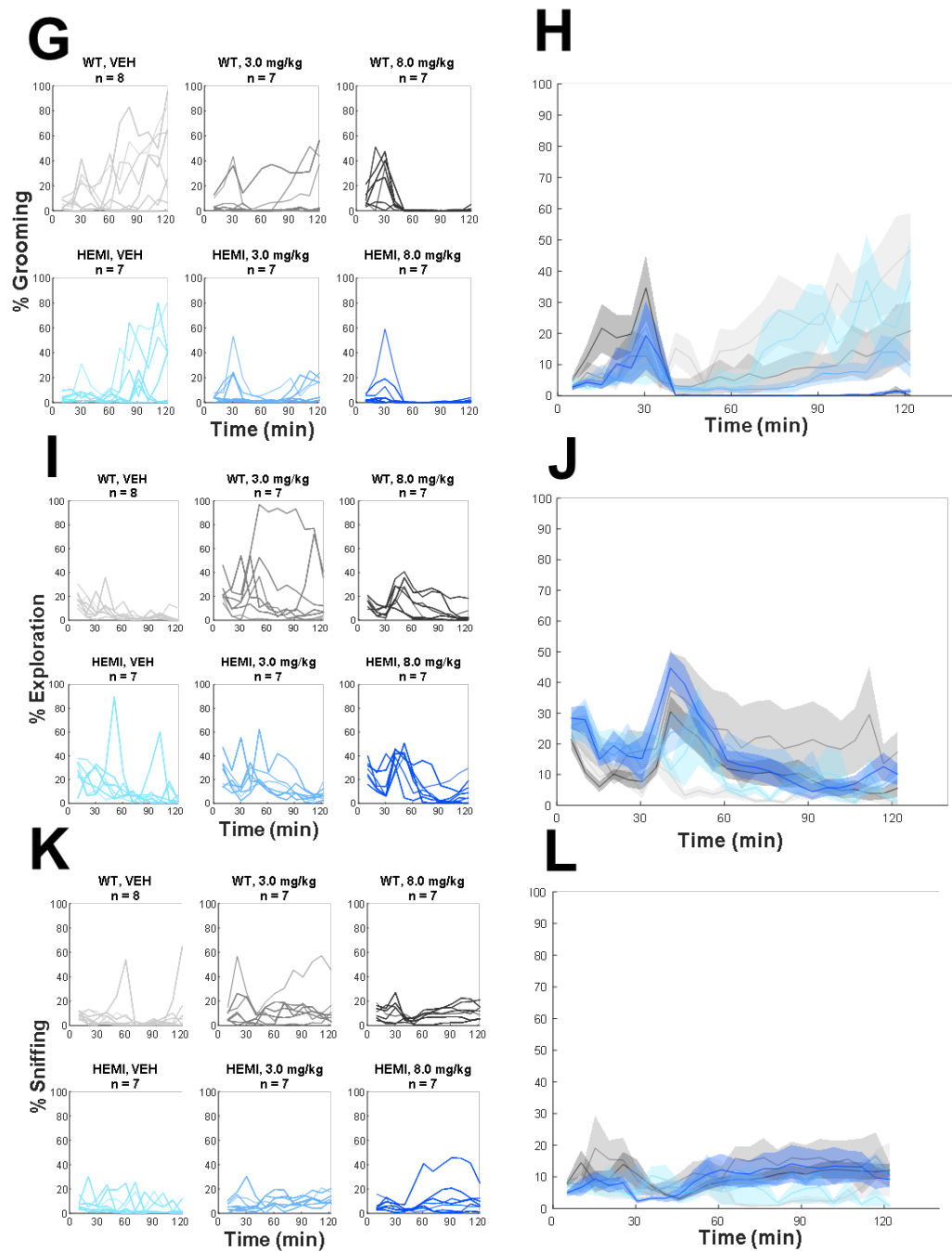


Figure A-5 Traces of B-SOID scored behavior, separated by genotype and drug treatment

Traces showing individual mouse and average mouse trace for % of total time in stereotypy (A & B), locomotion (C & D), quiescence (E & F), grooming (G & H), exploration (I & J), and sniffing (K & L). Data was analyzed in 5 minute bins. Injection of amphetamine or vehicle occurred at 30 minutes.

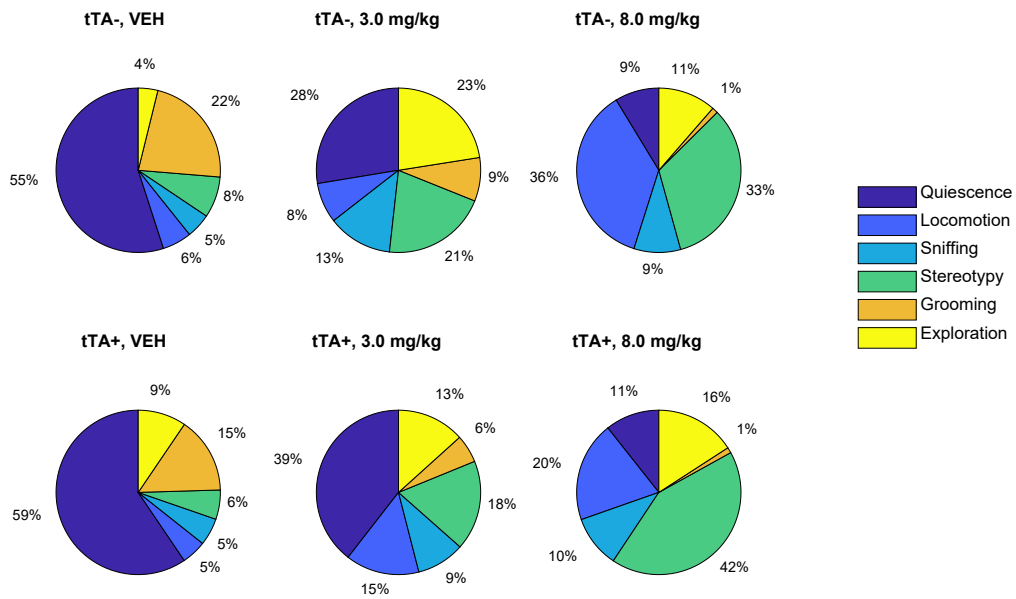


Figure A-6 Pie charts of B-SOID scored behavior, separated by genotype and drug treatment

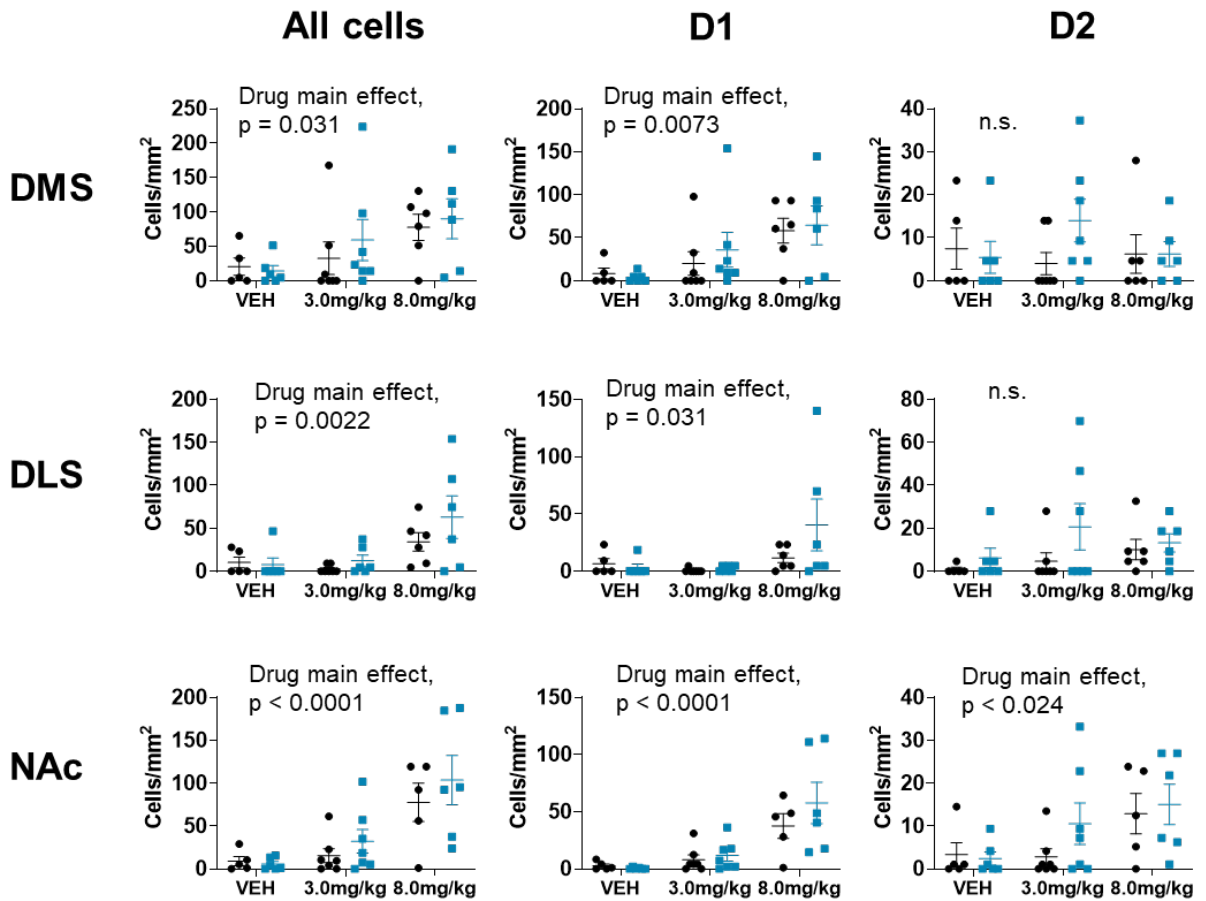


Figure A-7 Amphetamine increases overall cFos expression and D1 neuron cFos expression throughout the striatum and D2 neuron cFos in the NAc

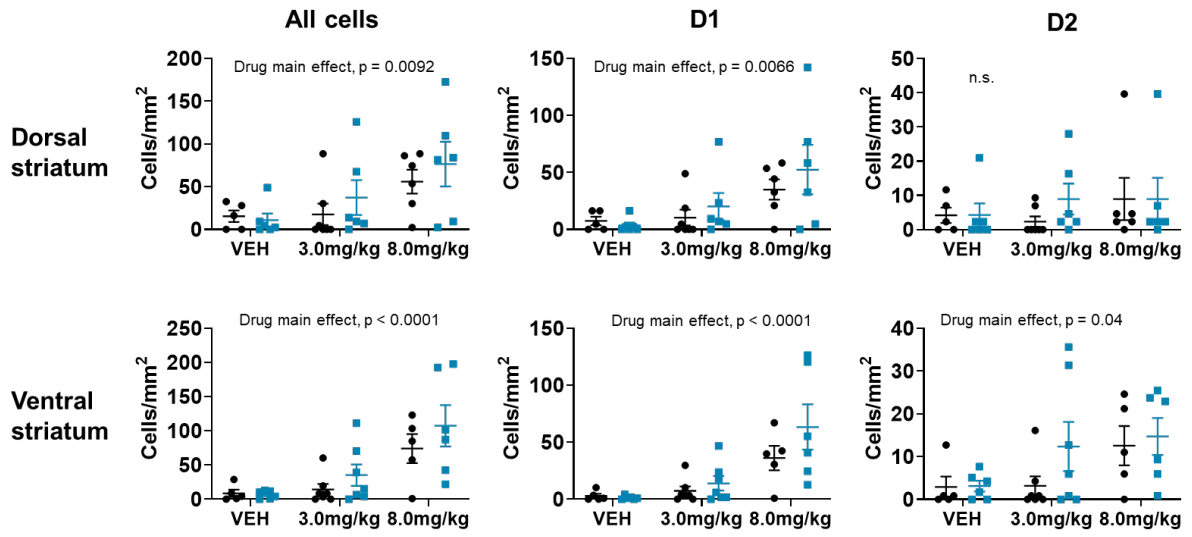


Figure A-8 Amphetamine increases cFos in dorsal and ventral striatum

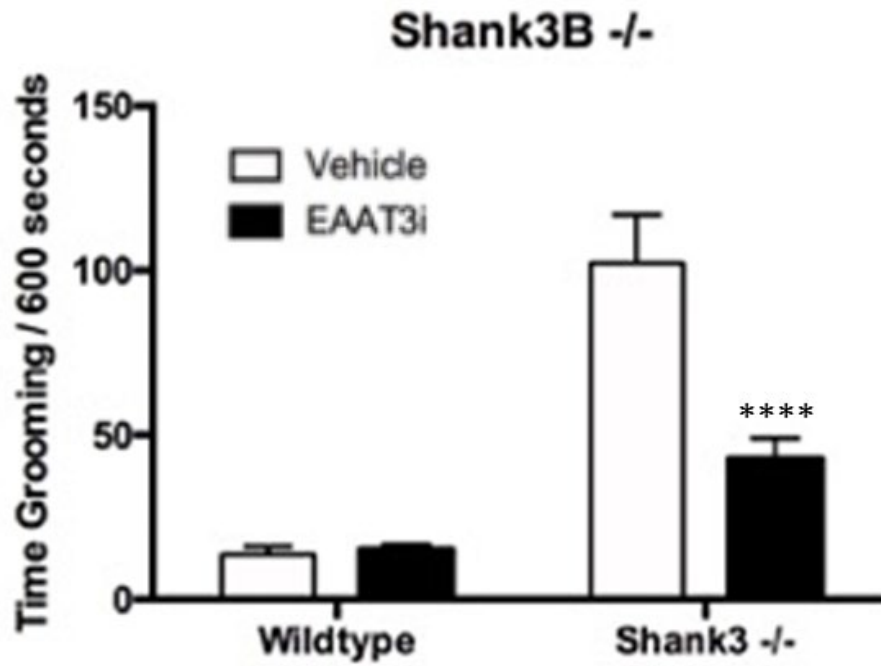


Figure A-9 Shank3-KO mice show increased grooming relative to WT mice, and this increased grooming is blunted by the administration of an EAAT3 inhibitor (EAAT3i, 30 mg/kg)

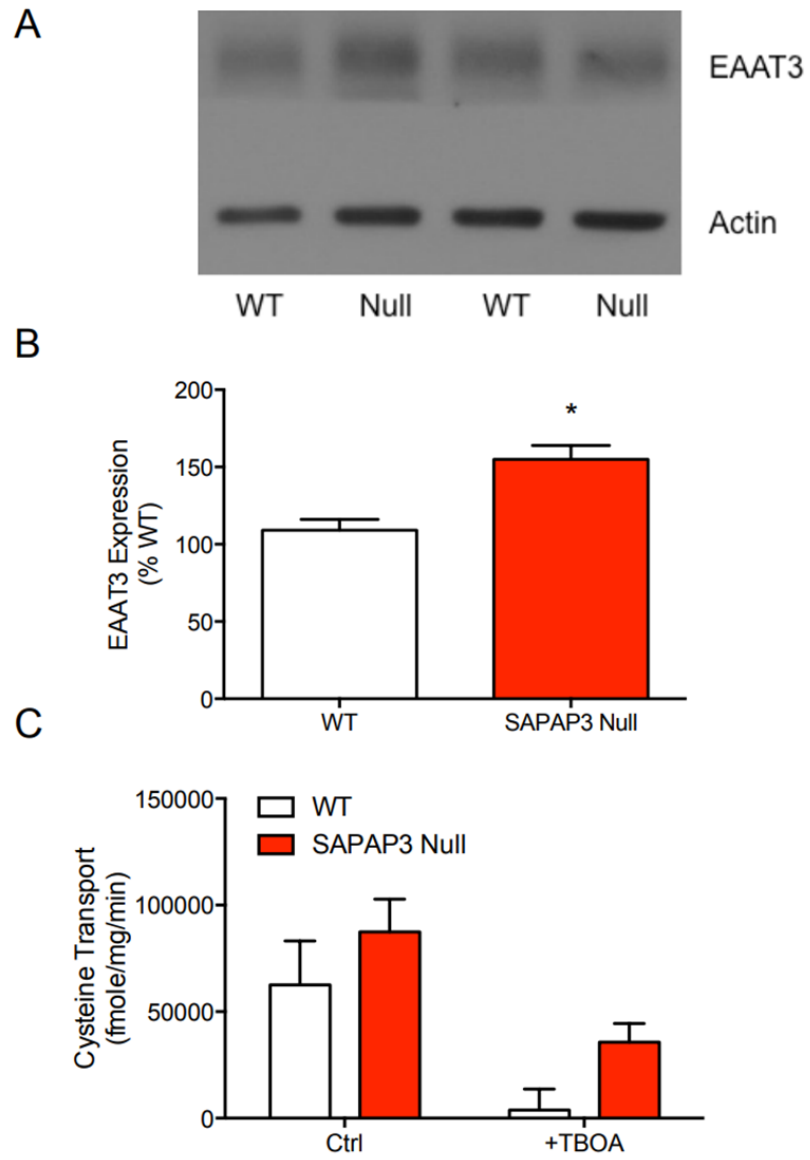


Figure A-10 *Sapap3*-KO mice show increased EAAT3 protein expression but no change in EAAT3 function

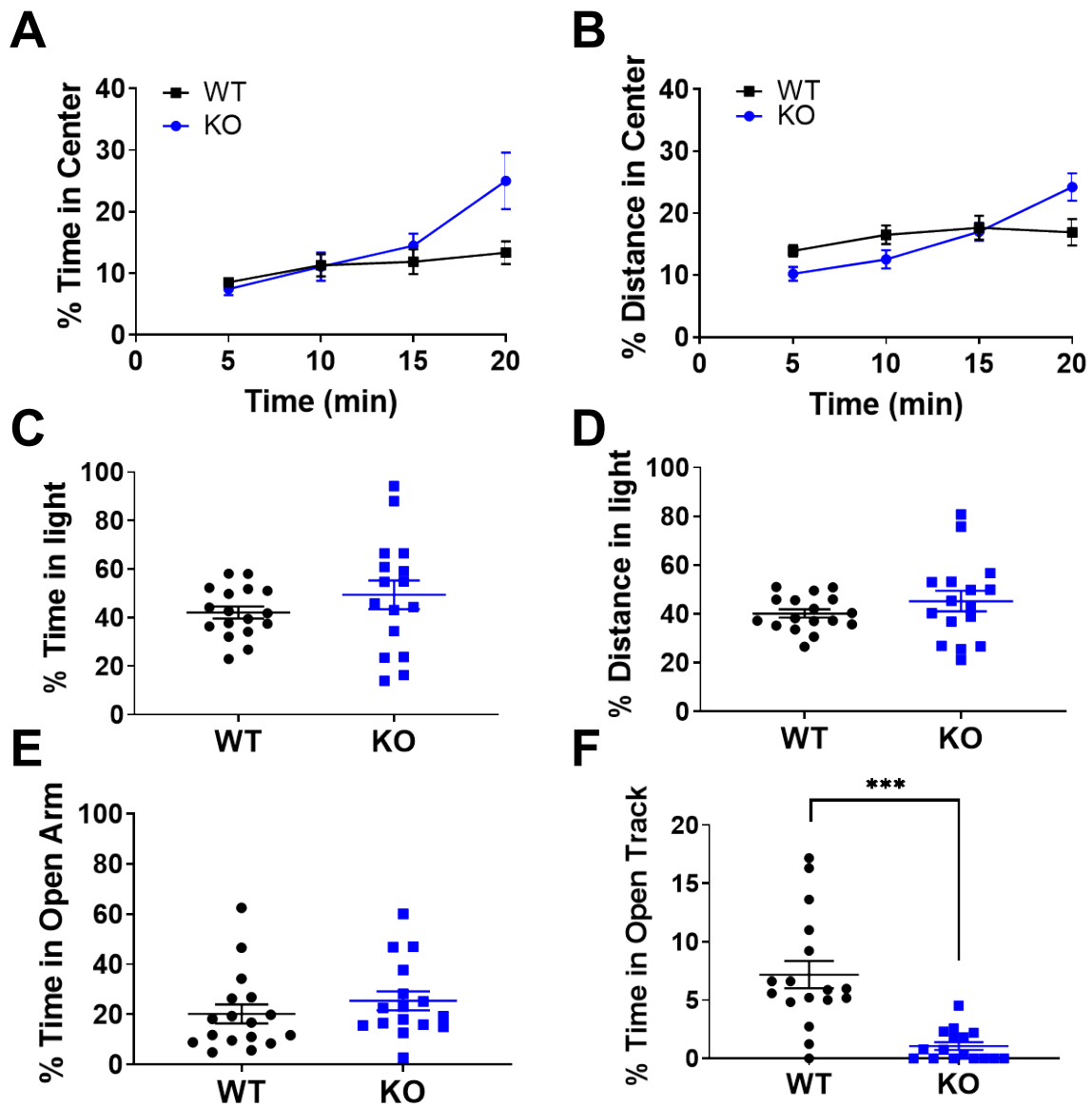


Figure A-11 *Sapap3* mice on C57Bl/6 background show an inconsistent anxiety-like phenotype

Sapap3-KO show no differences between from *Sapap3*-KO mice in the percent time or percent distance in center of the OF (A & B), the percent or percent distance in light side on the LD test (C & D), or the percent time in the open arm of the EPM (E). *Sapap3*-KO mice show a decrease in the time spent in the open track of the EZM relative to *Sapap3*-WT mice (Unpaired t-test, $t(31) = 4.88, p < 0.001$).

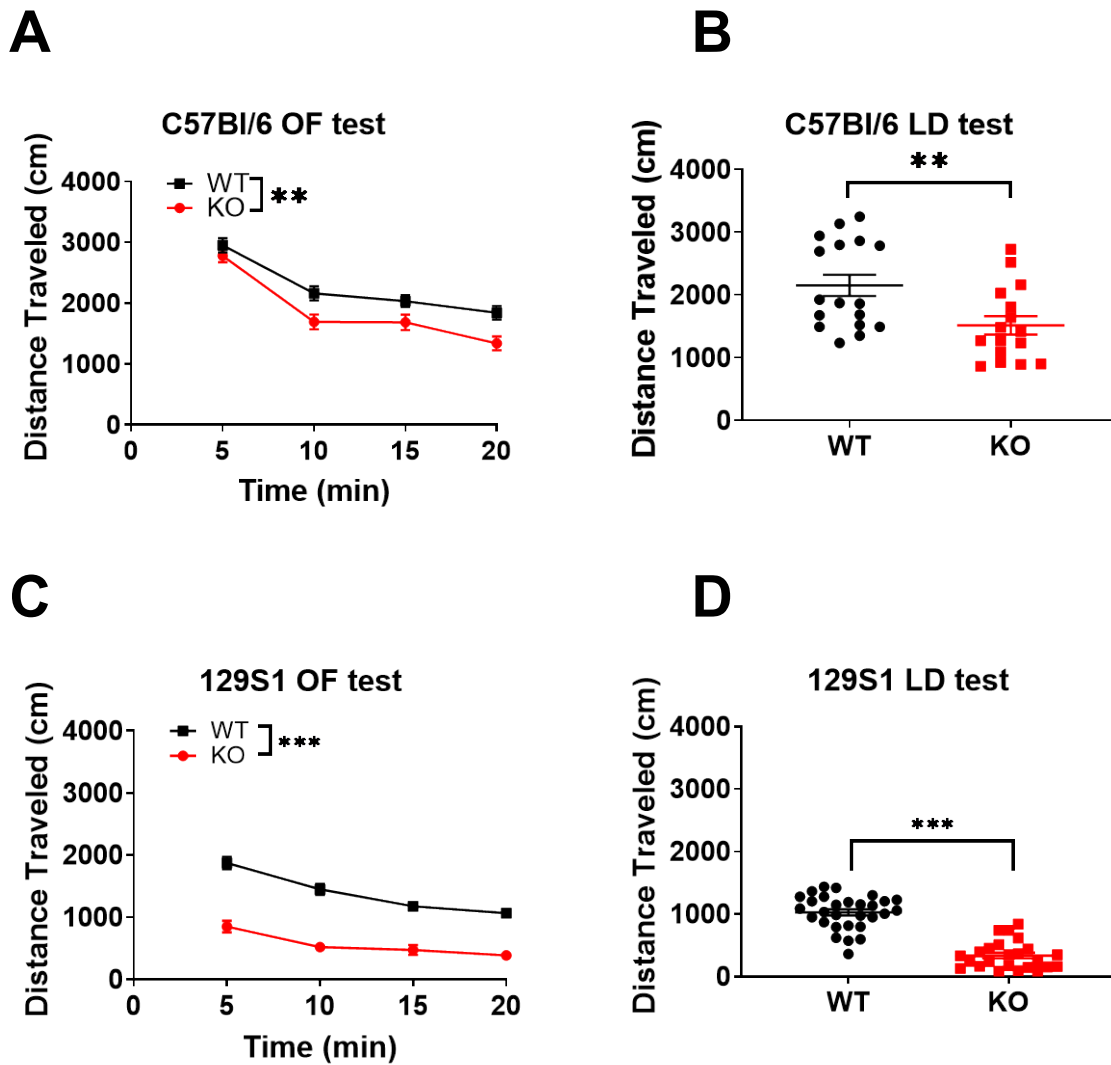


Figure A-12 *Sapap3*-KO mice on both C57Bl/6 and 129S background show lower levels of locomotion relative to *Sapap3*-WT mice

(A, B) *Sapap3*-KO mice on a C57Bl/6 background show lower levels of locomotion in both the OF test (Repeated measures Two-Way ANOVA, $F(1,31) = 8.55, p < 0.01$) and LD (Unpaired t-test, $t(31) = 2.82, p < 0.01$) relative to littermate *Sapap3*-WT controls. (C, D) *Sapap3*-KO mice on a 129S1 background show lower levels of locomotion in both the OF test (Repeated measures Two-Way ANOVA, $F(1,51) = 16.47, p < 0.001$) and LD (Unpaired t-test, $t(51) = 10.13, p < 0.001$) relative to littermate *Sapap3*-WT controls.

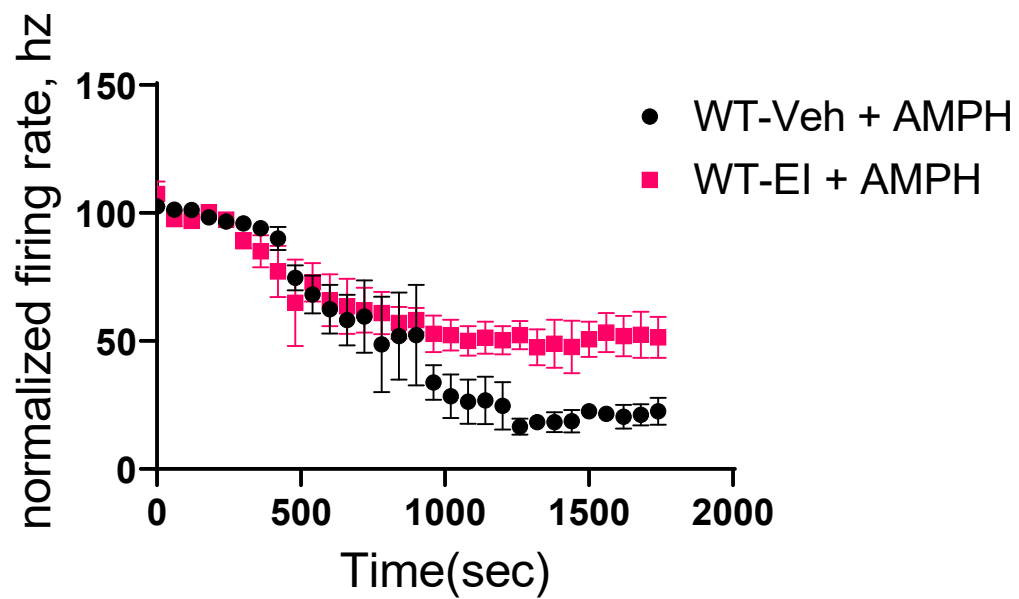


Figure A-13 Administration of an EAAT3 inhibitor blocks amphetamine-induced inhibition of midbrain dopamine firing rate

A



B

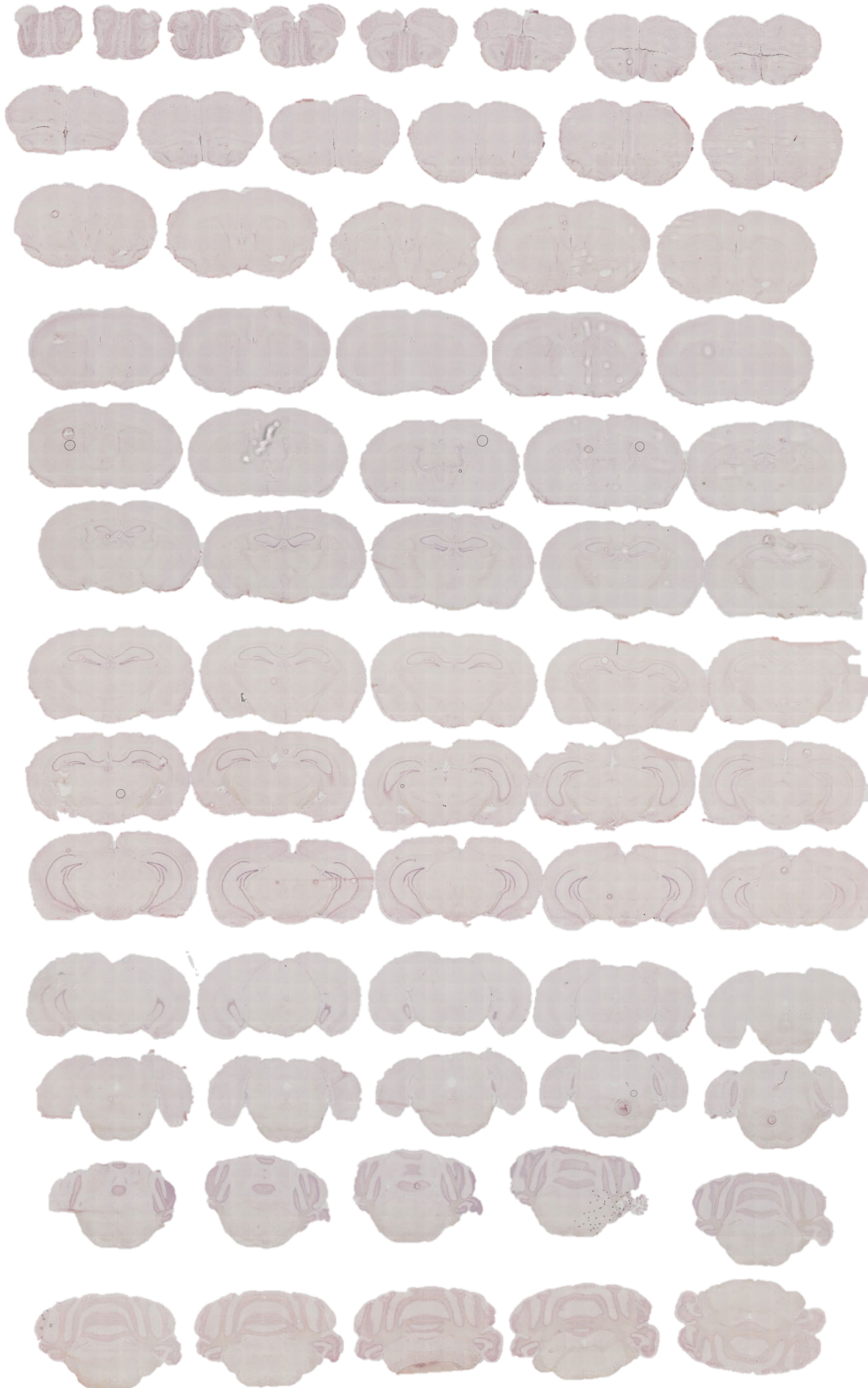


Figure A-14 *Slc1a1* mRNA expression in the whole mouse brain as measured by *in situ* hybridization histochemistry in *Slc1a1*-WT (A) and *Slc1a1*-STOP mice

Bibliography

- Abelson, J.F., Kwan, K.Y., O’Roak, B.J., et al. 2005. Sequence variants in SLITRK1 are associated with Tourette’s syndrome. *Science* 310(5746), pp. 317–320.
- Ade, K.K., Wan, Y., Hamann, H.C., et al. 2016. Increased Metabotropic Glutamate Receptor 5 Signaling Underlies Obsessive-Compulsive Disorder-like Behavioral and Striatal Circuit Abnormalities in Mice. *Biological Psychiatry* 80(7), pp. 522–533.
- Afshar, H., Roohafza, H., Mohammad-Beigi, H., et al. 2012. N-acetylcysteine add-on treatment in refractory obsessive-compulsive disorder: a randomized, double-blind, placebo-controlled trial. *Journal of Clinical Psychopharmacology* 32(6), pp. 797–803.
- Afshari, P., Yao, W.-D. and Middleton, F.A. 2017. Reduced Slc1a1 expression is associated with neuroinflammation and impaired sensorimotor gating and cognitive performance in mice: Implications for schizophrenia. *Plos One* 12(9), p. e0183854.
- Ahmari, S.E., Spellman, T., Douglass, N.L., et al. 2013. Repeated cortico-striatal stimulation generates persistent OCD-like behavior. *Science* 340(6137), pp. 1234–1239.
- Albrecht, J., Sidoryk-Węgrzynowicz, M., Zielińska, M. and Aschner, M. 2010. Roles of glutamine in neurotransmission. *Neuron Glia Biology* 6(4), pp. 263–276.
- Alexander, G.E., Crutcher, M.D. and DeLong, M.R. 1990. Basal ganglia-thalamocortical circuits: parallel substrates for motor, oculomotor, “prefrontal” and “limbic” functions. *Progress in Brain Research* 85, pp. 119–146.
- Alexander, G.E., DeLong, M.R. and Strick, P.L. 1986. Parallel organization of functionally segregated circuits linking basal ganglia and cortex. *Annual Review of Neuroscience* 9, pp. 357–381.

- Amara, S.G. and Fontana, A.C.K. 2002. Excitatory amino acid transporters: keeping up with glutamate. *Neurochemistry International* 41(5), pp. 313–318.
- Aoyama, K., Suh, S.W., Hamby, A.M., et al. 2006. Neuronal glutathione deficiency and age-dependent neurodegeneration in the EAAC1 deficient mouse. *Nature Neuroscience* 9(1), pp. 119–126.
- Arnold, P.D., Sicard, T., Burroughs, E., Richter, M.A. and Kennedy, J.L. 2006. Glutamate transporter gene SLC1A1 associated with obsessive-compulsive disorder. *Archives of General Psychiatry* 63(7), pp. 769–776.
- Arriza, J.L., Eliasof, S., Kavanaugh, M.P. and Amara, S.G. 1997. Excitatory amino acid transporter 5, a retinal glutamate transporter coupled to a chloride conductance. *Proceedings of the National Academy of Sciences of the United States of America* 94(8), pp. 4155–4160.
- Bailey, C.G., Ryan, R.M., Thoeng, A.D., et al. 2011. Loss-of-function mutations in the glutamate transporter SLC1A1 cause human dicarboxylic aminoaciduria. *The Journal of Clinical Investigation* 121(1), pp. 446–453.
- Baldan, L.C., Williams, K.A., Gallezot, J.-D., et al. 2014. Histidine decarboxylase deficiency causes tourette syndrome: parallel findings in humans and mice. *Neuron* 81(1), pp. 77–90.
- Bartha, R., Stein, M.B., Williamson, P.C., et al. 1998. A short echo 1H spectroscopy and volumetric MRI study of the corpus striatum in patients with obsessive-compulsive disorder and comparison subjects. *The American Journal of Psychiatry* 155(11), pp. 1584–1591.
- Baxter, L.R., Phelps, M.E., Mazziotta, J.C., Guze, B.H., Schwartz, J.M. and Selin, C.E. 1987. Local cerebral glucose metabolic rates in obsessive-compulsive disorder. A comparison

- with rates in unipolar depression and in normal controls. *Archives of General Psychiatry* 44(3), pp. 211–218.
- Baxter, L.R., Schwartz, J.M., Bergman, K.S., et al. 1992. Caudate glucose metabolic rate changes with both drug and behavior therapy for obsessive-compulsive disorder. *Archives of General Psychiatry* 49(9), pp. 681–689.
- Baxter, L.R., Schwartz, J.M., Mazziotta, J.C., et al. 1988. Cerebral glucose metabolic rates in nondepressed patients with obsessive-compulsive disorder. *The American Journal of Psychiatry* 145(12), pp. 1560–1563.
- Bellini, S., Fleming, K.E., De, M., et al. 2018. Neuronal glutamate transporters control dopaminergic signaling and compulsive behaviors. *The Journal of Neuroscience* 38(4), pp. 937–961.
- Berman, A.E., Chan, W.Y., Brennan, A.M., et al. 2011. N-acetylcysteine prevents loss of dopaminergic neurons in the EAAC1^{-/-} mouse. *Annals of Neurology* 69(3), pp. 509–520.
- Bernier, R., Golzio, C., Xiong, B., et al. 2014. Disruptive CHD8 mutations define a subtype of autism early in development. *Cell* 158(2), pp. 263–276.
- Bey, A.L. and Jiang, Y. 2014. Overview of mouse models of autism spectrum disorders. *Current protocols in pharmacology / editorial board, S.J. Enna (editor-in-chief) ... [et al.]* 66, pp. 5.66.1–26.
- Bhakar, A.L., Dölen, G. and Bear, M.F. 2012. The pathophysiology of fragile X (and what it teaches us about synapses). *Annual Review of Neuroscience* 35, pp. 417–443.
- Bienvenu, O.J., Samuels, J.F., Riddle, M.A., et al. 2000. The relationship of obsessive-compulsive disorder to possible spectrum disorders: results from a family study. *Biological Psychiatry* 48(4), pp. 287–293.

- Bienvenu, O.J., Wang, Y., Shugart, Y.Y., et al. 2009. Sapap3 and pathological grooming in humans: Results from the OCD collaborative genetics study. *American Journal of Medical Genetics. Part B, Neuropsychiatric Genetics* 150B(5), pp. 710–720.
- Bjørn-Yoshimoto, W.E. and Underhill, S.M. 2016. The importance of the excitatory amino acid transporter 3 (EAAT3). *Neurochemistry International* 98, pp. 4–18.
- Bloch, M.H., Wasylink, S., Landeros-Weisenberger, A., et al. 2012. Effects of ketamine in treatment-refractory obsessive-compulsive disorder. *Biological Psychiatry* 72(11), pp. 964–970.
- Bolton, J., Moore, G.J., MacMillan, S., Stewart, C.M. and Rosenberg, D.R. 2001. Case study: caudate glutamatergic changes with paroxetine persist after medication discontinuation in pediatric OCD. *Journal of the American Academy of Child and Adolescent Psychiatry* 40(8), pp. 903–906.
- Borges, K. and Dingledine, R. 1998. Chapter 11 AMPA receptors: Molecular and functional diversity. In: *Progress in brain research volume 116*. Progress in brain research. Elsevier, pp. 153–170.
- Burguière, E., Monteiro, P., Feng, G. and Graybiel, A.M. 2013. Optogenetic stimulation of lateral orbitofronto-striatal pathway suppresses compulsive behaviors. *Science* 340(6137), pp. 1243–1246.
- Cai, J., Zhang, W., Yi, Z., et al. 2013. Influence of polymorphisms in genes SLC1A1, GRIN2B, and GRIK2 on clozapine-induced obsessive-compulsive symptoms. *Psychopharmacology* 230(1), pp. 49–55.

- Campbell, K.M., de Lecea, L., Severynse, D.M., et al. 1999. OCD-Like behaviors caused by a neuropotentiating transgene targeted to cortical and limbic D1+ neurons. *The Journal of Neuroscience* 19(12), pp. 5044–5053.
- Canales, J.J. and Graybiel, A.M. 2000. A measure of striatal function predicts motor stereotypy. *Nature Neuroscience* 3(4), pp. 377–383.
- Cao, L., Li, L. and Zuo, Z. 2012. N-acetylcysteine reverses existing cognitive impairment and increased oxidative stress in glutamate transporter type 3 deficient mice. *Neuroscience* 220, pp. 85–89.
- Cappi, C., Oliphant, M.E., Péter, Z., et al. 2020. De Novo Damaging DNA Coding Mutations Are Associated With Obsessive-Compulsive Disorder and Overlap With Tourette’s Disorder and Autism. *Biological Psychiatry* 87(12), pp. 1035–1044.
- Del Casale, A., Sorice, S., Padovano, A., et al. 2019. Psychopharmacological Treatment of Obsessive-Compulsive Disorder (OCD). *Current neuropharmacology* 17(8), pp. 710–736.
- Chakrabarty, K., Bhattacharyya, S., Christopher, R. and Khanna, S. 2005. Glutamatergic dysfunction in OCD. *Neuropsychopharmacology* 30(9), pp. 1735–1740.
- Chamberlain, S.R., Menzies, L., Hampshire, A., et al. 2008. Orbitofrontal dysfunction in patients with obsessive-compulsive disorder and their unaffected relatives. *Science* 321(5887), pp. 421–422.
- Chartoff, E.H., Marck, B.T., Matsumoto, A.M., Dorsa, D.M. and Palmiter, R.D. 2001. Induction of stereotypy in dopamine-deficient mice requires striatal D1 receptor activation. *Proceedings of the National Academy of Sciences of the United States of America* 98(18), pp. 10451–10456.

- Cheng, C., Glover, G., Banker, G. and Amara, S.G. 2002. A novel sorting motif in the glutamate transporter excitatory amino acid transporter 3 directs its targeting in Madin-Darby canine kidney cells and hippocampal neurons. *The Journal of Neuroscience* 22(24), pp. 10643–10652.
- Choi, B.Y., Kim, J.H., Kim, H.J., et al. 2014. EAAC1 gene deletion increases neuronal death and blood brain barrier disruption after transient cerebral ischemia in female mice. *International Journal of Molecular Sciences* 15(11), pp. 19444–19457.
- Conti, F., DeBiasi, S., Minelli, A., Rothstein, J.D. and Melone, M. 1998. EAAC1, a high-affinity glutamate transporter, is localized to astrocytes and gabaergic neurons besides pyramidal cells in the rat cerebral cortex. *Cerebral Cortex* 8(2), pp. 108–116.
- Corbit, V.L., Manning, E.E., Gittis, A.H. and Ahmari, S.E. 2019. Strengthened Inputs from Secondary Motor Cortex to Striatum in a Mouse Model of Compulsive Behavior. *The Journal of Neuroscience* 39(15), pp. 2965–2975.
- Costa, D.L.C., Diniz, J.B., Requena, G., et al. 2017. Randomized, Double-Blind, Placebo-Controlled Trial of N-Acetylcysteine Augmentation for Treatment-Resistant Obsessive-Compulsive Disorder. *The Journal of Clinical Psychiatry* 78(7), pp. e766–e773.
- Crane, J., Fagerness, J., Osiecki, L., et al. 2011. Family-based genetic association study of DLGAP3 in Tourette Syndrome. *American Journal of Medical Genetics. Part B, Neuropsychiatric Genetics* 156B(1), pp. 108–114.
- Danbolt, N.C., Furness, D.N. and Zhou, Y. 2016. Neuronal vs glial glutamate uptake: Resolving the conundrum. *Neurochemistry International* 98, pp. 29–45.

- de Wit, S.J., Alonso, P., Schweren, L., et al. 2014. Multicenter voxel-based morphometry mega-analysis of structural brain scans in obsessive-compulsive disorder. *The American Journal of Psychiatry* 171(3), pp. 340–349.
- Dehnes, Y., Chaudhry, F.A., Ullensvang, K., Lehre, K.P., Storm-Mathisen, J. and Danbolt, N.C. 1998. The glutamate transporter EAAT4 in rat cerebellar Purkinje cells: a glutamate-gated chloride channel concentrated near the synapse in parts of the dendritic membrane facing astroglia. *The Journal of Neuroscience* 18(10), pp. 3606–3619.
- Delgado-Acevedo, C., Estay, S.F., Radke, A.K., et al. 2019. Behavioral and synaptic alterations relevant to obsessive-compulsive disorder in mice with increased EAAT3 expression. *Neuropsychopharmacology* 44(6), pp. 1163–1173.
- Dell’Osso, B., Cremaschi, L., Oldani, L. and Altamura, A.C. 2018. New Directions in the Use of Brain Stimulation Interventions in Patients with Obsessive-Compulsive Disorder. *Current Medicinal Chemistry* 25(41), pp. 5712–5721.
- Denys, D., Mantione, M., Figeet, M., et al. 2010. Deep brain stimulation of the nucleus accumbens for treatment-refractory obsessive-compulsive disorder. *Archives of General Psychiatry* 67(10), pp. 1061–1068.
- Denys, D., Zohar, J. and Westenberg, H.G.M. 2004. The role of dopamine in obsessive-compulsive disorder: preclinical and clinical evidence. *The Journal of Clinical Psychiatry* 65 Suppl 14, pp. 11–17.
- DeSilva, T.M., Kabakov, A.Y., Goldhoff, P.E., Volpe, J.J. and Rosenberg, P.A. 2009. Regulation of glutamate transport in developing rat oligodendrocytes. *The Journal of Neuroscience* 29(24), pp. 7898–7908.

- Diamond, J.S. 2001. Neuronal glutamate transporters limit activation of NMDA receptors by neurotransmitter spillover on CA1 pyramidal cells. *The Journal of Neuroscience* 21(21), pp. 8328–8338.
- Diamond, J.S. and Jahr, C.E. 1997. Transporters buffer synaptically released glutamate on a submillisecond time scale. *The Journal of Neuroscience* 17(12), pp. 4672–4687.
- Dickel, D.E., Veenstra-VanderWeele, J., Cox, N.J., et al. 2006. Association testing of the positional and functional candidate gene SLC1A1/EAAC1 in early-onset obsessive-compulsive disorder. *Archives of General Psychiatry* 63(7), pp. 778–785.
- Dougherty, D.D., Baer, L., Cosgrove, G.R., et al. 2002. Prospective long-term follow-up of 44 patients who received cingulotomy for treatment-refractory obsessive-compulsive disorder. *The American Journal of Psychiatry* 159(2), pp. 269–275.
- Dougherty, D.D., Rauch, S.L. and Jenike, M.A. 2004. Pharmacotherapy for obsessive-compulsive disorder. *Journal of Clinical Psychology* 60(11), pp. 1195–1202.
- DuPont, R.L., Rice, D.P., Shiraki, S. and Rowland, C.R. 1995. Economic costs of obsessive-compulsive disorder. *Medical interface* 8(4), pp. 102–109.
- Eaton, W.W., Martins, S.S., Nestadt, G., Bienvenu, O.J., Clarke, D. and Alexandre, P. 2008. The burden of mental disorders. *Epidemiologic Reviews* 30, pp. 1–14.
- Eliasof, S., Arriza, J.L., Leighton, B.H., Amara, S.G. and Kavanaugh, M.P. 1998. Localization and function of five glutamate transporters cloned from the salamander retina. *Vision Research* 38(10), pp. 1443–1454.
- Emamzadehfard, S., Kamaloo, A., Paydary, K., et al. 2016. Riluzole in augmentation of fluvoxamine for moderate to severe obsessive-compulsive disorder: Randomized, double-

- blind, placebo-controlled study. *Psychiatry and Clinical Neurosciences* 70(8), pp. 332–341.
- Engeln, M., Song, Y., Chandra, R., et al. 2020. Individual differences in stereotypy and neuron subtype transcriptome with TrkB deletion. *Molecular Psychiatry*.
- Fairman, W.A., Vandenberg, R.J., Arriza, J.L., Kavanaugh, M.P. and Amara, S.G. 1995. An excitatory amino-acid transporter with properties of a ligand-gated chloride channel. *Nature* 375(6532), pp. 599–603.
- Fernández de la Cruz, L., Rydell, M., Runeson, B., et al. 2017. Suicide in obsessive-compulsive disorder: a population-based study of 36 788 Swedish patients. *Molecular Psychiatry* 22(11), pp. 1626–1632.
- Fernandez, T.V., Leckman, J.F. and Pittenger, C. 2018. Genetic susceptibility in obsessive-compulsive disorder. *Handbook of Clinical Neurology* 148, pp. 767–781.
- Fouche, J.-P., du Plessis, S., Hattingh, C., et al. 2017. Cortical thickness in obsessive-compulsive disorder: multisite mega-analysis of 780 brain scans from six centres. *The British Journal of Psychiatry* 210(1), pp. 67–74.
- Ghaleiha, A., Entezari, N., Modabbernia, A., et al. 2013. Memantine add-on in moderate to severe obsessive-compulsive disorder: randomized double-blind placebo-controlled study. *Journal of Psychiatric Research* 47(2), pp. 175–180.
- Goodman, W.K., McDougle, C.J., Price, L.H., Riddle, M.A., Pauls, D.L. and Leckman, J.F. 1990. Beyond the serotonin hypothesis: a role for dopamine in some forms of obsessive compulsive disorder? *The Journal of Clinical Psychiatry* 51 Suppl, pp. 36–43; discussion 55.

- Graat, I., Figeet, M. and Denys, D. 2017. The application of deep brain stimulation in the treatment of psychiatric disorders. *International Review of Psychiatry* 29(2), pp. 178–190.
- Grados, M. and Wilcox, H.C. 2007. Genetics of obsessive-compulsive disorder: a research update. *Expert Review of Neurotherapeutics* 7(8), pp. 967–980.
- Grados, M.A., Riddle, M.A., Samuels, J.F., et al. 2001. The familial phenotype of obsessive-compulsive disorder in relation to tic disorders: the Hopkins OCD family study. *Biological Psychiatry* 50(8), pp. 559–565.
- Grant, P.J., Joseph, L.A., Farmer, C.A., et al. 2014. 12-week, placebo-controlled trial of add-on riluzole in the treatment of childhood-onset obsessive-compulsive disorder. *Neuropsychopharmacology* 39(6), pp. 1453–1459.
- Greer, J.B., Khuri, S. and Fieber, L.A. 2017. Phylogenetic analysis of ionotropic L-glutamate receptor genes in the Bilateria, with special notes on *Aplysia californica*. *BMC Evolutionary Biology* 17(1), p. 11.
- Grewer, C., Watzke, N., Wiessner, M. and Rauen, T. 2000. Glutamate translocation of the neuronal glutamate transporter EAAC1 occurs within milliseconds. *Proceedings of the National Academy of Sciences of the United States of America* 97(17), pp. 9706–9711.
- Han, S., Tai, C., Westenbroek, R.E., et al. 2012. Autistic-like behaviour in *Scn1a*^{+/-} mice and rescue by enhanced GABA-mediated neurotransmission. *Nature* 489(7416), pp. 385–390.
- Hanna, G.L., Piacentini, J., Cantwell, D.P., Fischer, D.J., Himle, J.A. and Van Etten, M. 2002. Obsessive-compulsive disorder with and without tics in a clinical sample of children and adolescents. *Depression and Anxiety* 16(2), pp. 59–63.

- Hanna, G.L., Veenstra-VanderWeele, J., Cox, N.J., et al. 2002. Genome-wide linkage analysis of families with obsessive-compulsive disorder ascertained through pediatric probands. *American Journal of Medical Genetics* 114(5), pp. 541–552.
- Harrison, B.J., Soriano-Mas, C., Pujol, J., et al. 2009. Altered corticostriatal functional connectivity in obsessive-compulsive disorder. *Archives of General Psychiatry* 66(11), pp. 1189–1200.
- Herring, B.E. and Nicoll, R.A. 2016. Long-Term Potentiation: From CaMKII to AMPA Receptor Trafficking. *Annual Review of Physiology* 78, pp. 351–365.
- Hettema, J.M., Neale, M.C. and Kendler, K.S. 2001. A review and meta-analysis of the genetic epidemiology of anxiety disorders. *The American Journal of Psychiatry* 158(10), pp. 1568–1578.
- Hirschtritt, M.E., Bloch, M.H. and Mathews, C.A. 2017. Obsessive-Compulsive Disorder: Advances in Diagnosis and Treatment. *The Journal of the American Medical Association* 317(13), pp. 1358–1367.
- Hollmann, M. and Heinemann, S. 1994. Cloned glutamate receptors. *Annual Review of Neuroscience* 17, pp. 31–108.
- Holmseth, S., Dehnes, Y., Huang, Y.H., et al. 2012. The density of EAAC1 (EAAT3) glutamate transporters expressed by neurons in the mammalian CNS. *The Journal of Neuroscience* 32(17), pp. 6000–6013.
- Holmseth, S., Lehre, K.P. and Danbolt, N.C. 2006. Specificity controls for immunocytochemistry. *Anatomy and embryology* 211(4), pp. 257–266.

- Horiuchi, Y., Iida, S., Koga, M., et al. 2012. Association of SNPs linked to increased expression of SLC1A1 with schizophrenia. *American Journal of Medical Genetics. Part B, Neuropsychiatric Genetics* 159B(1), pp. 30–37.
- Hsu, A.I. and Yttri, E.A. 2019. B-SOiD: An Open Source Unsupervised Algorithm for Discovery of Spontaneous Behaviors. *BioRxiv*.
- Hu, W., MacDonald, M.L., Elswick, D.E. and Sweet, R.A. 2015. The glutamate hypothesis of schizophrenia: evidence from human brain tissue studies. *Annals of the New York Academy of Sciences* 1338, pp. 38–57.
- Huang, Y.H., Dykes-Hoberg, M., Tanaka, K., Rothstein, J.D. and Bergles, D.E. 2004. Climbing fiber activation of EAAT4 transporters and kainate receptors in cerebellar Purkinje cells. *The Journal of Neuroscience* 24(1), pp. 103–111.
- Jarzylo, L.A. and Man, H.-Y. 2012. Parasynaptic NMDA receptor signaling couples neuronal glutamate transporter function to AMPA receptor synaptic distribution and stability. *The Journal of Neuroscience* 32(7), pp. 2552–2563.
- Jiang, Y.-H. and Ehlers, M.D. 2013. Modeling autism by SHANK gene mutations in mice. *Neuron* 78(1), pp. 8–27.
- Kanai, Y. and Hediger, M.A. 1992. Primary structure and functional characterization of a high-affinity glutamate transporter. *Nature* 360(6403), pp. 467–471.
- Kelley, A.E. 2001. Measurement of rodent stereotyped behavior. *Current Protocols in Neuroscience* Chapter 8, p. Unit 8.8.
- Kessler, R.C., Berglund, P., Demler, O., Jin, R., Merikangas, K.R. and Walters, E.E. 2005. Lifetime prevalence and age-of-onset distributions of DSM-IV disorders in the National Comorbidity Survey Replication. *Archives of General Psychiatry* 62(6), pp. 593–602.

- Koran, L.M. 2000. Quality of life in obsessive-compulsive disorder. *The Psychiatric Clinics of North America* 23(3), pp. 509–517.
- Koran, L.M., Hanna, G.L., Hollander, E., Nestadt, G., Simpson, H.B. and American Psychiatric Association 2007. Practice guideline for the treatment of patients with obsessive-compulsive disorder. *The American Journal of Psychiatry* 164(7 Suppl), pp. 5–53.
- Kouser, M., Speed, H.E., Dewey, C.M., et al. 2013. Loss of predominant Shank3 isoforms results in hippocampus-dependent impairments in behavior and synaptic transmission. *The Journal of Neuroscience* 33(47), pp. 18448–18468.
- Kugler, P. and Schmitt, A. 1999. Glutamate transporter EAAC1 is expressed in neurons and glial cells in the rat nervous system. *Glia* 27(2), pp. 129–142.
- Lee, Y., Kim, H., Kim, J.-E., et al. 2018. Excessive D1 Dopamine Receptor Activation in the Dorsal Striatum Promotes Autistic-Like Behaviors. *Molecular Neurobiology* 55(7), pp. 5658–5671.
- Lehre, K.P. and Danbolt, N.C. 1998. The number of glutamate transporter subtype molecules at glutamatergic synapses: chemical and stereological quantification in young adult rat brain. *The Journal of Neuroscience* 18(21), pp. 8751–8757.
- Lehre, K.P., Levy, L.M., Ottersen, O.P., Storm-Mathisen, J. and Danbolt, N.C. 1995. Differential expression of two glial glutamate transporters in the rat brain: quantitative and immunocytochemical observations. *The Journal of Neuroscience* 15(3 Pt 1), pp. 1835–1853.
- Lewis, M. and Kim, S.-J. 2009. The pathophysiology of restricted repetitive behavior. *Journal of neurodevelopmental disorders* 1(2), pp. 114–132.

- Li, M.-H., Underhill, S.M., Reed, C., Phillips, T.J., Amara, S.G. and Ingram, S.L. 2017. Amphetamine and Methamphetamine Increase NMDAR-GluN2B Synaptic Currents in Midbrain Dopamine Neurons. *Neuropsychopharmacology* 42(7), pp. 1539–1547.
- Liang, J., Chao, D., Sandhu, H.K., et al. 2014. δ -Opioid receptors up-regulate excitatory amino acid transporters in mouse astrocytes. *British Journal of Pharmacology* 171(23), pp. 5417–5430.
- Manning, E.E., Dombrovski, A.Y., Torregrossa, M.M. and Ahmari, S.E. 2019. Impaired instrumental reversal learning is associated with increased medial prefrontal cortex activity in Sapap3 knockout mouse model of compulsive behavior. *Neuropsychopharmacology* 44(8), pp. 1494–1504.
- Marinova, Z., Chuang, D.-M. and Fineberg, N. 2017. Glutamate-Modulating Drugs as a Potential Therapeutic Strategy in Obsessive-Compulsive Disorder. *Current neuropharmacology* 15(7), pp. 977–995.
- Mataix-Cols, D., Boman, M., Monzani, B., et al. 2013. Population-based, multigenerational family clustering study of obsessive-compulsive disorder. *JAMA psychiatry* 70(7), pp. 709–717.
- Mathews, G.C. and Diamond, J.S. 2003. Neuronal glutamate uptake Contributes to GABA synthesis and inhibitory synaptic strength. *The Journal of Neuroscience* 23(6), pp. 2040–2048.
- Mathis, A., Mamidanna, P., Cury, K.M., et al. 2018. DeepLabCut: markerless pose estimation of user-defined body parts with deep learning. *Nature Neuroscience* 21(9), pp. 1281–1289.
- Mattheisen, M., Samuels, J.F., Wang, Y., et al. 2015. Genome-wide association study in obsessive-compulsive disorder: results from the OCGAS. *Molecular Psychiatry* 20(3), pp. 337–344.

- McCullumsmith, R.E. and Meador-Woodruff, J.H. 2002. Striatal excitatory amino acid transporter transcript expression in schizophrenia, bipolar disorder, and major depressive disorder. *Neuropsychopharmacology* 26(3), pp. 368–375.
- McDougle, C.J., Barr, L.C., Goodman, W.K. and Price, L.H. 1999. Possible role of neuropeptides in obsessive compulsive disorder. *Psychoneuroendocrinology* 24(1), pp. 1–24.
- McKay, D., Sookman, D., Neziroglu, F., et al. 2015. Efficacy of cognitive-behavioral therapy for obsessive-compulsive disorder. *Psychiatry Research* 225(3), pp. 236–246.
- Menzies, L., Chamberlain, S.R., Laird, A.R., Thelen, S.M., Sahakian, B.J. and Bullmore, E.T. 2008. Integrating evidence from neuroimaging and neuropsychological studies of obsessive-compulsive disorder: the orbitofronto-striatal model revisited. *Neuroscience and Biobehavioral Reviews* 32(3), pp. 525–549.
- Milardi, D., Quartarone, A., Bramanti, A., et al. 2019. The Cortico-Basal Ganglia-Cerebellar Network: Past, Present and Future Perspectives. *Frontiers in Systems Neuroscience* 13, p. 61.
- Monyer, H., Sprengel, R., Schoepfer, R., et al. 1992. Heteromeric NMDA receptors: molecular and functional distinction of subtypes. *Science* 256(5060), pp. 1217–1221.
- Morein-Zamir, S., Pappmeyer, M., Pertusa, A., et al. 2014. The profile of executive function in OCD hoarders and hoarding disorder. *Psychiatry Research* 215(3), pp. 659–667.
- Muehlmann, A.M. and Lewis, M.H. 2012. Abnormal repetitive behaviours: shared phenomenology and pathophysiology. *Journal of Intellectual Disability Research* 56(5), pp. 427–440.
- Myles-Worsley, M., Tiobech, J., Browning, S.R., et al. 2013. Deletion at the SLC1A1 glutamate transporter gene co-segregates with schizophrenia and bipolar schizoaffective disorder in

- a 5-generation family. *American Journal of Medical Genetics. Part B, Neuropsychiatric Genetics* 162B(2), pp. 87–95.
- Nagarajan, N., Jones, B.W., West, P.J., Marc, R.E. and Capecchi, M.R. 2018. Corticostriatal circuit defects in Hoxb8 mutant mice. *Molecular Psychiatry* 23(9), pp. 1868–1877.
- Nakanishi, S. 1992. Molecular diversity of glutamate receptors and implications for brain function. *Science* 258(5082), pp. 597–603.
- Nakanishi, S., Masu, M., Bessho, Y., Nakajima, Y., Hayashi, Y. and Shigemoto, R. 1994. Molecular diversity of glutamate receptors and their physiological functions. *Exs* 71, pp. 71–80.
- Nath, T., Mathis, A., Chen, A.C., Patel, A., Bethge, M. and Mathis, M.W. 2019. Using DeepLabCut for 3D markerless pose estimation across species and behaviors. *Nature Protocols* 14(7), pp. 2152–2176.
- Nicholls, D. and Attwell, D. 1990. The release and uptake of excitatory amino acids. *Trends in Pharmacological Sciences* 11(11), pp. 462–468.
- Niswender, C.M. and Conn, P.J. 2010. Metabotropic glutamate receptors: physiology, pharmacology, and disease. *Annual Review of Pharmacology and Toxicology* 50, pp. 295–322.
- Nordahl, T.E., Benkelfat, C., Semple, W.E., Gross, M., King, A.C. and Cohen, R.M. 1989. Cerebral glucose metabolic rates in obsessive compulsive disorder. *Neuropsychopharmacology* 2(1), pp. 23–28.
- Ozawa, S., Kamiya, H. and Tsuzuki, K. 1998. Glutamate receptors in the mammalian central nervous system. *Progress in Neurobiology* 54(5), pp. 581–618.

- Pallanti, S., Grassi, G., Sarrecchia, E.D., Cantisani, A. and Pellegrini, M. 2011. Obsessive-compulsive disorder comorbidity: clinical assessment and therapeutic implications. *Frontiers in psychiatry* 2, p. 70.
- Pardiñas, A.F., Holmans, P., Pocklington, A.J., et al. 2018. Common schizophrenia alleles are enriched in mutation-intolerant genes and in regions under strong background selection. *Nature Genetics* 50(3), pp. 381–389.
- Parmar, A. and Sarkar, S. 2016. Neuroimaging studies in obsessive compulsive disorder: A narrative review. *Indian journal of psychological medicine* 38(5), pp. 386–394.
- Pauls, D.L. 2008. The genetics of obsessive compulsive disorder: a review of the evidence. *American Journal of Medical Genetics. Part C, Seminars in Medical Genetics* 148C(2), pp. 133–139.
- Pauls, D.L., Abramovitch, A., Rauch, S.L. and Geller, D.A. 2014. Obsessive-compulsive disorder: an integrative genetic and neurobiological perspective. *Nature Reviews. Neuroscience* 15(6), pp. 410–424.
- Paydary, K., Akamaloo, A., Ahmadipour, A., Pishgar, F., Emamzadehfard, S. and Akhondzadeh, S. 2016. N-acetylcysteine augmentation therapy for moderate-to-severe obsessive-compulsive disorder: randomized, double-blind, placebo-controlled trial. *Journal of Clinical Pharmacy and Therapeutics* 41(2), pp. 214–219.
- Peghini, P., Janzen, J. and Stoffel, W. 1997. Glutamate transporter EAAC-1-deficient mice develop dicarboxylic aminoaciduria and behavioral abnormalities but no neurodegeneration. *The EMBO Journal* 16(13), pp. 3822–3832.
- Pence, S.L., Sulkowski, M.L., Jordan, C. and Storch, E.A. 2010. When exposures go wrong: troubleshooting guidelines for managing difficult scenarios that arise in exposure-based

- treatment for obsessive-compulsive disorder. *American journal of psychotherapy* 64(1), pp. 39–53.
- Piantadosi, S.C., Chamberlain, B.L., Glausier, J.R., Lewis, D.A. and Ahmari, S.E. 2019. Lower excitatory synaptic gene expression in orbitofrontal cortex and striatum in an initial study of subjects with obsessive compulsive disorder. *Molecular Psychiatry*.
- Pittenger, C. 2015. Glutamatergic agents for OCD and related disorders. *Current treatment options in psychiatry* 2(3), pp. 271–283.
- Pittenger, C., Bloch, M.H., Wasylink, S., et al. 2015. Riluzole augmentation in treatment-refractory obsessive-compulsive disorder: a pilot randomized placebo-controlled trial. *The Journal of Clinical Psychiatry* 76(8), pp. 1075–1084.
- Pittenger, C., Bloch, M.H. and Williams, K. 2011. Glutamate abnormalities in obsessive compulsive disorder: neurobiology, pathophysiology, and treatment. *Pharmacology & Therapeutics* 132(3), pp. 314–332.
- Pittenger, C., Kelmendi, B., Bloch, M., Krystal, J.H. and Coric, V. 2005. Clinical treatment of obsessive compulsive disorder. *Psychiatry (Edgmont)* 2(11), pp. 34–43.
- Pujol, J., Soriano-Mas, C., Alonso, P., et al. 2004. Mapping structural brain alterations in obsessive-compulsive disorder. *Archives of General Psychiatry* 61(7), pp. 720–730.
- Radua, J. and Mataix-Cols, D. 2009. Voxel-wise meta-analysis of grey matter changes in obsessive-compulsive disorder. *The British Journal of Psychiatry* 195(5), pp. 393–402.
- Radua, J., van den Heuvel, O.A., Surguladze, S. and Mataix-Cols, D. 2010. Meta-analytical comparison of voxel-based morphometry studies in obsessive-compulsive disorder vs other anxiety disorders. *Archives of General Psychiatry* 67(7), pp. 701–711.

- Rajendram, R., Kronenberg, S., Burton, C.L. and Arnold, P.D. 2017. Glutamate Genetics in Obsessive-Compulsive Disorder: A Review. *Journal of the Canadian Academy of Child and Adolescent Psychiatry* 26(3), pp. 205–213.
- Rasmussen, A.H., Rasmussen, H.B. and Silaharoglu, A. 2017. The DLGAP family: neuronal expression, function and role in brain disorders. *Molecular Brain* 10(1), p. 43.
- Robbins, T.W., Vaghi, M.M. and Banca, P. 2019. Obsessive-Compulsive Disorder: Puzzles and Prospects. *Neuron* 102(1), pp. 27–47.
- Robins, L.N., Helzer, J.E., Weissman, M.M., et al. 1984. Lifetime prevalence of specific psychiatric disorders in three sites. *Archives of General Psychiatry* 41(10), pp. 949–958.
- Rodriguez, C.I., Levinson, A., Zwerling, J., Vermes, D. and Simpson, H.B. 2016. Open-Label trial on the effects of memantine in adults with obsessive-compulsive disorder after a single ketamine infusion. *The Journal of Clinical Psychiatry* 77(5), pp. 688–689.
- Rodriguez, C.I., Wheaton, M., Zwerling, J., et al. 2016. Can exposure-based CBT extend the effects of intravenous ketamine in obsessive-compulsive disorder? an open-label trial. *The Journal of Clinical Psychiatry* 77(3), pp. 408–409.
- Rosenberg, D.R., MacMaster, F.P., Keshavan, M.S., Fitzgerald, K.D., Stewart, C.M. and Moore, G.J. 2000. Decrease in caudate glutamatergic concentrations in pediatric obsessive-compulsive disorder patients taking paroxetine. *Journal of the American Academy of Child and Adolescent Psychiatry* 39(9), pp. 1096–1103.
- Rosenberg, D.R., Mirza, Y., Russell, A., et al. 2004. Reduced anterior cingulate glutamatergic concentrations in childhood OCD and major depression versus healthy controls. *Journal of the American Academy of Child and Adolescent Psychiatry* 43(9), pp. 1146–1153.

- Ruscio, A.M., Stein, D.J., Chiu, W.T. and Kessler, R.C. 2010. The epidemiology of obsessive-compulsive disorder in the National Comorbidity Survey Replication. *Molecular Psychiatry* 15(1), pp. 53–63.
- Samuels, J., Wang, Y., Riddle, M.A., et al. 2011. Comprehensive family-based association study of the glutamate transporter gene SLC1A1 in obsessive-compulsive disorder. *American Journal of Medical Genetics. Part B, Neuropsychiatric Genetics* 156B(4), pp. 472–477.
- Sanders, S.J., Murtha, M.T., Gupta, A.R., et al. 2012. De novo mutations revealed by whole-exome sequencing are strongly associated with autism. *Nature* 485(7397), pp. 237–241.
- Sarris, J., Oliver, G., Camfield, D.A., et al. 2015. N-Acetyl Cysteine (NAC) in the Treatment of Obsessive-Compulsive Disorder: A 16-Week, Double-Blind, Randomised, Placebo-Controlled Study. *CNS Drugs* 29(9), pp. 801–809.
- Schizophrenia Working Group of the Psychiatric Genomics Consortium 2014. Biological insights from 108 schizophrenia-associated genetic loci. *Nature* 511(7510), pp. 421–427.
- Scimemi, A., Fine, A., Kullmann, D.M. and Rusakov, D.A. 2004. NR2B-containing receptors mediate cross talk among hippocampal synapses. *The Journal of Neuroscience* 24(20), pp. 4767–4777.
- Scimemi, A., Tian, H. and Diamond, J.S. 2009. Neuronal transporters regulate glutamate clearance, NMDA receptor activation, and synaptic plasticity in the hippocampus. *The Journal of Neuroscience* 29(46), pp. 14581–14595.
- Sepkuty, J.P., Cohen, A.S., Eccles, C., et al. 2002. A neuronal glutamate transporter contributes to neurotransmitter GABA synthesis and epilepsy. *The Journal of Neuroscience* 22(15), pp. 6372–6379.

- Shahbazian, M., Young, J., Yuva-Paylor, L., et al. 2002. Mice with truncated MeCP2 recapitulate many Rett syndrome features and display hyperacetylation of histone H3. *Neuron* 35(2), pp. 243–254.
- Shigeri, Y., Seal, R.P. and Shimamoto, K. 2004. Molecular pharmacology of glutamate transporters, EAATs and VGLUTs. *Brain Research. Brain Research Reviews* 45(3), pp. 250–265.
- Shmelkov, S.V., Hormigo, A., Jing, D., et al. 2010. Slitrk5 deficiency impairs corticostriatal circuitry and leads to obsessive-compulsive-like behaviors in mice. *Nature Medicine* 16(5), pp. 598–602, 1p following 602.
- Shugart, Y.Y., Wang, Y., Samuels, J.F., et al. 2009. A family-based association study of the glutamate transporter gene SLC1A1 in obsessive-compulsive disorder in 378 families. *American Journal of Medical Genetics. Part B, Neuropsychiatric Genetics* 150B(6), pp. 886–892.
- Sommer, B., Monyer, H., Wisden, W., et al. 1992. Glutamate-gated ion channels in the brain. Genetic mechanism for generating molecular and functional diversity. *Arzneimittel-Forschung* 42(2A), pp. 209–210.
- Starck, G., Ljungberg, M., Nilsson, M., et al. 2008. A ¹H magnetic resonance spectroscopy study in adults with obsessive compulsive disorder: relationship between metabolite concentrations and symptom severity. *Journal of Neural Transmission* 115(7), pp. 1051–1062.
- Steinhausen, H.-C., Bisgaard, C., Munk-Jørgensen, P. and Helenius, D. 2013. Family aggregation and risk factors of obsessive-compulsive disorders in a nationwide three-generation study. *Depression and Anxiety* 30(12), pp. 1177–1184.

- Stewart, S.E., Fagerness, J.A., Platko, J., et al. 2007. Association of the SLC1A1 glutamate transporter gene and obsessive-compulsive disorder. *American Journal of Medical Genetics. Part B, Neuropsychiatric Genetics* 144B(8), pp. 1027–1033.
- Stewart, S.E., Mayerfeld, C., Arnold, P.D., et al. 2013. Meta-analysis of association between obsessive-compulsive disorder and the 3' region of neuronal glutamate transporter gene SLC1A1. *American Journal of Medical Genetics. Part B, Neuropsychiatric Genetics* 162B(4), pp. 367–379.
- Stewart, S.E., Yu, D., Scharf, J.M., et al. 2013. Genome-wide association study of obsessive-compulsive disorder. *Molecular Psychiatry* 18(7), pp. 788–798.
- Tanaka, K., Watase, K., Manabe, T., et al. 1997. Epilepsy and exacerbation of brain injury in mice lacking the glutamate transporter GLT-1. *Science* 276(5319), pp. 1699–1702.
- Tanaka, K.F., Ahmari, S.E., Leonardo, E.D., et al. 2010. Flexible Accelerated STOP Tetracycline Operator-knockin (FAST): a versatile and efficient new gene modulating system. *Biological Psychiatry* 67(8), pp. 770–773.
- Taylor, S. 2013. Molecular genetics of obsessive-compulsive disorder: a comprehensive meta-analysis of genetic association studies. *Molecular Psychiatry* 18(7), pp. 799–805.
- Thamby, A. and Jaisoorya, T.S. 2019. Antipsychotic augmentation in the treatment of obsessive-compulsive disorder. *Indian journal of psychiatry* 61(Suppl 1), pp. S51–S57.
- Traynelis, S.F., Wollmuth, L.P., McBain, C.J., et al. 2010. Glutamate receptor ion channels: structure, regulation, and function. *Pharmacological Reviews* 62(3), pp. 405–496.
- Underhill, S.M., Wheeler, D.S., Li, M., Watts, S.D., Ingram, S.L. and Amara, S.G. 2014. Amphetamine modulates excitatory neurotransmission through endocytosis of the glutamate transporter EAAT3 in dopamine neurons. *Neuron* 83(2), pp. 404–416.

- Vaghi, M.M., Vértes, P.E., Kitzbichler, M.G., et al. 2017. Specific Frontostriatal Circuits for Impaired Cognitive Flexibility and Goal-Directed Planning in Obsessive-Compulsive Disorder: Evidence From Resting-State Functional Connectivity. *Biological Psychiatry* 81(8), pp. 708–717.
- van den Heuvel, O.A., Remijnse, P.L., Mataix-Cols, D., et al. 2009. The major symptom dimensions of obsessive-compulsive disorder are mediated by partially distinct neural systems. *Brain: A Journal of Neurology* 132(Pt 4), pp. 853–868.
- van Grootheest, D.S., Cath, D.C., Beekman, A.T. and Boomsma, D.I. 2005. Twin studies on obsessive-compulsive disorder: a review. *Twin Research and Human Genetics* 8(5), pp. 450–458.
- Veenstra-VanderWeele, J., Xu, T., Ruggiero, A.M., et al. 2012. Functional studies and rare variant screening of SLC1A1/EAAC1 in males with obsessive-compulsive disorder. *Psychiatric Genetics* 22(5), pp. 256–260.
- Velaz-Faircloth, M., McGraw, T.S., alandro, M.S., Fremeau, R.T., Kilberg, M.S. and Anderson, K.J. 1996. Characterization and distribution of the neuronal glutamate transporter EAAC1 in rat brain. *The American Journal of Physiology* 270(1 Pt 1), pp. C67–75.
- Wadiche, J.I., Arriza, J.L., Amara, S.G. and Kavanaugh, M.P. 1995. Kinetics of a human glutamate transporter. *Neuron* 14(5), pp. 1019–1027.
- Wan, Y., Ade, K.K., Caffall, Z., et al. 2014. Circuit-selective striatal synaptic dysfunction in the Sapap3 knockout mouse model of obsessive-compulsive disorder. *Biological Psychiatry* 75(8), pp. 623–630.
- Welch, J.M., Lu, J., Rodriguiz, R.M., et al. 2007. Cortico-striatal synaptic defects and OCD-like behaviours in Sapap3-mutant mice. *Nature* 448(7156), pp. 894–900.

- Wendland, J.R., Moya, P.R., Timpano, K.R., et al. 2009. A haplotype containing quantitative trait loci for SLC1A1 gene expression and its association with obsessive-compulsive disorder. *Archives of General Psychiatry* 66(4), pp. 408–416.
- Whiteside, S.P., Port, J.D., Deacon, B.J. and Abramowitz, J.S. 2006. A magnetic resonance spectroscopy investigation of obsessive-compulsive disorder and anxiety. *Psychiatry Research* 146(2), pp. 137–147.
- Willour, V.L., Yao Shugart, Y., Samuels, J., et al. 2004. Replication study supports evidence for linkage to 9p24 in obsessive-compulsive disorder. *American Journal of Human Genetics* 75(3), pp. 508–513.
- Wolgin, D.L. 2012. Amphetamine stereotypy, the basal ganglia, and the “selection problem”. *Behavioural Brain Research* 231(2), pp. 297–308.
- Wood, J. and Ahmari, S.E. 2015. A Framework for Understanding the Emerging Role of Corticolimbic-Ventral Striatal Networks in OCD-Associated Repetitive Behaviors. *Frontiers in Systems Neuroscience* 9, p. 171.
- Wood, J., LaPalombara, Z. and Ahmari, S.E. 2018. Monoamine abnormalities in the SAPAP3 knockout model of obsessive-compulsive disorder-related behaviour. *Philosophical Transactions of the Royal Society of London. Series B, Biological Sciences* 373(1742).
- Wu, M.-Y., Lin, Y.-C., Liao, W.-J., et al. 2014. Inhibition of the plasma SCUBE1, a novel platelet adhesive protein, protects mice against thrombosis. *Arteriosclerosis, Thrombosis, and Vascular Biology* 34(7), pp. 1390–1398.
- Yates, J.W., Meij, J.T.A., Sullivan, J.R., Richtand, N.M. and Yu, L. 2007. Bimodal effect of amphetamine on motor behaviors in C57BL/6 mice. *Neuroscience Letters* 427(1), pp. 66–70.

- Yüksel, C. and Öngür, D. 2010. Magnetic resonance spectroscopy studies of glutamate-related abnormalities in mood disorders. *Biological Psychiatry* 68(9), pp. 785–794.
- Zerangue, N. and Kavanaugh, M.P. 1996. Flux coupling in a neuronal glutamate transporter. *Nature* 383(6601), pp. 634–637.
- Zhou, Y. and Danbolt, N.C. 2014. Glutamate as a neurotransmitter in the healthy brain. *Journal of Neural Transmission* 121(8), pp. 799–817.
- Zike, I.D., Chohan, M.O., Kopelman, J.M., et al. 2017. OCD candidate gene SLC1A1/EAAT3 impacts basal ganglia-mediated activity and stereotypic behavior. *Proceedings of the National Academy of Sciences of the United States of America* 114(22), pp. 5719–5724.